Precision Measurements

Particle Physics
Toni Baroncelli
Haiping Peng
USTC

LEP and LEP Data

LEP was an electron-positron collider ring with a circumference of approximately 27 km
four interaction regions with **multipurpose detector: L3, ALEPH, OPAL and DELPHI**

- In the summer of 1989 the first Z bosons were produced at LEP
- At the end of LEP (~2000) approximately 1000 Z bosons were *recorded* every hour by each of the four experiments,

LEP was a true Z factory.

The LEP Collaborations:

Experiment	Aleph	Delphi	L3	Opal
# Institutes	34	60	49	34

Number of members/authors ~ 10/Institute
I was a DELPHI member!

11 years of operation

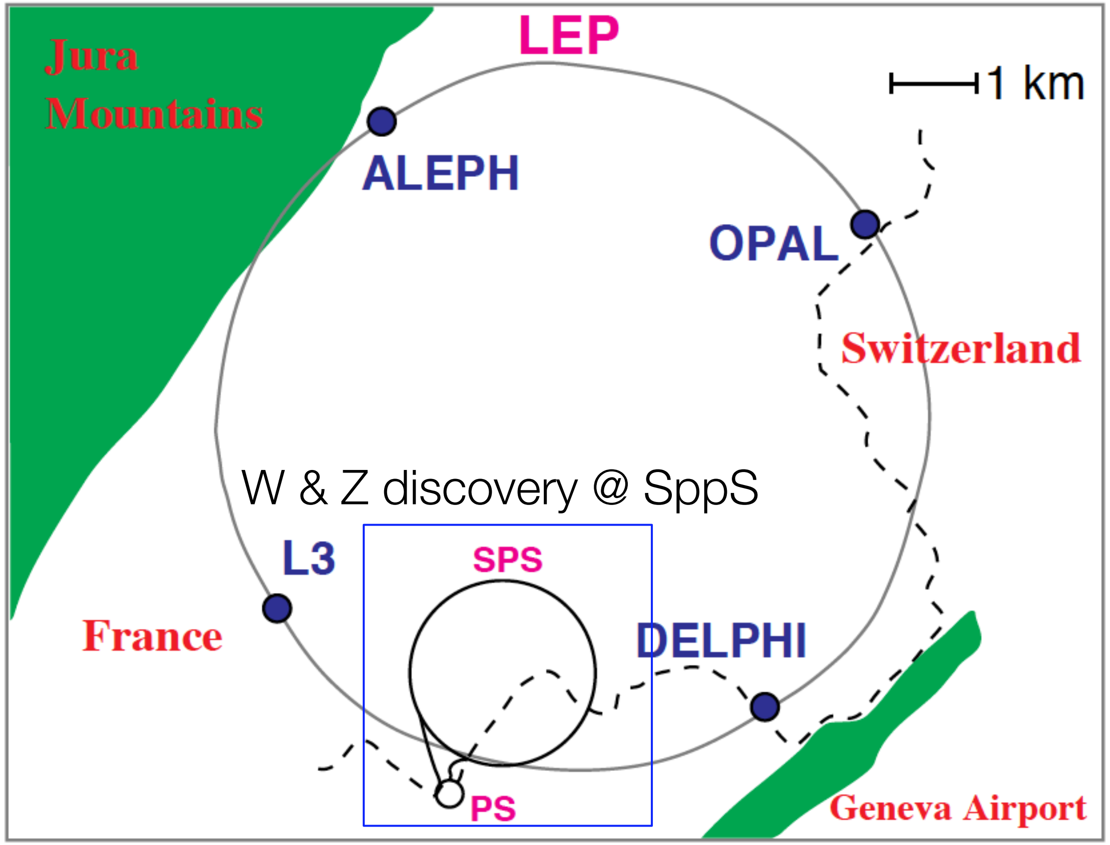

W & Z discovery @ SppS

The Energy Points

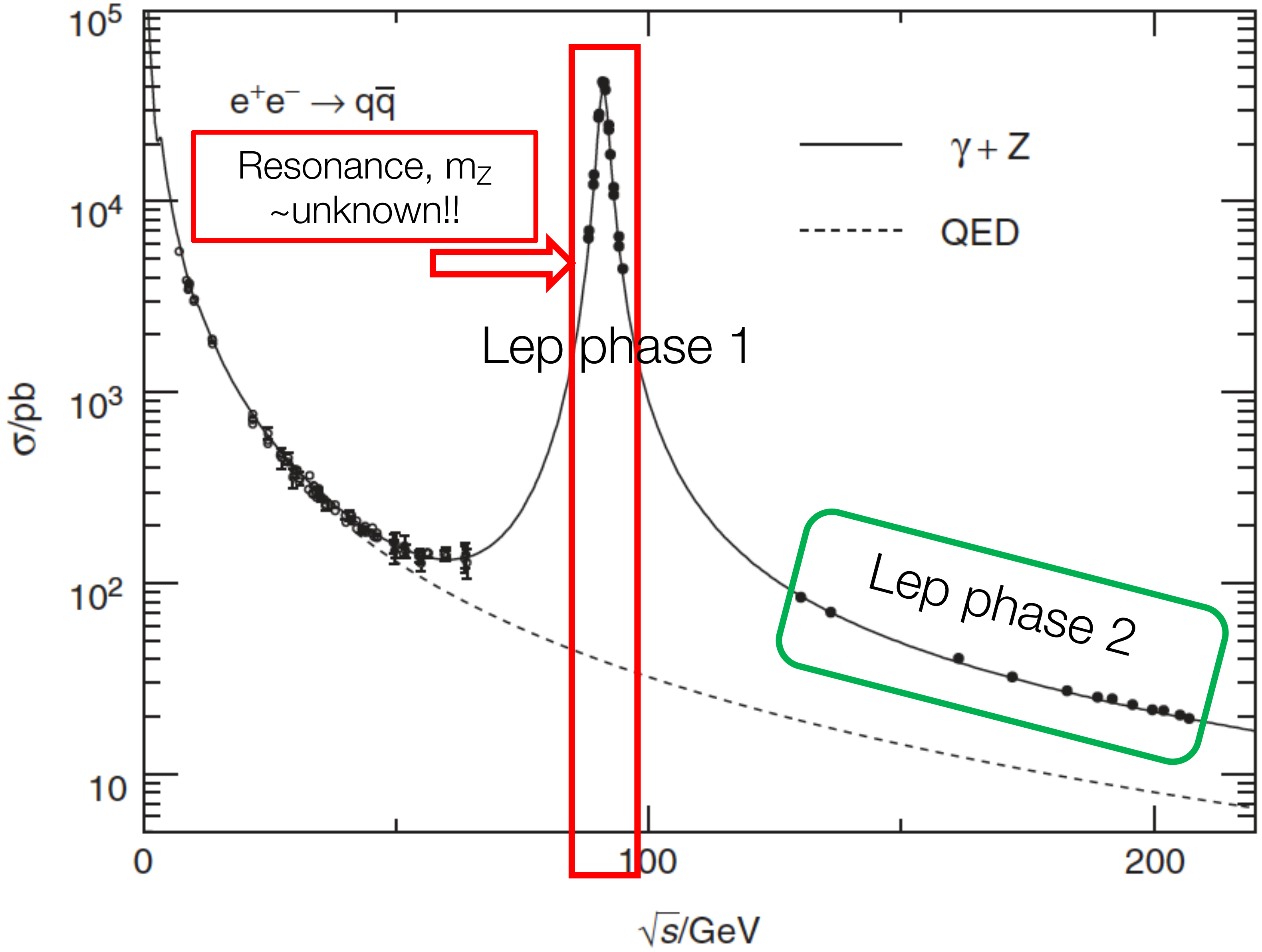

Resonance, m_Z
~unknown!!

Lep phase 1

Lep phase 2

LEP phase 1 : Study the Z
Precision measurement

- The position of energy points optimised to get the best possible determination of m_Z
- Points away from the top are very important to determine the peak position →
- You have to run longer to collect enough statistics!

LEP phase 2 : Search of the Higgs

- Increase energy up to maximum

LEP Data Taking Periods

- 1989 → first Z peak
- 1990 and 1991 “energy scans” ~ one GeV apart.
- In 1992 and 1994 high-statistics at the peak energy.
- In 1993 and 1995 about 1.8 GeV below, above the peak and at the peak.

LEP Phase 1 → Z mass (& first quest for the Higgs)

Year	Centre-of-mass energy range [GeV]	Integrated luminosity [pb^{-1}]
1989	88.2 – 94.2	1.7
1990	88.2 – 94.2	8.6
1991	88.5 – 93.7	18.9
1992	91.3	28.6
1993	89.4, 91.2, 93.0	40.0
1994	91.2	64.5
1995	89.4, 91.3, 93.0	39.8

Energy Scans

Peak Energy

About 17 million Z decays recorded by the four experiments.

LEP Phase 2 → W properties (& quest for the Higgs)

Period	Energy (GeV)	Luminosity (pb^{-1})
1995	130/136	6.2
1996	161	12.1
1996	172	11.3
1997	183	63.8
1998	189	196.4
1999	192	30.

LEP Experiments

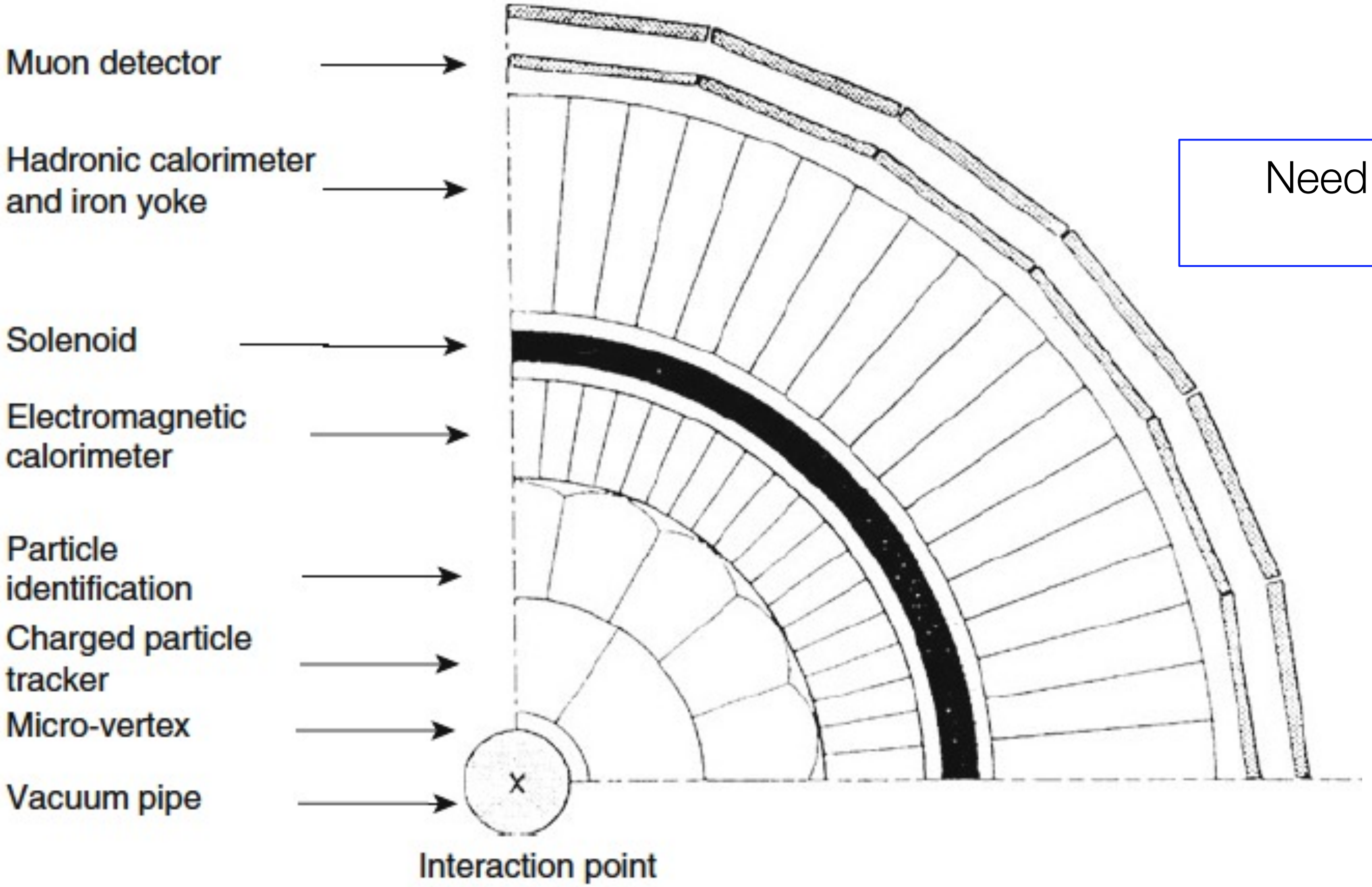

- four large detectors: ALEPH, DELPHI, L3 and OPAL.

Need to rely on multiple measurements (~cost allowed)

- Cylindrical structure, with dimensions of at least 10m in diameter, 10m in length.
- Typical collider experiment: a set of subdetectors, cylindrical structure concentric with the LEP beam.
- The detectors were closed on each side by two end-caps.

x-y view of a typical LEP detector

These multipurpose devices were able to detect, in any direction, any type of particle produced (except neutrinos) at the interaction point. Experiments of this type are sometimes called *4π detectors* because they are able to detect particles emitted in almost the full solid angle.

Toni Baroncelli: Precision Measurements

Cut-View of OPAL

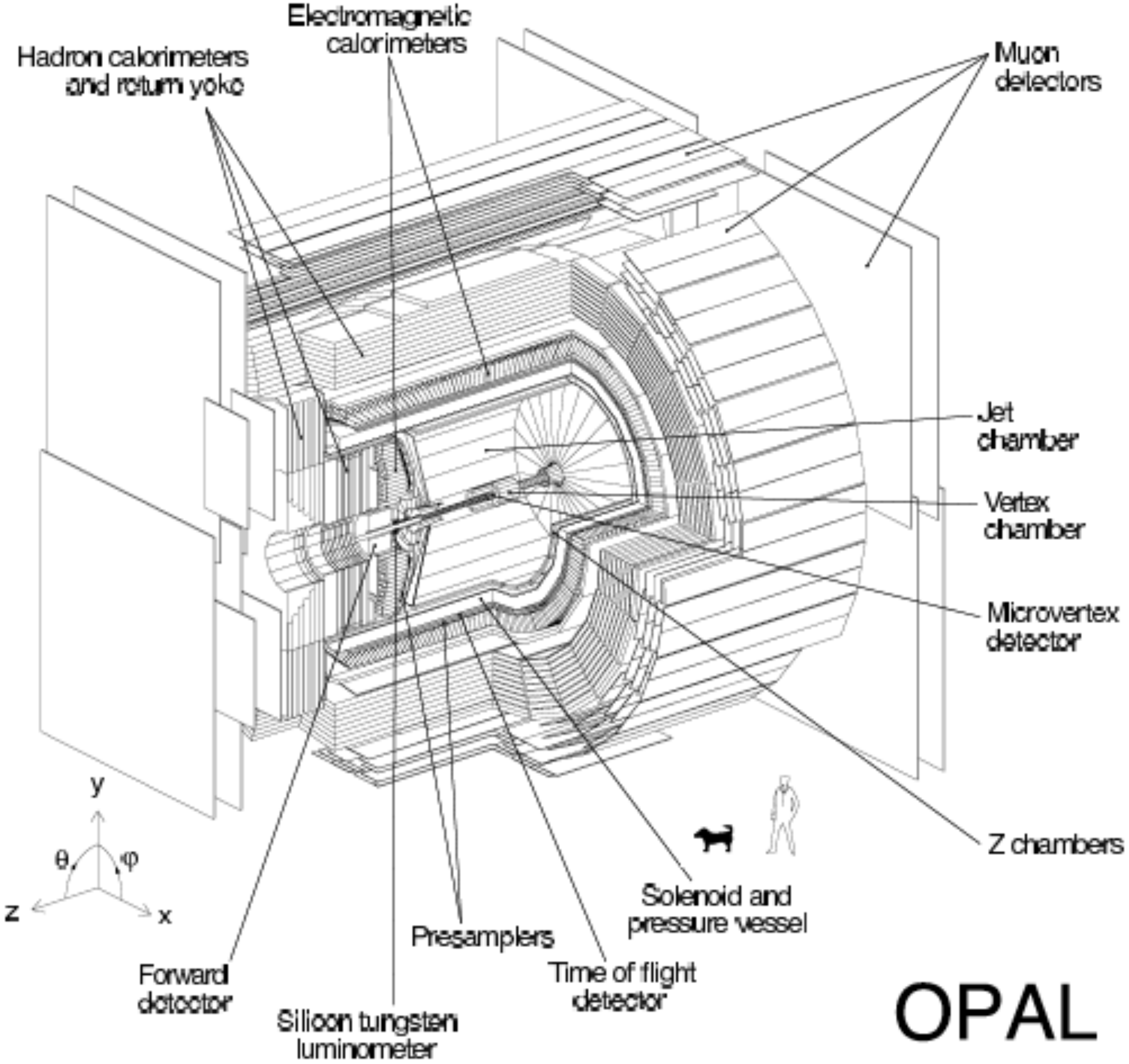

Detectors @ Aleph, DELPHI, L3, Opal

Toni Baroncelli: Precision Measurements

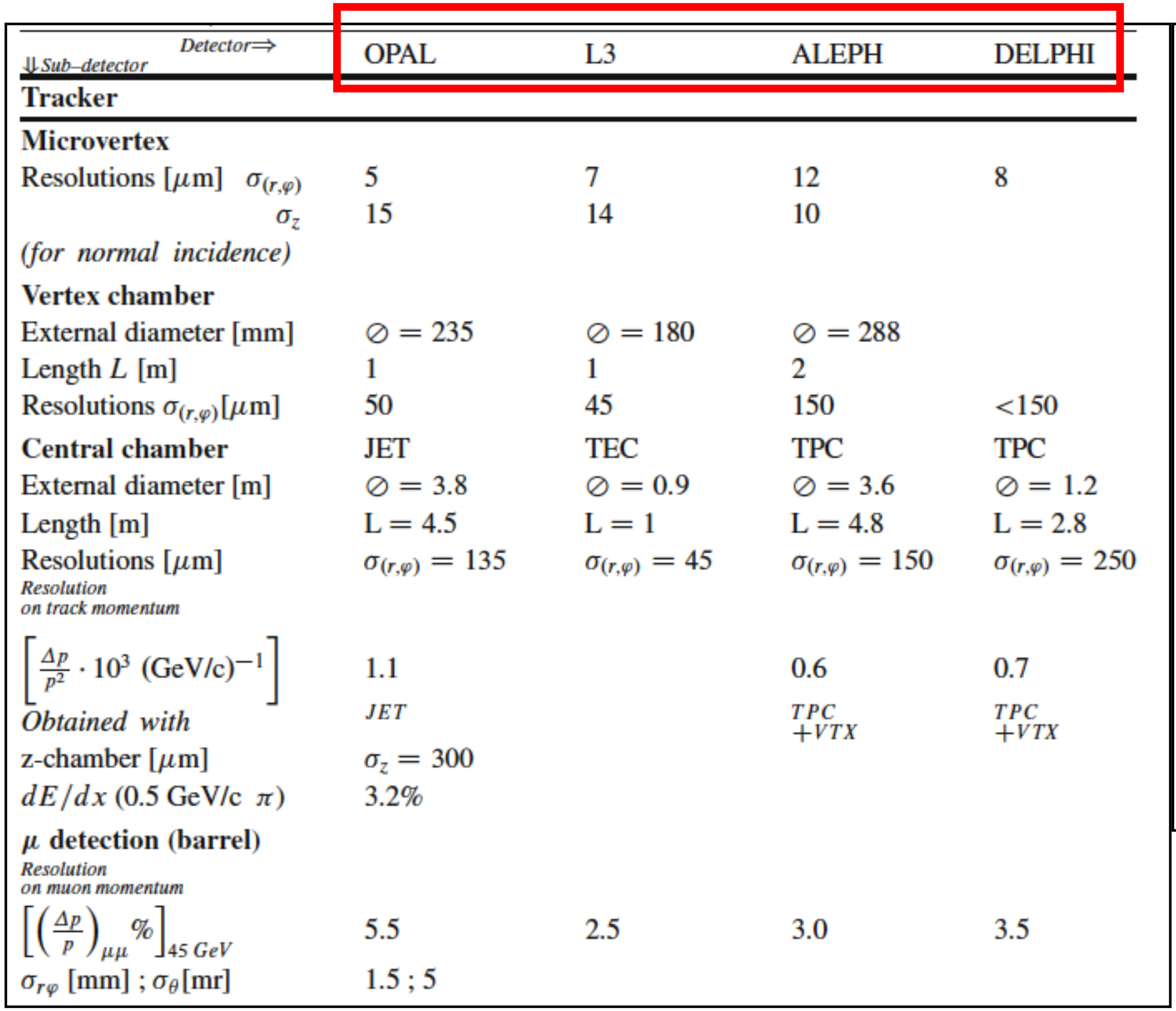

Detector⇒ ⇓Sub–detector	OPAL	L3	ALEPH	DELPHI
Tracker				
Microvertex				
Resolutions [μm] $\sigma_{(r,\varphi)}$	5	7	12	8
σ_z	15	14	10	
(for normal incidence)				
Vertex chamber				
External diameter [mm]	$\oslash = 235$	$\oslash = 180$	$\oslash = 288$	
Length L [m]	1	1	2	
Resolutions $\sigma_{(r,\varphi)}$[μm]	50	45	150	<150
Central chamber	JET	TEC	TPC	TPC
External diameter [m]	$\oslash = 3.8$	$\oslash = 0.9$	$\oslash = 3.6$	$\oslash = 1.2$
Length [m]	L = 4.5	L = 1	L = 4.8	L = 2.8
Resolutions [μm]	$\sigma_{(r,\varphi)} = 135$	$\sigma_{(r,\varphi)} = 45$	$\sigma_{(r,\varphi)} = 150$	$\sigma_{(r,\varphi)} = 250$
Resolution on track momentum				
$\left[\frac{\Delta p}{p^2} \cdot 10^3\ (\mathrm{GeV/c})^{-1}\right]$	1.1		0.6	0.7
Obtained with	*JET*		*TPC +VTX*	*TPC +VTX*
z-chamber [μm]	$\sigma_z = 300$			
dE/dx (0.5 GeV/c π)	3.2%			
μ detection (barrel)				
Resolution on muon momentum				
$\left[\left(\frac{\Delta p}{p}\right)_{\mu\mu} \%\right]_{45\ GeV}$	5.5	2.5	3.0	3.5
$\sigma_{r\varphi}$ [mm] ; σ_θ[mr]	1.5 ; 5			

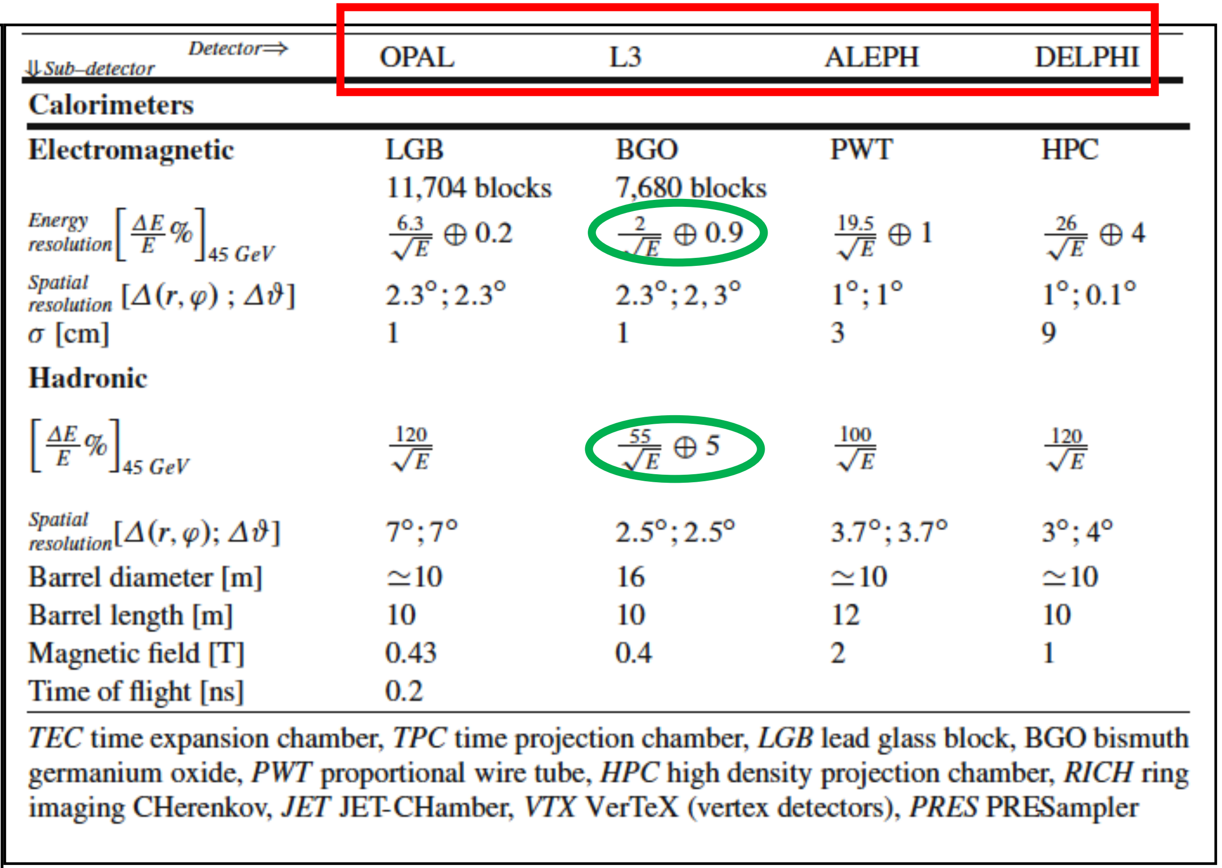

Detector⇒ ⇓Sub–detector	OPAL	L3	ALEPH	DELPHI
Calorimeters				
Electromagnetic	LGB	BGO	PWT	HPC
	11,704 blocks	7,680 blocks		
Energy resolution $\left[\frac{\Delta E}{E}\%\right]_{45\ GeV}$	$\frac{6.3}{\sqrt{E}} \oplus 0.2$	$\frac{2}{\sqrt{E}} \oplus 0.9$	$\frac{19.5}{\sqrt{E}} \oplus 1$	$\frac{26}{\sqrt{E}} \oplus 4$
Spatial resolution $[\Delta(r,\varphi)\ ;\ \Delta\vartheta]$	2.3°; 2.3°	2.3°; 2, 3°	1°; 1°	1°; 0.1°
σ [cm]	1	1	3	9
Hadronic				
$\left[\frac{\Delta E}{E}\%\right]_{45\ GeV}$	$\frac{120}{\sqrt{E}}$	$\frac{55}{\sqrt{E}} \oplus 5$	$\frac{100}{\sqrt{E}}$	$\frac{120}{\sqrt{E}}$
Spatial resolution $[\Delta(r,\varphi);\ \Delta\vartheta]$	7°; 7°	2.5°; 2.5°	3.7°; 3.7°	3°; 4°
Barrel diameter [m]	$\simeq$10	16	$\simeq$10	$\simeq$10
Barrel length [m]	10	10	12	10
Magnetic field [T]	0.43	0.4	2	1
Time of flight [ns]	0.2			

TEC time expansion chamber, *TPC* time projection chamber, *LGB* lead glass block, BGO bismuth germanium oxide, *PWT* proportional wire tube, *HPC* high density projection chamber, *RICH* ring imaging CHerenkov, *JET* JET-CHamber, *VTX* VerTeX (vertex detectors), *PRES* PRESampler

The main features of the four LEP detectors are summarized in the Table above

Physics at LEP

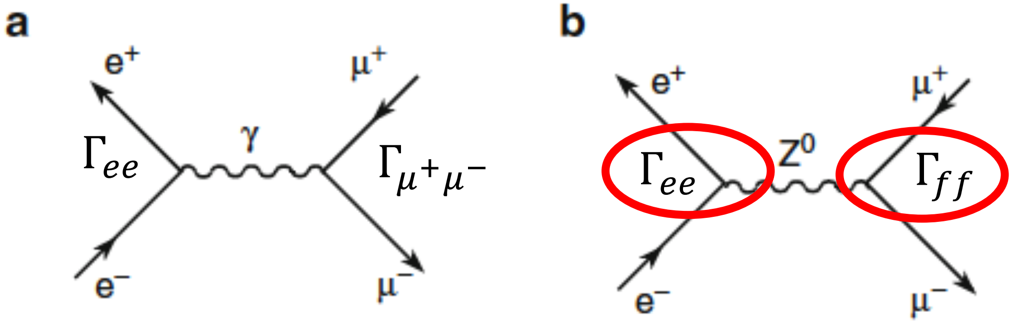

Diagrams at LEP:

- Photon exchange (a); dominant below m_Z, ~ 1/s
- Z exchange (b), dominant @cms = m_Z

The example for $e^+e^- \to \mu^+\mu^-$ but the same diagrams works for all $f\bar{f}$ final states.

At the “Z peak”, “real” (on mass shell) Z are produced → the Z boson is produced such that $E^2 - p^2 = m_Z^2$.

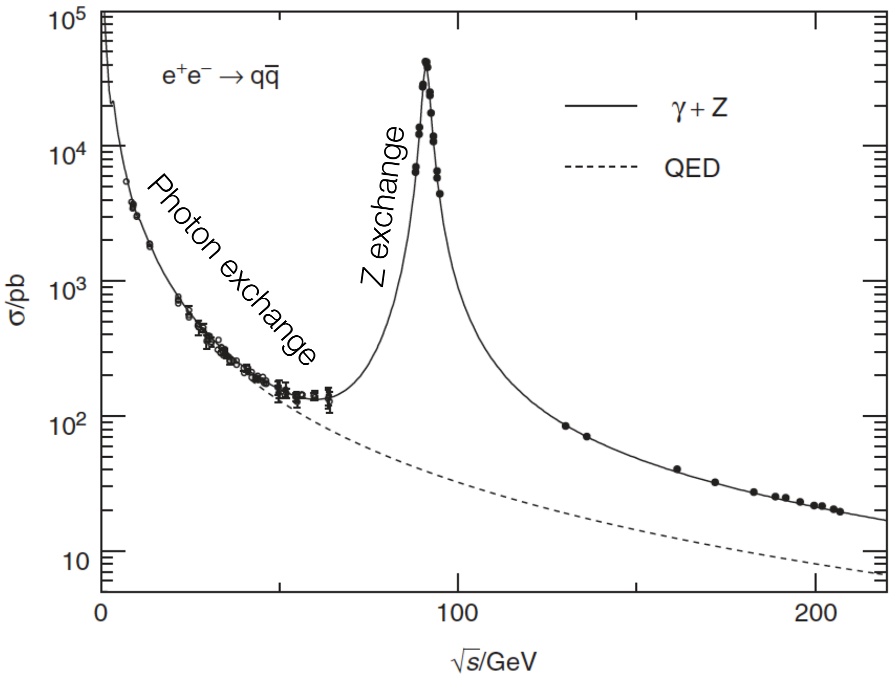

$$\sigma_{el}(E;J) = 4\pi\bar{\lambda}^2\frac{(2J+1)}{(2s_a+1)(2s_b+1)}\left[\frac{\Gamma^2/4}{(E_R-E)^2+\Gamma^2/4}\right].$$

⇧

$e^+e^- \to e^+e^-$

J=1, s_1=s_2=1/2,

the de Broglie wavelength $\lambda = \frac{\hbar}{p}$ (me~0. $p \to \sqrt{s}$). → $\hbar/(\sqrt{s}/2)$

$$\sigma_{el}(E;J) \to \sigma(s)$$
$$\Gamma^2 \to \Gamma_{ee}\cdot\Gamma_{ff}$$

$e^+e^- \to q\bar{q}$

$$\sigma(s) = \frac{4\pi}{(s/4)}\,\frac{3}{4}\left[\frac{\Gamma_{ee}\Gamma_{ff}/4}{(\sqrt{s}-m_Z)^2+\Gamma_Z^2/4}\right] = \frac{12\pi}{m_Z^2}\,s\,\frac{\Gamma_{ee}\Gamma_{ff}}{(s-m_Z^2)^2+s^2\Gamma_Z^2/m_Z^2}$$

Cross Section at the Z

$$\sigma(s) = \frac{4\pi}{(s/4)}\,\frac{3}{4}\left[\frac{\Gamma_{ee}\Gamma_{ff}/4}{(\sqrt{s}-m_Z)^2+\Gamma_Z^2/4}\right] = \frac{12\pi}{m_Z^2}\,s\,\frac{\Gamma_{ee}\Gamma_{ff}}{(s-m_Z^2)^2+s^2\Gamma_Z^2/m_Z^2}$$

at $s = m_Z^2$

$$\sigma^0 \equiv \sigma(s = m_Z^2) = \frac{12\pi}{m_Z^2}\,\frac{\Gamma_{ee}\Gamma_{ff}}{\Gamma_Z^2}.$$

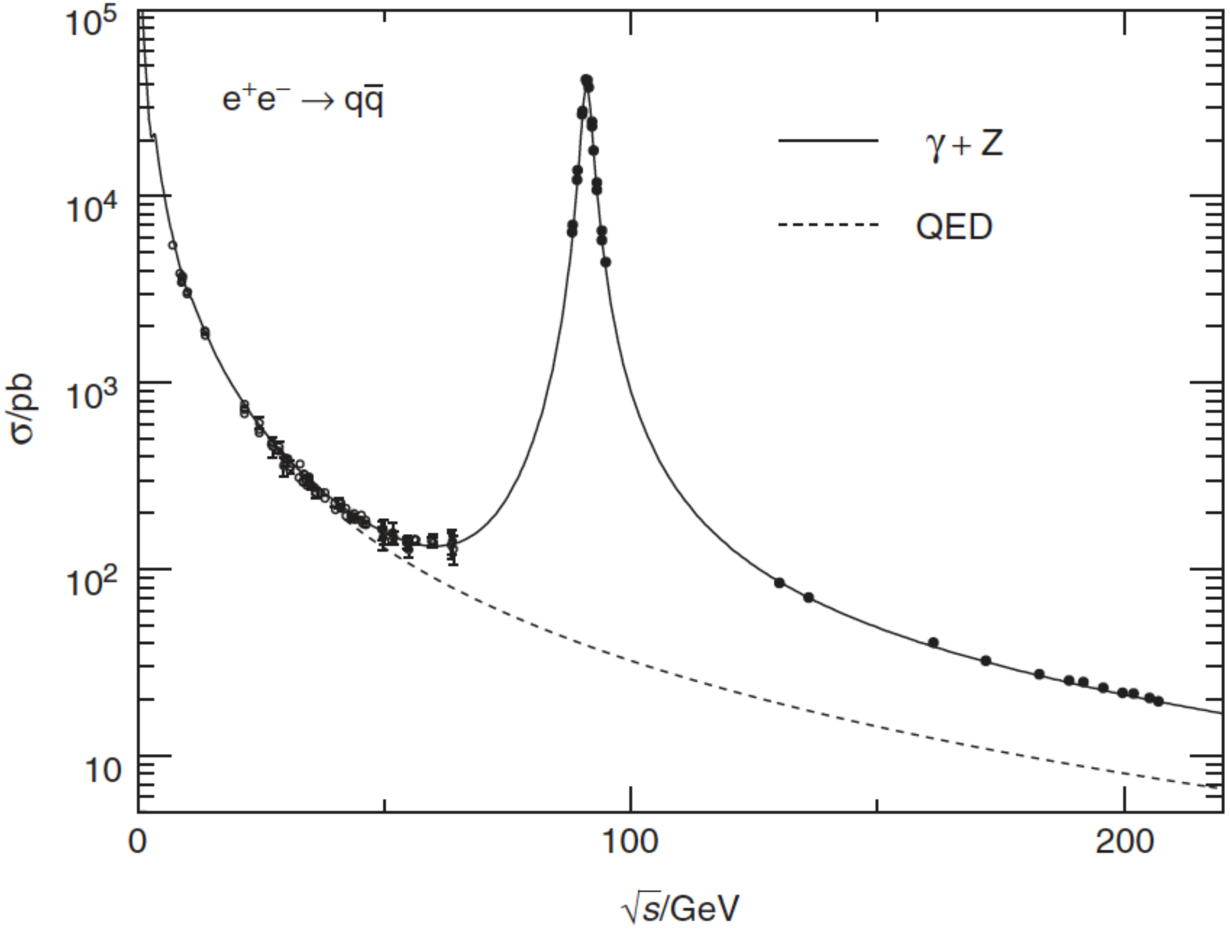

Number of events collected by the 4 LEP experiments at LEP phase 1 in units 10^3

- 4 millions of Z hadronic decays per experiment
- ~ half million of Z leptonic decays

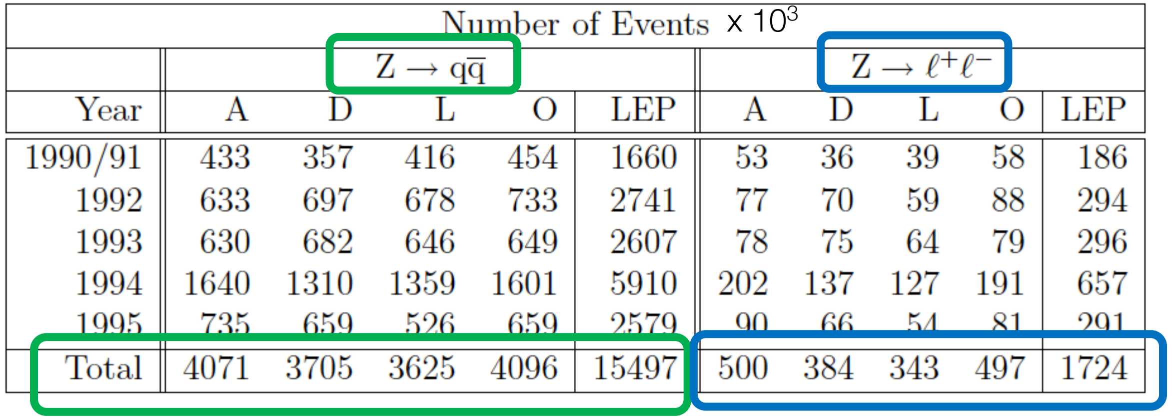

Number of Events x 10^3										
	$Z \to q\bar{q}$					$Z \to \ell^+\ell^-$				
Year	A	D	L	O	LEP	A	D	L	O	LEP
1990/91	433	357	416	454	1660	53	36	39	58	186
1992	633	697	678	733	2741	77	70	59	88	294
1993	630	682	646	649	2607	78	75	64	79	296
1994	1640	1310	1359	1601	5910	202	137	127	191	657
1995	735	659	526	659	2579	90	66	54	81	291
Total	4071	3705	3625	4096	15497	500	384	343	497	1724

The Z Width, Γ_{ff}

Γ_Z is determined by the number of species of kinematically accessible (with a mass < $m_Z/2$)
All species with weak interactions contribute to Γ_Z.

$$\Gamma = \frac{\hbar}{\tau}$$

$$BR(\rightarrow xy) = \frac{\Gamma_{xy}}{\Gamma}$$

Decay fractions of the Z to different pairs of fermions → predicted by the SM

- leptons do not have a color multiplicity $N_c^f = 1$
- each quark has three degrees of freedom (one for each color quantum number) $N_c^f = 3$
- SM: an axial and a vector part.

The partial width Γ_{ff} represents the transition probability per time unit for the Z boson decay to a given final state $f\bar{f}$.

$$\Gamma_{ff} = \frac{G_F m_Z^3}{6\sqrt{2}\pi}(a_f^2 + v_f^2)N_C^f = 330(a_f^2 + v_f^2)N_C^f \text{ MeV}$$

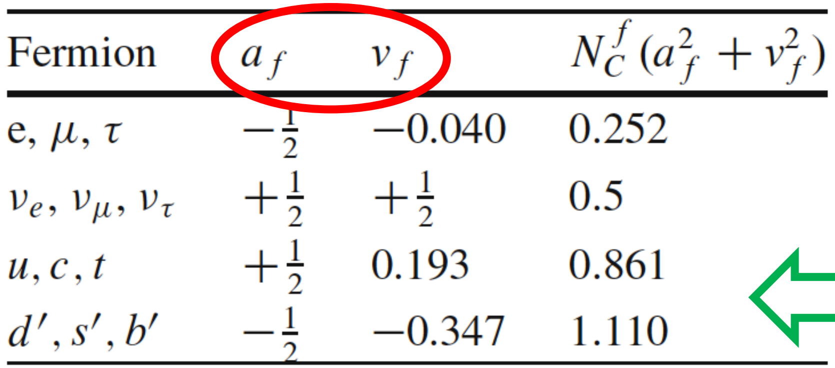

Fermion	a_f	v_f	$N_C^f(a_f^2 + v_f^2)$
e, μ, τ	$-\frac{1}{2}$	-0.040	0.252
ν_e, ν_μ, ν_τ	$+\frac{1}{2}$	$+\frac{1}{2}$	0.5
u, c, t	$+\frac{1}{2}$	0.193	0.861
d', s', b'	$-\frac{1}{2}$	-0.347	1.110

Measurements

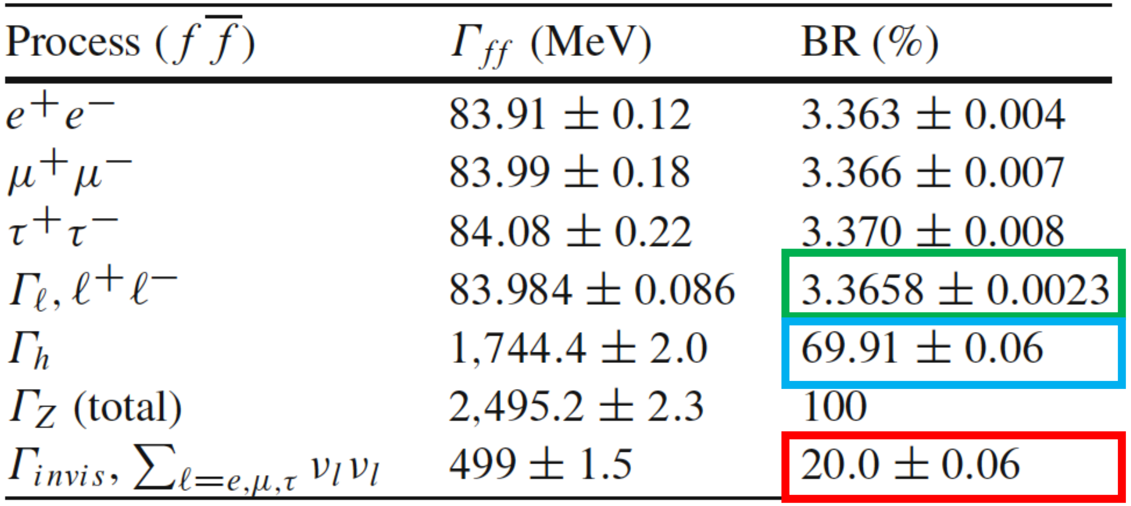

Process ($f\bar{f}$)	Γ_{ff} (MeV)	BR (%)
e^+e^-	83.91 ± 0.12	3.363 ± 0.004
$\mu^+\mu^-$	83.99 ± 0.18	3.366 ± 0.007
$\tau^+\tau^-$	84.08 ± 0.22	3.370 ± 0.008
$\Gamma_\ell, \ell^+\ell^-$	83.984 ± 0.086	3.3658 ± 0.0023
Γ_h	$1{,}744.4 \pm 2.0$	69.91 ± 0.06
Γ_Z (total)	$2{,}495.2 \pm 2.3$	100
$\Gamma_{invis}, \sum_{\ell=e,\mu,\tau} \nu_l \nu_l$	499 ± 1.5	20.0 ± 0.06

Topologies at LEP

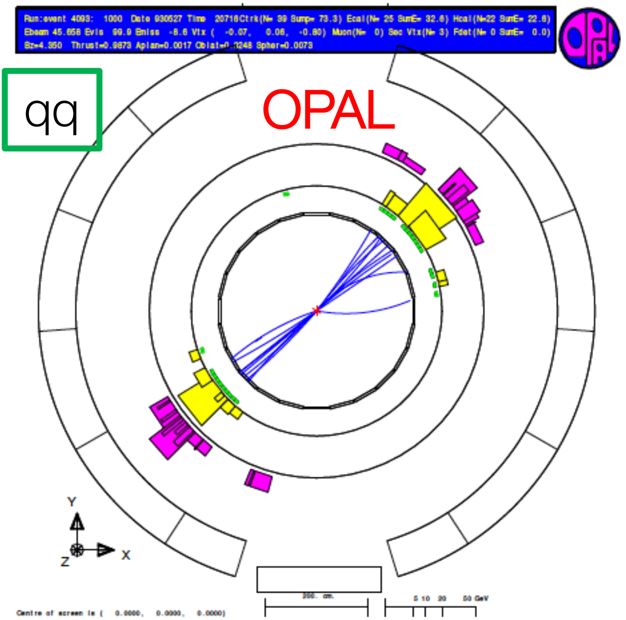

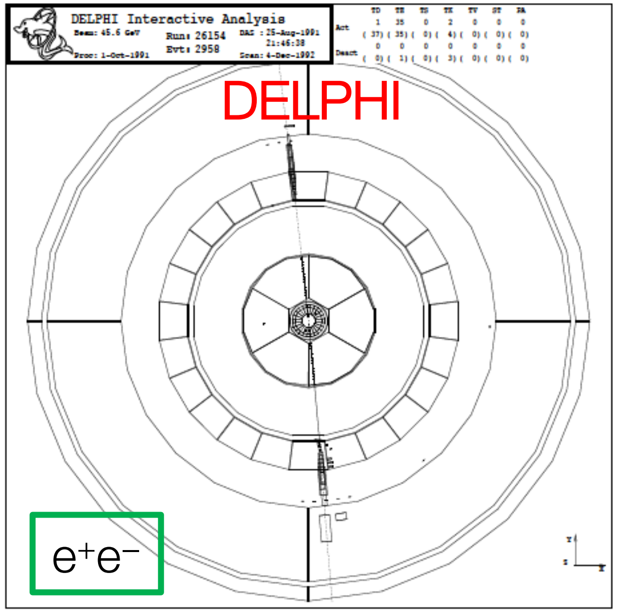

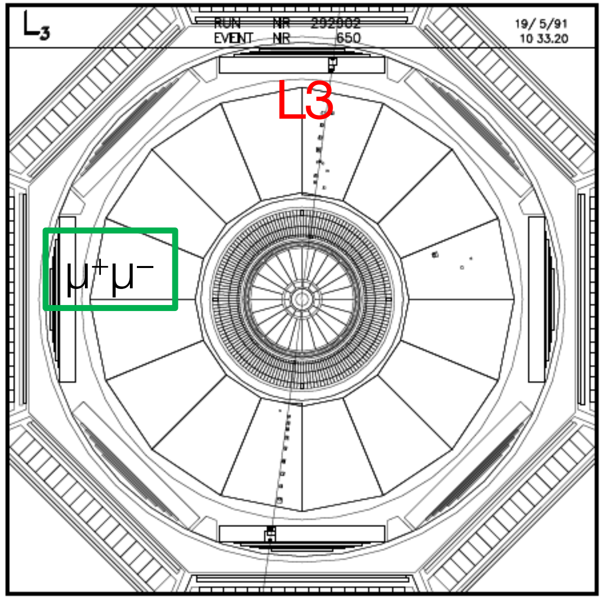

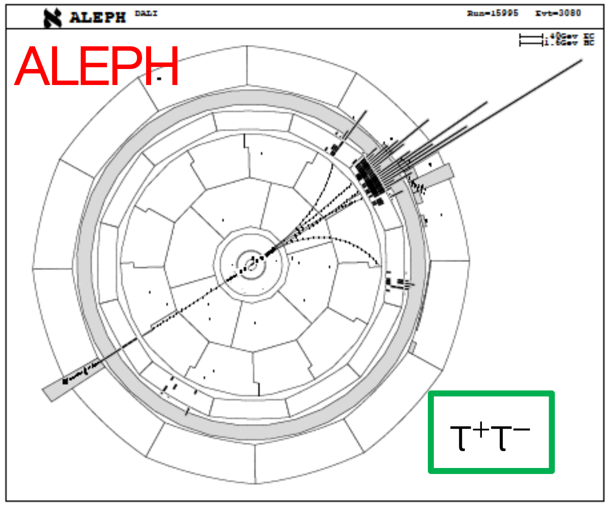

At LEP the kinematics is completely determined by the fact electrons and positrons are point-like particles: no PDF!
→ 4 conservation laws can be used: p_x, p_y, p_z, E_{tot}
Pairs of $f\bar{f}$ are back to back in all views

If you have a species on one side
→ anti-species on the opposite

Reaction	$q\bar{q}$	e^+e^-	$\mu^+\mu^-$	$\tau^+\tau^-$
Topology	2 jets	Two em showers	Two penetrating particles	Two narrow jets

Topologies in ALEPH

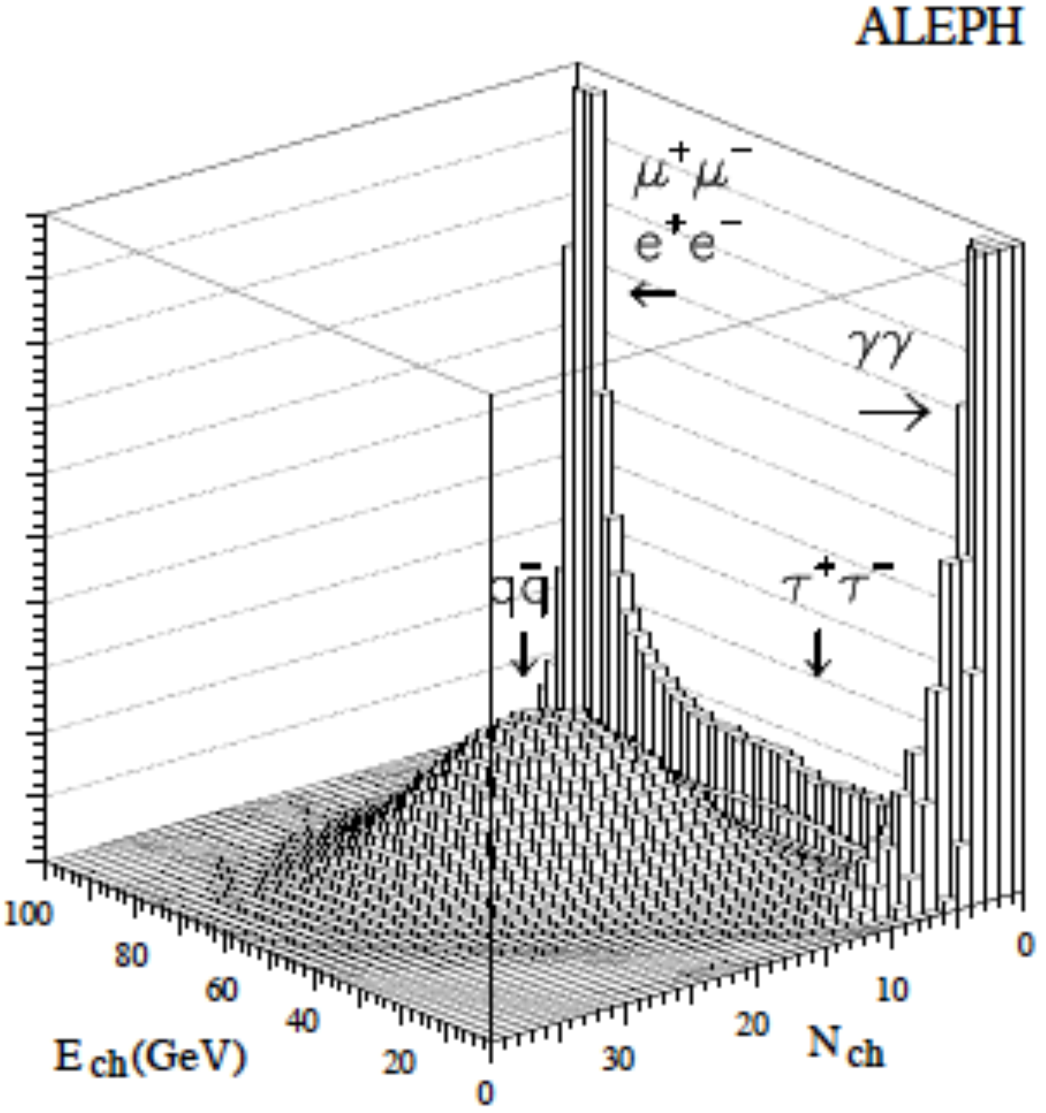

Example: final states distinguished with two variables

- the sum of the track momenta, E_{ch}
- and the track multiplicity, N_{ch}, (ALEPH experiment)

Reaction	$q\bar{q}$	e^+e^-	$\mu^+\mu^-$	$\tau^+\tau^-$
E_{ch}	2 jets → medium to large energy	Two em showers → large energy $\sim 2 \cdot E_{beam}$	Two penetrating particles $\sim 2 \cdot E_{beam}$	Two narrow jets → medium to large energy
N_{ch}	~large	2	2	~few

The Z Scan and Γ_{ff}

$$\sigma(s) = \frac{4\pi}{(s/4)}\,\frac{3}{4}\left[\frac{\Gamma_{ee}\Gamma_{ff}/4}{(\sqrt{s}-m_Z)^2+\Gamma_Z^2/4}\right] = \frac{12\pi}{m_Z^2}\,s\,\frac{\Gamma_{ee}\Gamma_{ff}}{(s-m_Z^2)^2+s^2\Gamma_Z^2/m_Z^2}$$

$\Gamma_Z = total\ Z\ width$

One sees that the cross section falls to half of its peak value at

$$\sqrt{s} = m_Z + \frac{\Gamma_Z}{2}$$

→ Γ_Z total decay rate of the Z boson and also the full-width half-maximum (FWHM) of the cross section vs E_{cms}

→ The mass and Γ_Z of the Z boson can be determined from a 'scan' of the cross-section

$$e^+e^- \rightarrow Z \rightarrow f\bar{f}$$

→ Once m_Z and Γ_Z are known, the measured value of the peak cross-section for a particular final-state $\sigma^0_{f\bar{f}}$ is given by the formula

$$\Gamma_{ee}\Gamma_{ff} = \frac{\sigma^0_{ff}\Gamma_Z^2 m_Z^2}{12\pi}.$$

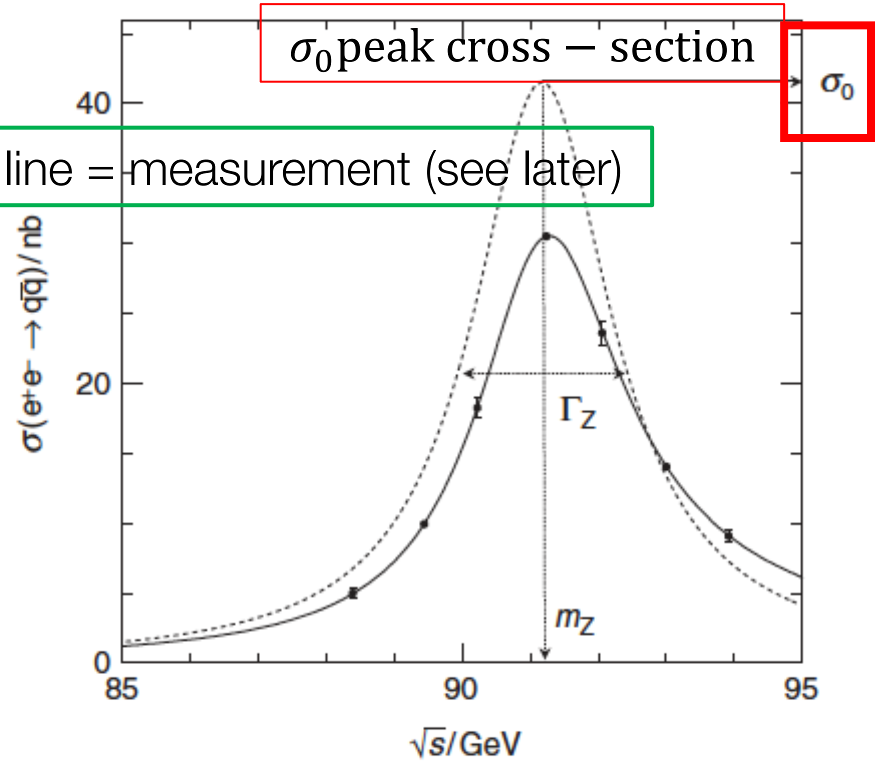

$\sigma_0$peak cross − section

Solid line = measurement (see later)

Initial State Radiation ISR

LEP: the mass and width of the Z boson measured with a ‘scan’ of the cross section → Breit–Wigner resonance

$$e^+e^- \rightarrow Z \rightarrow f\bar{f}$$

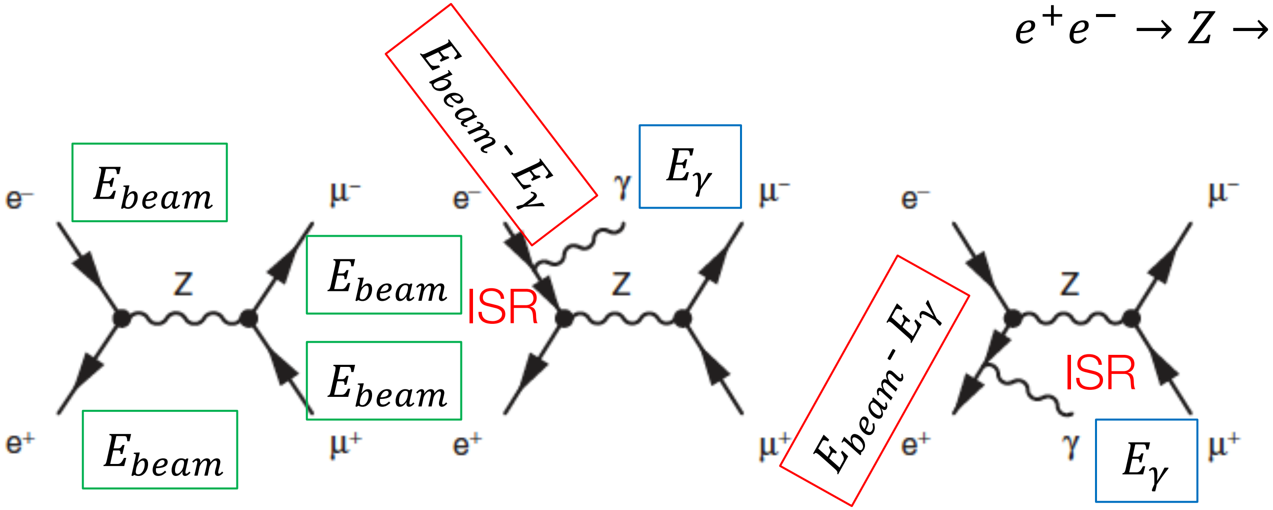

In practice, this is more complicated. Two higher-order QED diagrams where a photon is radiated from either the initial-state electron or positron, distort the shape of the Z resonance curve

ISR photon with energy E_γ is radiated → at the Z production vertex

$$p_1 = \left(E_{beam} - E_\gamma, 0{,}0, E_{beam} - E_\gamma\right), p_2 = (E_{beam}, 0{,}0, -E_{beam})$$

→ The effective centre-of-mass energy squared at vertex s’ = q^2_Z, given by the square of the sum of four-momenta of the e+ and e– after ISR

$$s' = q_Z^2 = (p_1 + p_2)^2 = (2 \cdot E_{beam} - E_\gamma)^2 - E_\gamma^2 = 4 \cdot E_{beam}^2 \cdot \left(1 - E_\gamma / E_{beam}\right) = \boxed{s \cdot \left(1 - E_\gamma / E_{beam}\right)}$$

Distorsion of the Z-Line-Shape

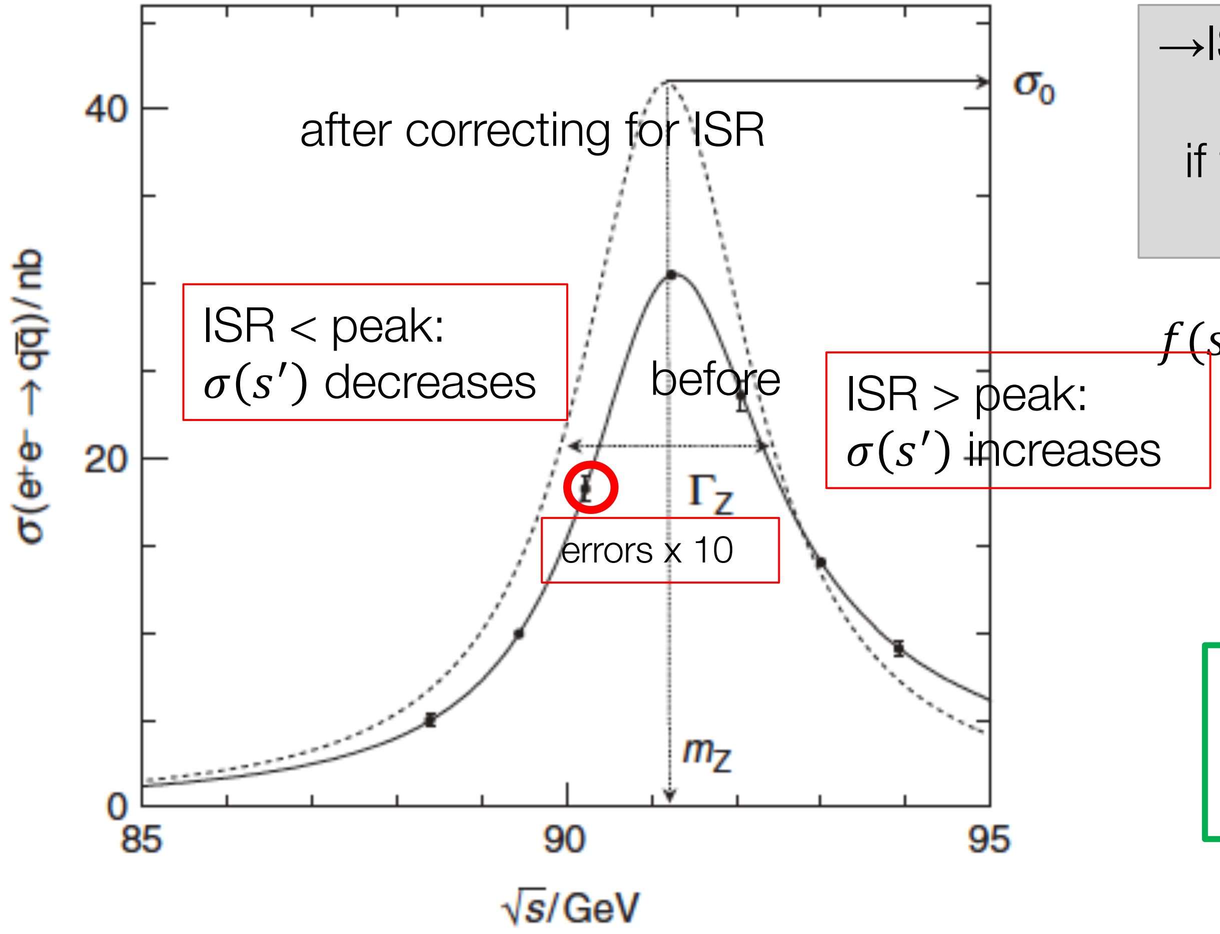

after correcting for ISR

before

ISR < peak: $\sigma(s')$ decreases

ISR > peak: $\sigma(s')$ increases

errors x 10

→ISR reduces

s to s'

if the accelerator runs at $s = m_Z$ a fraction of the Z bosons are produced $q_Z^2 < m_Z^2$

$f(s,s')$ probability that $s \rightarrow s'$ .The measured cross section

$$\sigma_{measured}(s) = \int \sigma(s') f(s,s') ds'$$

ISR is a QED process → $f(s,s')$ can be calculated to high precision. $\sigma_{measured}(s)$ can be corrected back to the Breit–Wigner distribution with 'no ISR'.

- $e^+e^- \rightarrow Z \rightarrow q\bar{q}$
- Solid line Breit–Wigner distribution with ISR.
- Dotted line Breit–Wigner distribution with no ISR

The Invisible Width (neutrino families!)

$$\Gamma_{ff} = \frac{G_F m_Z^3}{6\sqrt{2}\pi}\boxed{(a_f^2 + v_f^2)}N_C^f = 330(a_f^2 + v_f^2)N_C^f \text{ MeV}$$

Fermion	a_f	v_f	$N_C^f(a_f^2 + v_f^2)$
e, μ, τ	$-\frac{1}{2}$	-0.040	0.252
ν_e, ν_μ, ν_τ	$+\frac{1}{2}$	$+\frac{1}{2}$	0.5
u, c, t	$+\frac{1}{2}$	0.193	0.861
d', s', b'	$-\frac{1}{2}$	-0.347	1.110

What discussed already

Process ($f\overline{f}$)	Γ_{ff} (MeV)	BR (%)
e^+e^-	83.91 ± 0.12	3.363 ± 0.004
$\mu^+\mu^-$	83.99 ± 0.18	3.366 ± 0.007
$\tau^+\tau^-$	84.08 ± 0.22	3.370 ± 0.008
$\Gamma_\ell, \ell^+\ell^-$	83.984 ± 0.086	3.3658 ± 0.0023
Γ_h	$1{,}744.4 \pm 2.0$	69.91 ± 0.06
Γ_Z (total)	$2{,}495.2 \pm 2.3$	100
$\Gamma_{invis}, \sum_{\ell=e,\mu,\tau} \nu_l \nu_l$	499 ± 1.5	20.0 ± 0.06

Measurements

The hadronic width Γ_h = sum of partial widths of $q\bar{q}$ pairs ***kinematically accessible*** (top quark too heavy!)

$$\Gamma_h = \Gamma_{uu} + \Gamma_{dd} + \Gamma_{ss} + \Gamma_{cc} + \Gamma_{bb}$$

The leptonic widths ($\Gamma_{ee}, \Gamma_{\mu\mu}, \Gamma_{\tau\tau}$ *and* $\Gamma_{\nu\nu}$) include also the ‘invisible width Γ_{invis} carried by all N_ν neutrinos (we expect $N_\nu = 3$). Assuming lepton universality (all neutrinos behave the same!)

$$\boxed{\Gamma_{invis} = N_\nu \cdot \Gamma_{\nu\nu}}$$

The Number of (ν) Families

Cannot measure Γ_{invis} → is derived by subtracting all ***visible*** widths from Γ_Z (if there was a neutrino with $m_\nu > \frac{m_Z}{2}$ → it would not contribute)

$$\Gamma_{\mathrm{invis}} = \Gamma_{\mathrm{Z}} - \Gamma_{\mathrm{h}} - \Gamma_{\mathrm{ee}} - \Gamma_{\mu\mu} - \Gamma_{\tau\tau} \rightarrow \boxed{\Gamma_{\mathrm{invis}} = \Gamma_{\mathrm{Z}} - \Gamma_{\mathrm{h}} - 3 * \Gamma_{\mathrm{ll}}}$$

Strategy:

$$assuming\ \Gamma_{\mathrm{ll}} = \Gamma_{\mathrm{ee}} = \Gamma_{\mu\mu} = \Gamma_{\tau\tau}$$

- Identify Z decays topologies
- the largest cross section that can be measured at the peak of the Z (and the one statistically better defined) is the one into hadrons

$$\sigma^0_{had} = \frac{12\pi\Gamma_{ee}\Gamma_h}{m_Z^2\Gamma_Z^2} \rightarrow \boxed{\Gamma_Z} = \sqrt{\frac{12\pi\Gamma_{ee}\Gamma_h}{m_Z^2\sigma^0_{had}}}$$

$$\boxed{\text{Define } R^0_l = \Gamma_h/\Gamma_{ll}} \quad \boxed{\Gamma_{ee}/\Gamma_{ll} = 1}$$

$$\boxed{\Gamma_Z/\Gamma_{ll} = \sqrt{\frac{12\pi\Gamma_{ee}\Gamma_h}{m_Z^2\sigma^0_{had}\Gamma^2_{ll}}} = \sqrt{\frac{12\pi R^0_l}{m_Z^2\sigma^0_{had}}}}$$

- One additional family with light members, would determine a larger Γ_{Z}.
- → a larger Z width (a smaller lifetime) and a $\sigma_0(s) \propto \Gamma_Z^{-2}$
- measure the number of families is based on the ratio (assuming lepton universality)

$$R^0_{invis} = \Gamma_{invis}/\Gamma_{ll}$$

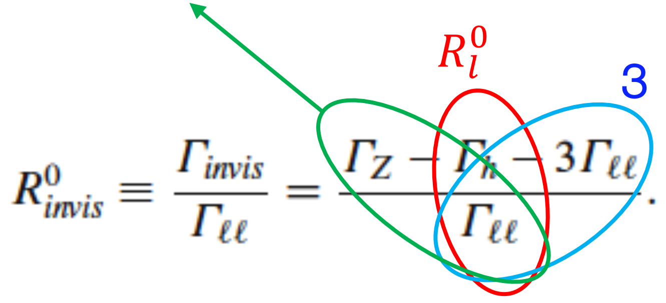

$$R^0_{invis} \equiv \frac{\Gamma_{invis}}{\Gamma_{\ell\ell}} = \frac{\Gamma_Z - \Gamma_h - 3\Gamma_{\ell\ell}}{\Gamma_{\ell\ell}}.$$

Toni Baroncelli: Precision Measurements

The Number of (ν) Families

$$\Gamma_Z/\Gamma_{ll} = \sqrt{\frac{12\pi\Gamma_{ee}\Gamma_h}{m_Z^2\sigma_{had}^0\Gamma_{ll}^2}} = \sqrt{\frac{12\pi R_l^0}{m_Z^2\sigma_{had}^0}}$$

$R^0_{invis} = \sqrt{\frac{12\pi R_l^0}{m_Z^2\sigma_{had}^0}} - R_l^0 - 3$ measured to be 5.943±0.016

$$R^0_{invis} = N_\nu\left(\frac{\Gamma_{\nu\bar{\nu}}}{\Gamma_{ll}}\right)_{SM}$$

$\left(\frac{\Gamma_{\nu\bar{\nu}}}{\Gamma_{ll}}\right)_{SM}$ = 1.99125±0.00083 computed using (*)

$$\boxed{N_\nu = \frac{5.943 \pm 0.016}{1.99125 \pm 0.00083} = 2.984 \pm 0.0082}$$

Combined analysis of 4 LEP experiments using all available statistics

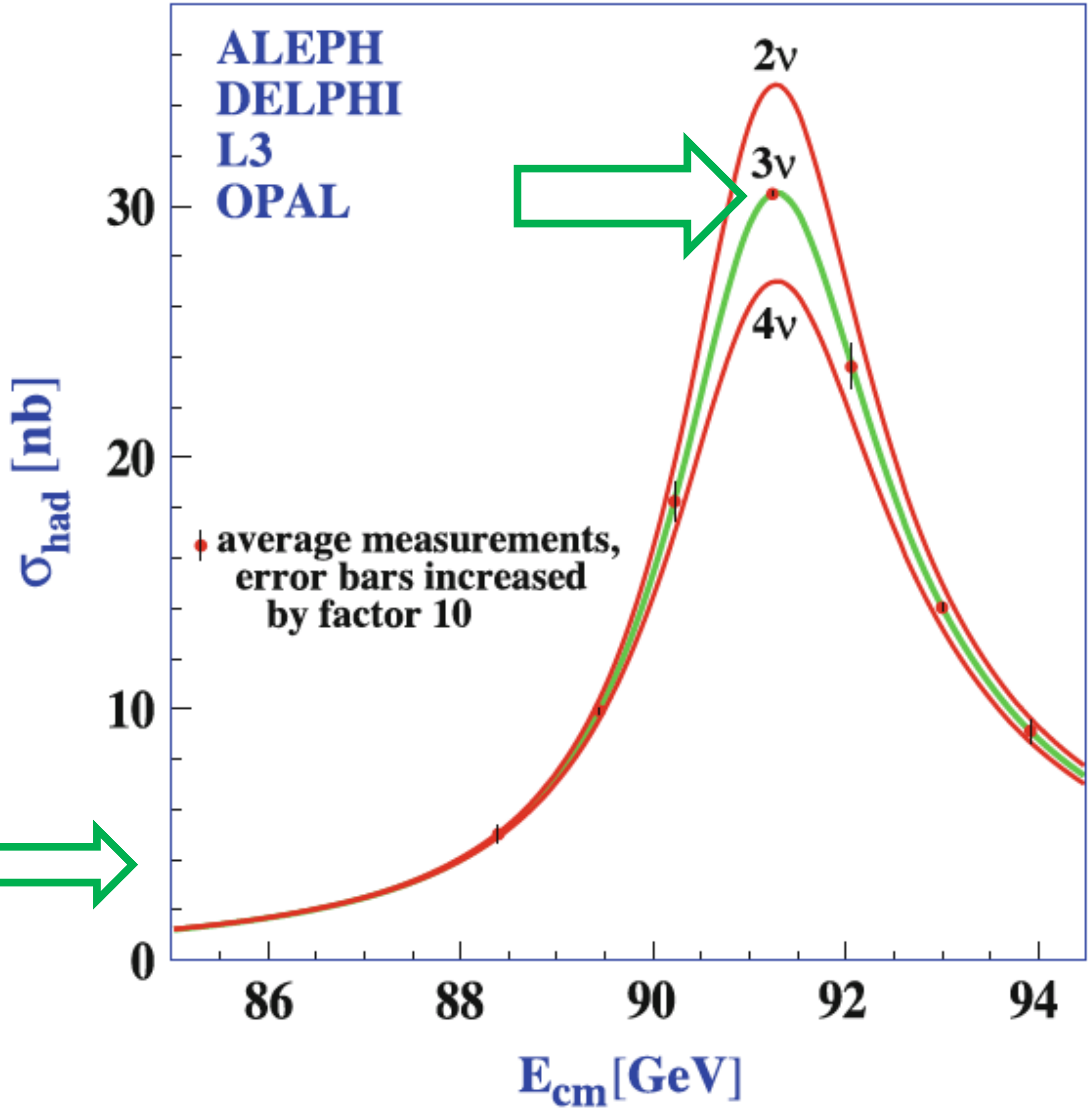

(*) $\Gamma_{ff} = \frac{G_F m_Z^3}{6\sqrt{2}\pi}(a_f^2 + v_f^2)N_C^f = 330(a_f^2 + v_f^2)N_C^f$ MeV

The Forward-Backward Asymmetry A^{μ}_{FB}

There are more complex observables at LEP than cross-sections and widths: forward-backward asymmetry (A_{FB}) measures asymmetries in the polar angle predicted by SM

The asymmetry in the angular distribution of the process

$$e^+e^- \to \gamma/Z \to \mu^+\mu^-$$

is easy to measure:

$$A^{\mu}_{FB} = \frac{N^{\mu}_F - N^{\mu}_B}{N^{\mu}_F + N^{\mu}_B} = \frac{\sigma^{\mu}_F - \sigma^{\mu}_B}{\sigma^{\mu}_F + \sigma^{\mu}_B}$$

- “F (B)” means “forward (backward)”,
- N^{μ}_F (N^{μ}_B) is the number of muons scattered in the forward (backward) hemisphere, with respect to the e beam.
- The corresponding cross-sections $\sigma^{\mu}_F(\sigma^{\mu}_B)$ are the given by

$$\frac{d\ \sigma}{d\ \cos\theta} = \frac{3}{8}\,\sigma^0\left[(1+\cos^2\theta) + 2\ A_e\ A_f \cos\theta\right]$$

Fermion	a_f	v_f	$N_C^f\,(a_f^2 + v_f^2)$
e, μ, τ	$-\frac{1}{2}$	-0.040	0.252
ν_e, ν_μ, ν_τ	$+\frac{1}{2}$	$+\frac{1}{2}$	0.5
u, c, t	$+\frac{1}{2}$	0.193	0.861
d', s', b'	$-\frac{1}{2}$	-0.347	1.110

→ AFB is an observable that establishes a relation between v_f and a_f

$$A_f = \frac{2v_f a_f}{v_f^2 + a_f^2} = 2\frac{v_f/a_f}{1+(v_f/a_f)^2}$$

Asymmetries at the Peak of the Z

At the Z peak of the Z: $A_{FB}^{0,f} = \frac{3}{4} A_e A_f$

- The lepton FB asymmetry is easily measured (tracks well measured, flavour clear!)
- The hadrons FB asymmetry is more difficult: how to distinguish jets from d, u, s, c, b? Only c and b induced jets can be identified using secondary jets (heavy flavours decays)

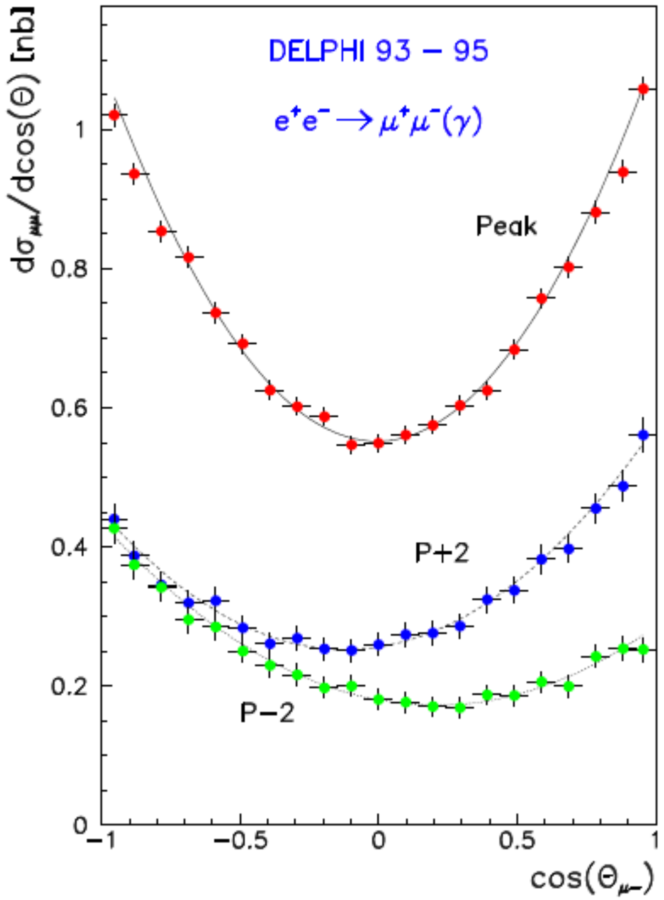

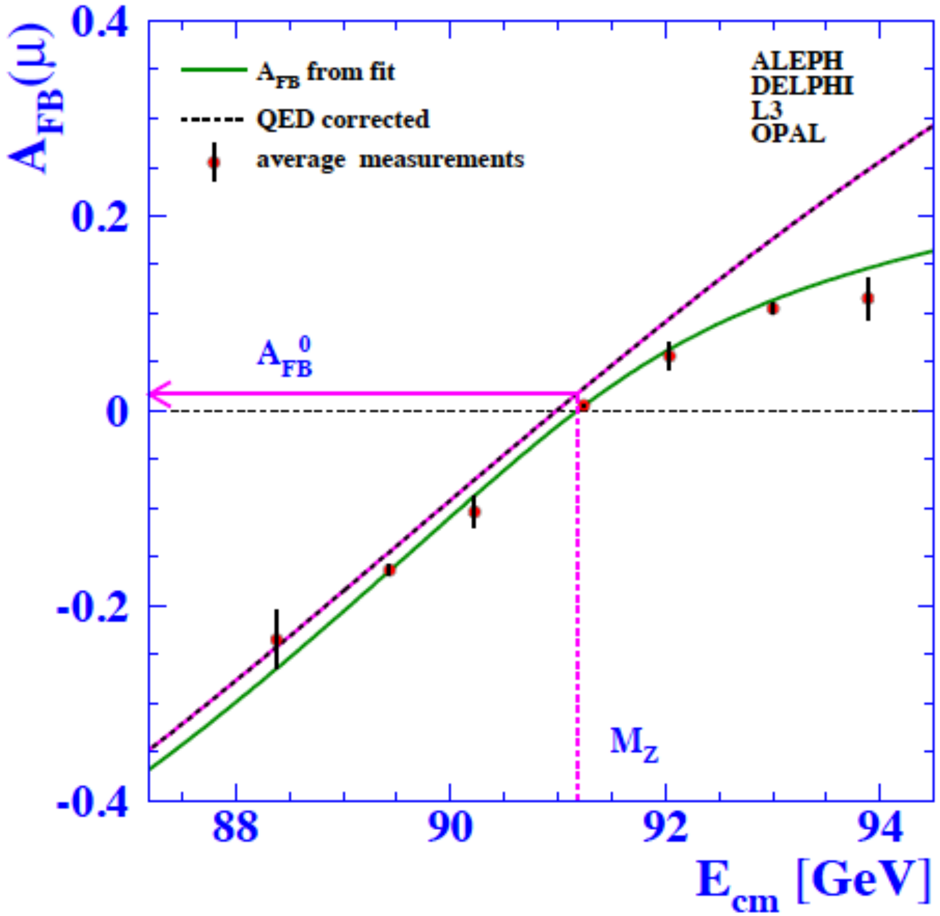

- A_{FB} has an energy dependence due to the different energy dependence of the
    - γ component,
    - the Z component and
    - the interference between the two cross-sections
- A_{FB} has a detector-related 'complication': it depends on the efficiency and acceptance. These have a direct impact on the observable

Measurements at LEP

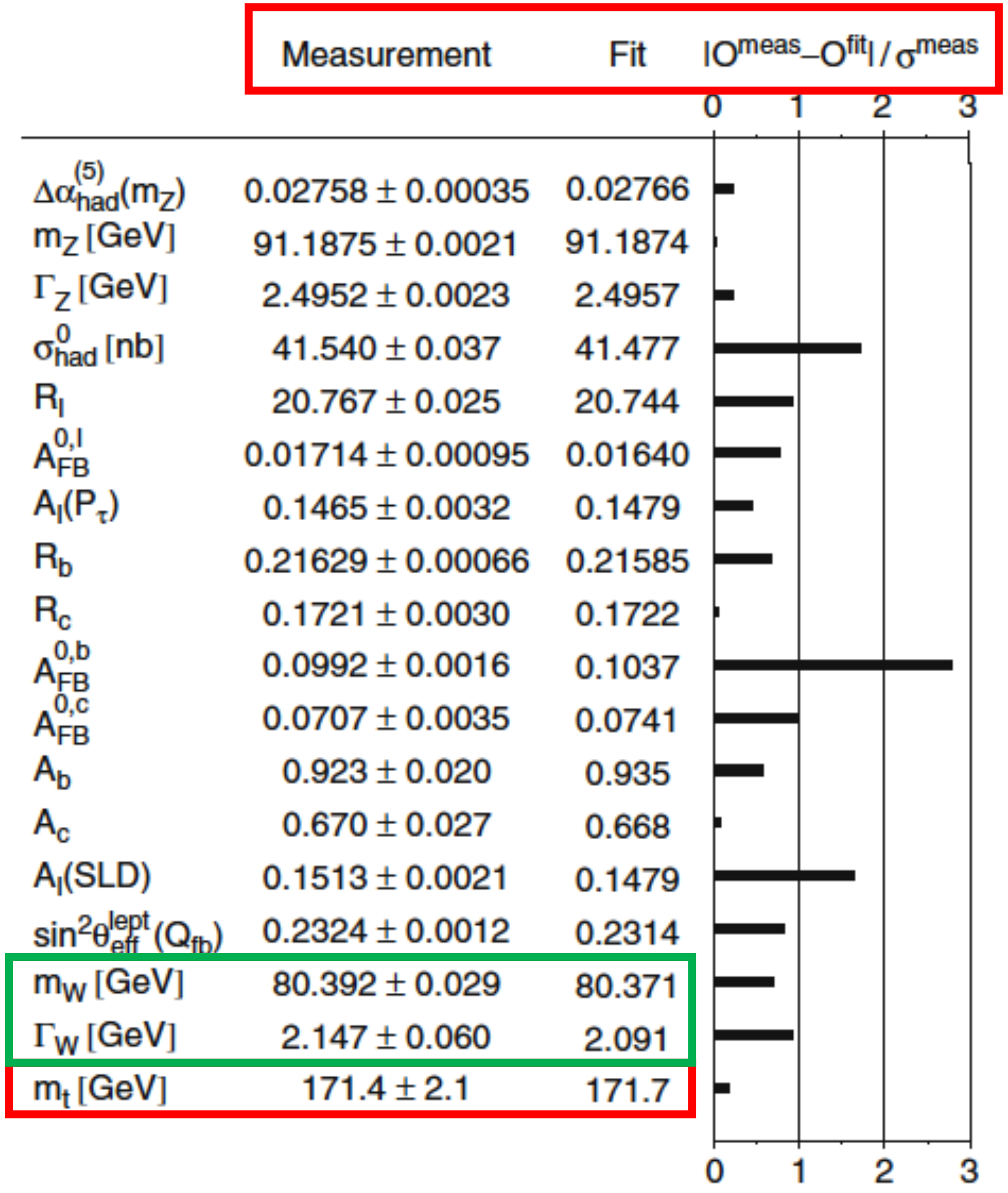

	Measurement	Fit
$\Delta\alpha_{had}^{(5)}(m_Z)$	0.02758 ± 0.00035	0.02766
m_Z [GeV]	91.1875 ± 0.0021	91.1874
Γ_Z [GeV]	2.4952 ± 0.0023	2.4957
σ_{had}^{0} [nb]	41.540 ± 0.037	41.477
R_l	20.767 ± 0.025	20.744
$A_{FB}^{0,l}$	0.01714 ± 0.00095	0.01640
$A_l(P_\tau)$	0.1465 ± 0.0032	0.1479
R_b	0.21629 ± 0.00066	0.21585
R_c	0.1721 ± 0.0030	0.1722
$A_{FB}^{0,b}$	0.0992 ± 0.0016	0.1037
$A_{FB}^{0,c}$	0.0707 ± 0.0035	0.0741
A_b	0.923 ± 0.020	0.935
A_c	0.670 ± 0.027	0.668
A_l(SLD)	0.1513 ± 0.0021	0.1479
$\sin^2\theta_{eff}^{lept}(Q_{fb})$	0.2324 ± 0.0012	0.2314
m_W [GeV]	80.392 ± 0.029	80.371
Γ_W [GeV]	2.147 ± 0.060	2.091
m_t [GeV]	171.4 ± 2.1	171.7

$$\chi^2 = \frac{|Observable^{measured} - Observable^{fitted(SM)}|}{\sigma^{measured}}$$

Compare all observables with SM. Agreement (χ^2) given by the ratio above → large deviations indicate a deviation from the fit

- m_Z corresponds to maximum of Breit-Wigner curve
- the width Γ_Z to FWHM
- The hadronic cross-section σ_{had}^0 corresponds to the maximum of the cross-section of the resonance of events with hadronic topologies.
- As for the case of hadronic events, the cross-section of different leptonic species has been measured
- The partial widths have also been measured $\frac{\Gamma_{ff}}{\Gamma_{ee}} = \sigma_f/\sigma_e$

Lep phase-2, see next slides

Also indirect measurement from higher order diagrams

Statistics: Reminder

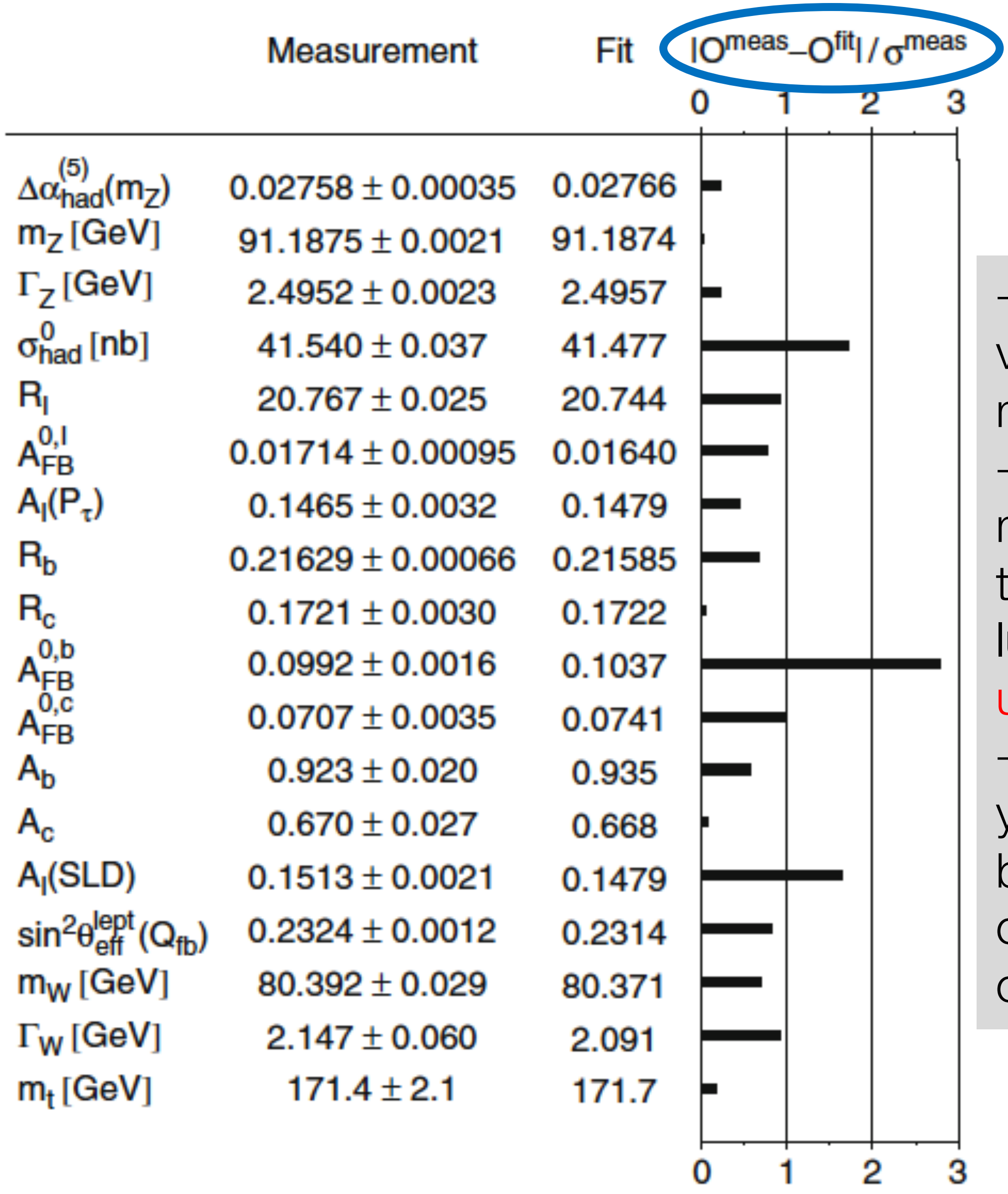

	Measurement	Fit	$\lvert O^{meas} - O^{fit} \rvert / \sigma^{meas}$
$\Delta\alpha^{(5)}_{had}(m_Z)$	0.02758 ± 0.00035	0.02766	
m_Z [GeV]	91.1875 ± 0.0021	91.1874	
Γ_Z [GeV]	2.4952 ± 0.0023	2.4957	
σ^0_{had} [nb]	41.540 ± 0.037	41.477	
R_l	20.767 ± 0.025	20.744	
$A^{0,l}_{FB}$	0.01714 ± 0.00095	0.01640	
$A_l(P_\tau)$	0.1465 ± 0.0032	0.1479	
R_b	0.21629 ± 0.00066	0.21585	
R_c	0.1721 ± 0.0030	0.1722	
$A^{0,b}_{FB}$	0.0992 ± 0.0016	0.1037	
$A^{0,c}_{FB}$	0.0707 ± 0.0035	0.0741	
A_b	0.923 ± 0.020	0.935	
A_c	0.670 ± 0.027	0.668	
A_l(SLD)	0.1513 ± 0.0021	0.1479	
$\sin^2\theta^{lept}_{eff}(Q_{fb})$	0.2324 ± 0.0012	0.2314	
m_W [GeV]	80.392 ± 0.029	80.371	
Γ_W [GeV]	2.147 ± 0.060	2.091	
m_t [GeV]	171.4 ± 2.1	171.7	

If you repeat the same measurement (characterised by a measurement error) many times, in a small number of cases you get large variations relative to measurement error.

→ expect some ~significant variations in a large sample of measurements
→ if too many of your measurements are 'too' close to the expected value you are not lucky, you are probably underestimating your errors
→ the probability distribution of your measurements has to be flat between 0 and 1 if your model is correct (&& and if your errors are correctly computed)

# std.deviations	Two sides probability
0	1.00
0.5	0.62
1.0	0.31
1.5	0.13
2.0	0.045
2.5	0.012
3.0	0.0027

All is quantified by the ratio $\chi^2/ndof$
where ndof = # measurements – #degrees of freedom

From Combination Paper of Four LEP Experiments

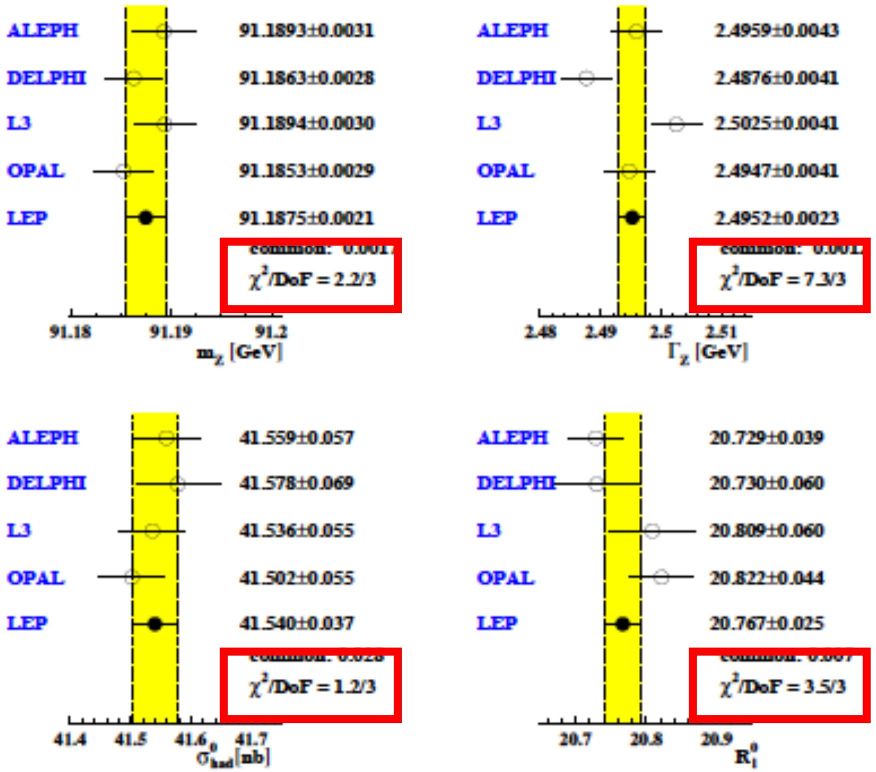

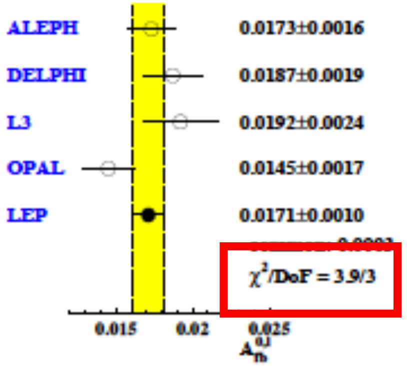

Figure 2.9: Measurements of m_Z, Γ_Z, $\sigma^0_{\rm had}$, R^0_ℓ and $A^{0,\ell}_{\rm FB}$. The averages indicated were obtained using the common errors and combination method discussed in the text. The values of χ^2 per degree of freedom were calculated considering error correlations between measurements of the same parameter, but not error correlations between different parameters.

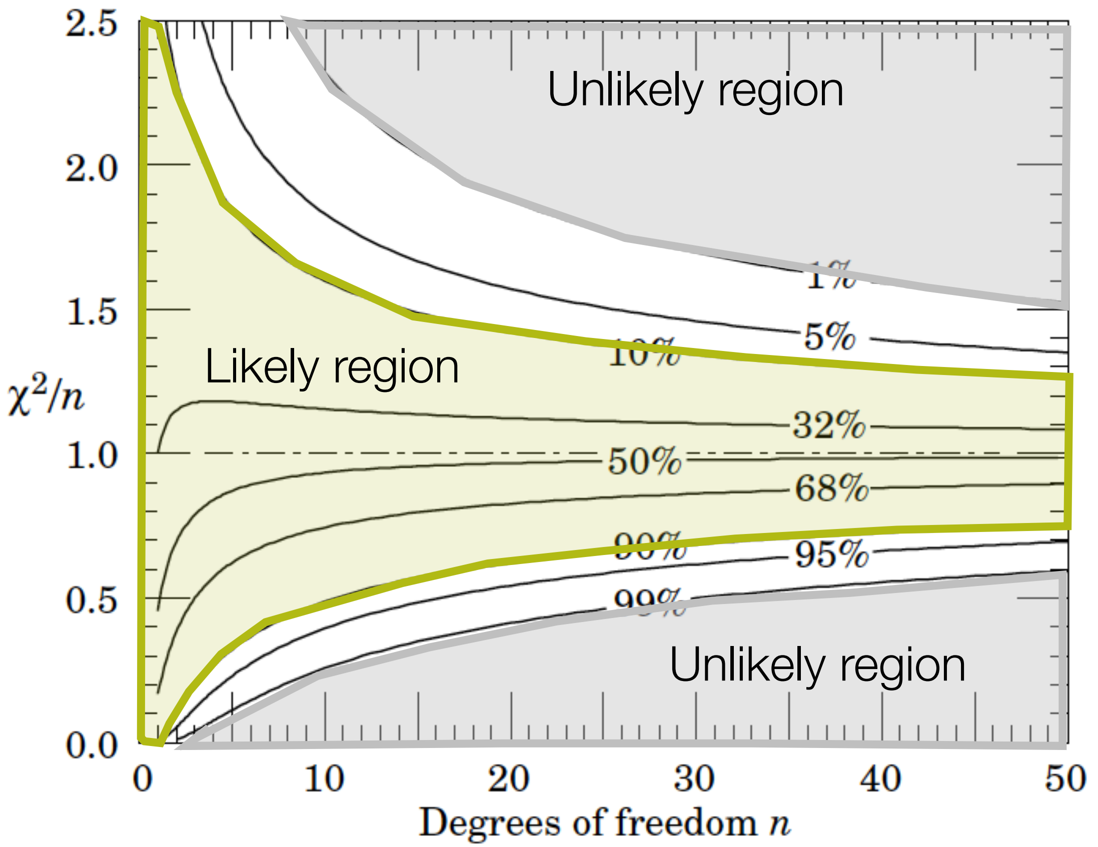

Figure 38.2: The 'reduced' χ^2, equal to χ^2/n, for n degrees of freedom. The curves show as a function of n the χ^2/n that corresponds to a given p-value.

Particle Data Group: http://pdg.lbl.gov/2015/reviews/rpp2015-rev-statistics.pdf

Precision of $m_Z \longrightarrow$ Impact of Beam Energy

Precision on m_Z

- Stat ± 2 MeV
- ΔE_{beam} had to be known to 2MeV

$$\begin{aligned}\Delta m_Z &\approx \tfrac{1}{2}\cdot\Delta(E_{+2}+E_{-2}) \text{ and}\\ \Delta\Gamma_Z &\approx \frac{\Gamma_Z}{E_{+2}-E_{-2}}\Delta(E_{+2}-E_{-2})\,.\end{aligned}$$

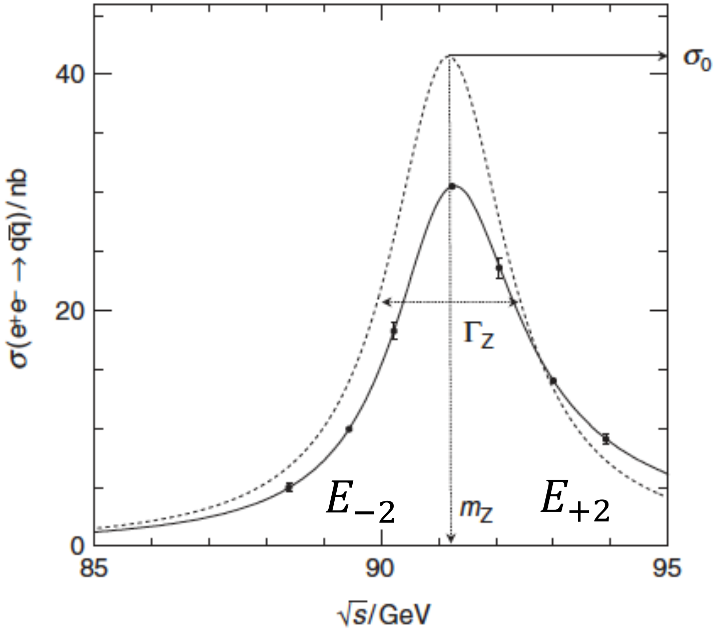

Consider very small effects:

- tidal effects: the Moon distort the rocks around LEP by ±0.15mm in the accelerator. Induced ΔE_{beam} ±10MeV. Moon movements are known → effect corrected.
- Ununderstood effect for some time: jumps in the beam energies at specific times of the day. After much investigation (and a box of bottles of champagne!), the origin → leakage currents from the local high-speed railway. Once understood, the affected data could be corrected for this effect.

Accurate Measurement of Beam Energy

momentum of particles circulating in a ring is proportional to the magnetic bending field

The needed ΔE_{beam} in LEP achieved with the technique of

resonant spin depolarisation (*)

precession of the average spin vector of the polarised bunches.

→ The beam energy is therefore proportional to the number of spin precessions per turn ("spin tune", ν). It is measured with the help of a weak oscillating radial magnetic field, by observing the depolarisation which occurs when an artificial spin resonance is excited.

This method offers a very high precision, as good as ±0.2 MeV, on the beam energy at the time of the measurement.

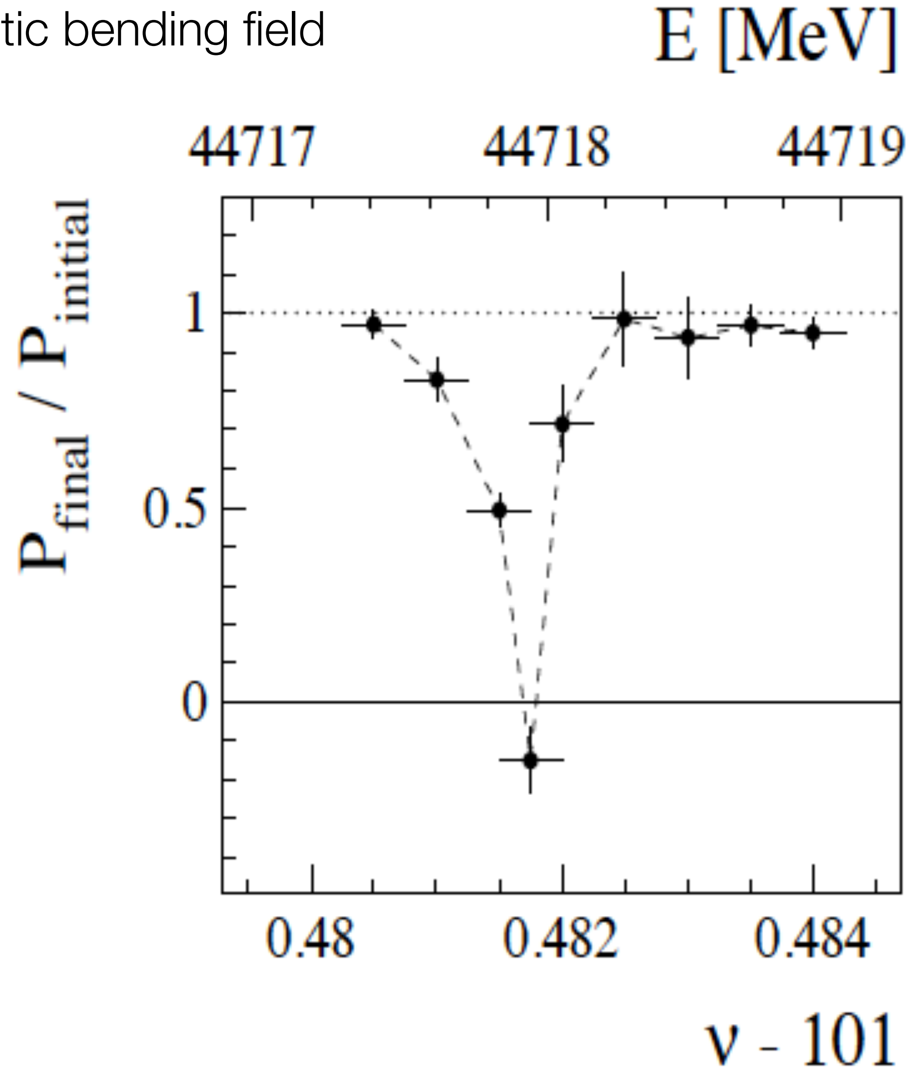

(*) available in 1991, when a small transverse polarisation of the electron beam in LEP was observed.

Energy Calibration of the Beams at LEP

Typical variations of the beam energy around the LEP ring due to energy losses from synchrotron radiation in the arcs: compensated by radio frequency cavities

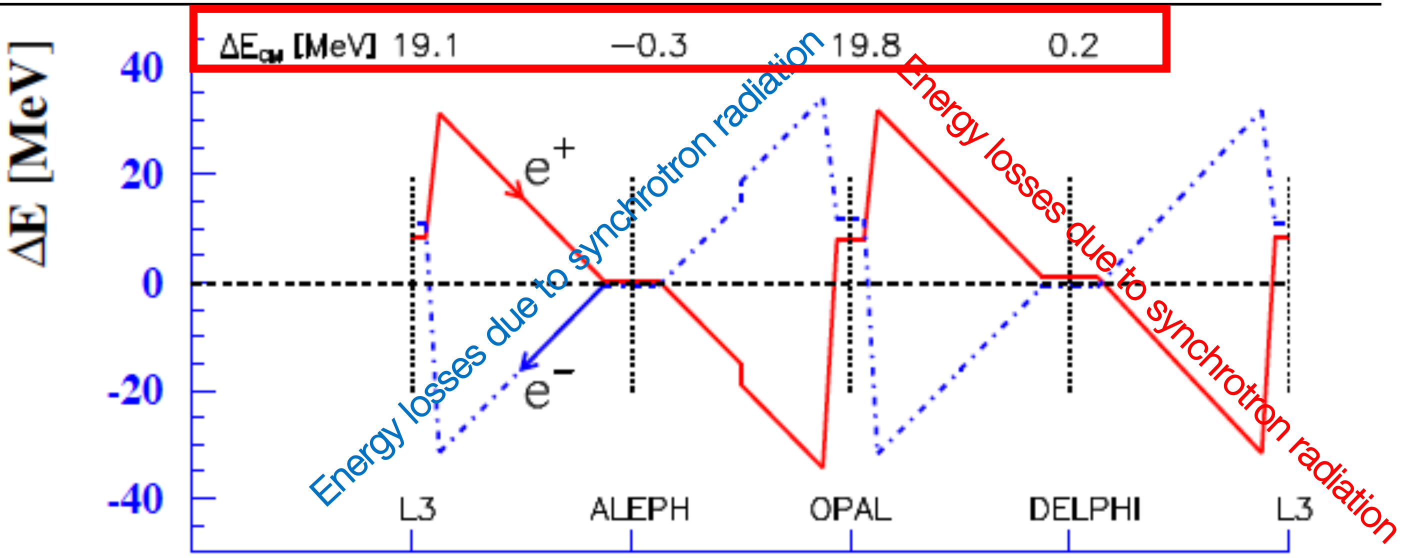

Energy losses due to synchrotron radiation

Energy losses due to synchrotron radiation

→ Effects on the centre-of mass energy. The last two columns give the approximate contribution of each effect to the error on m_Z and on Γ_Z. (specific to each year and energy)

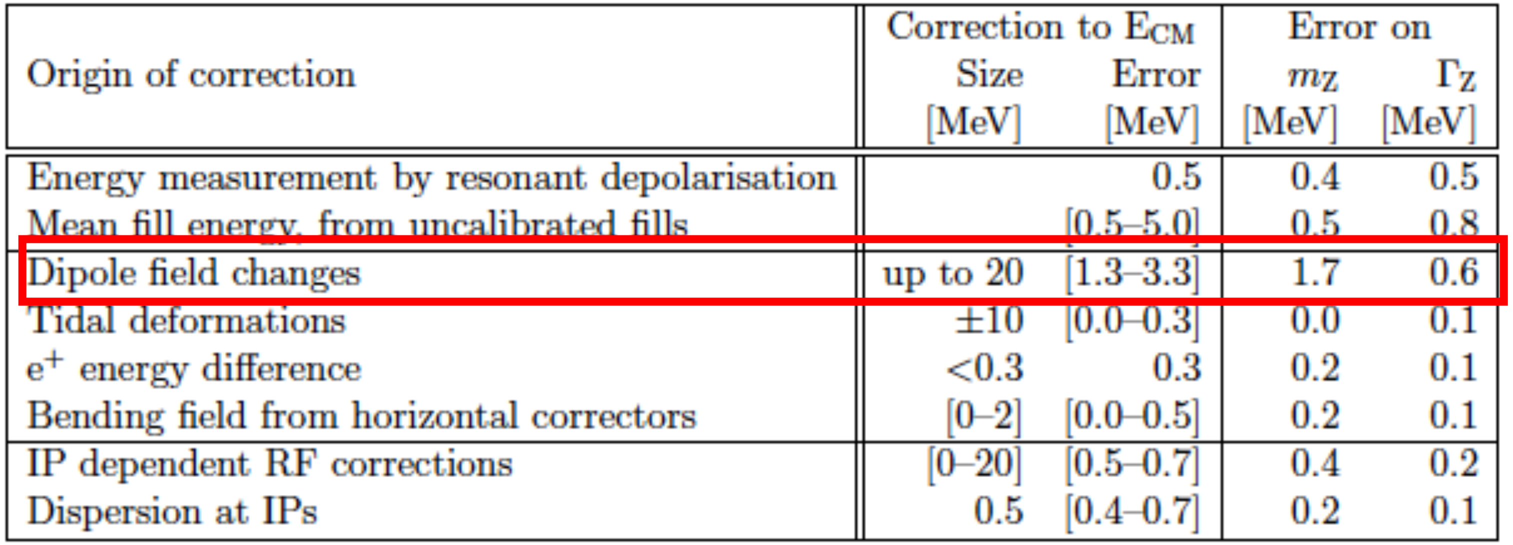

Origin of correction	Correction to E_{CM} Size [MeV]	Error [MeV]	Error on m_Z [MeV]	Γ_Z [MeV]
Energy measurement by resonant depolarisation		0.5	0.4	0.5
Mean fill energy, from uncalibrated fills		[0.5–5.0]	0.5	0.8
Dipole field changes	up to 20	[1.3–3.3]	1.7	0.6
Tidal deformations	±10	[0.0–0.3]	0.0	0.1
e^+ energy difference	<0.3	0.3	0.2	0.1
Bending field from horizontal correctors	[0–2]	[0.0–0.5]	0.2	0.1
IP dependent RF corrections	[0–20]	[0.5–0.7]	0.4	0.2
Dispersion at IPs	0.5	[0.4–0.7]	0.2	0.1

Luminosity Measurement at LEP

$$\mathcal{L} = \frac{N_{selected}}{\sigma^{signal} \cdot Acceptance \cdot Efficiency}$$

The small-angle Bhabha scattering was used to measure the luminosity at LEP.

$$e^+ \, e^+ \, e^- \rightarrow mostly \, \gamma \; at \; small \; angles \rightarrow e^+ \, e^-$$

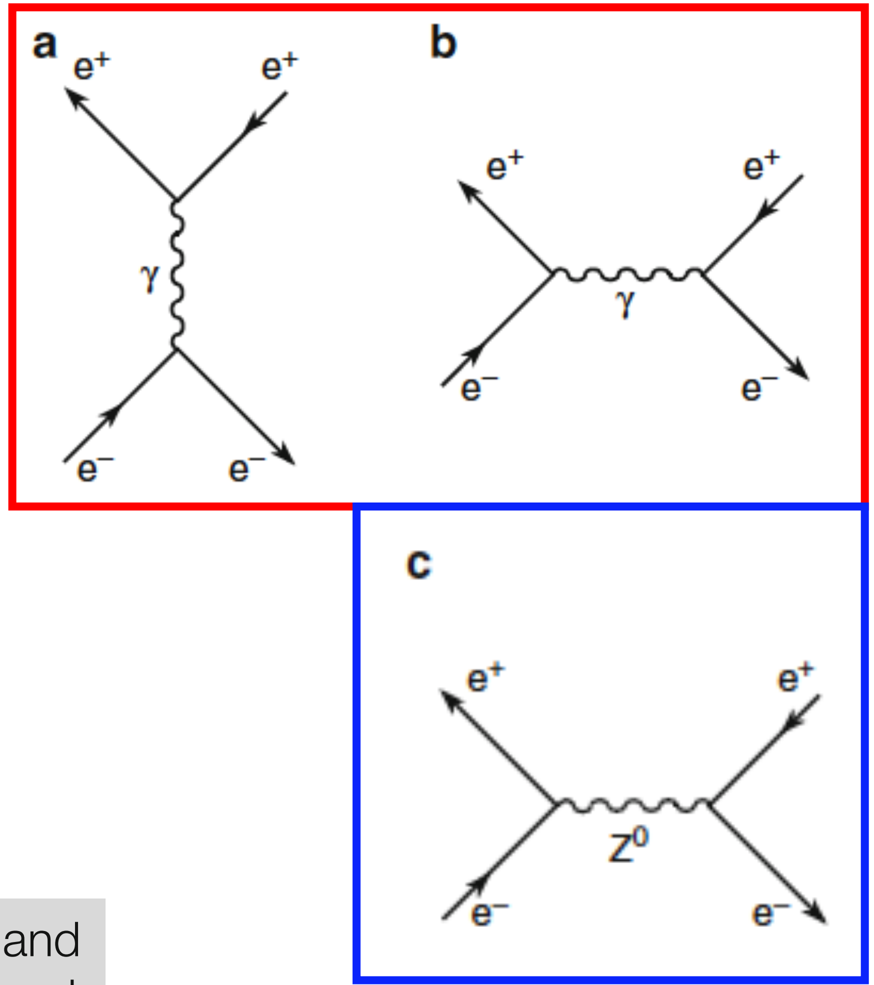

It can be described by two contributions:

- at small angles, the cross section has a dependence on the polar angle of the type $1/\theta^4 \approx 1/q^4$ due to the EM terms → very rapid variation with θ;
- at large angles, the exchange of the Z has also to be included.

The large cross-section at small angles is only due to the EM interaction and is calculated with a precision better than 1% (compared to 3% achievable at LHC using Van der Mer scan).

Luminosity Measurement at LEP

- Events with forward going electrons are recorded at the same time of all other processes → reflect any data-taking inefficiencies (readout deadtimes and detector downtimes).
- The cross-section is high → many events produced → the statistical precision of this process is high, matching well even the high statistics of hadronic events at the Z resonance.

The topology of these events is extremely clear:

- **back-to-back electrons and positrons close to the beam direction.** Their positions and energies (E_L and E_R) are measured by calorimeters placed at small angles with respect to the beam line, polar angle range: 25 to 60 mrad.
- The energy of electrons and positrons is equal to the energy of the beams → $E_{L/R} / E_{beam} = 1$.
- The cross-section is twice the hadronic peak cross-section → small statistical errors arising due to luminosity.

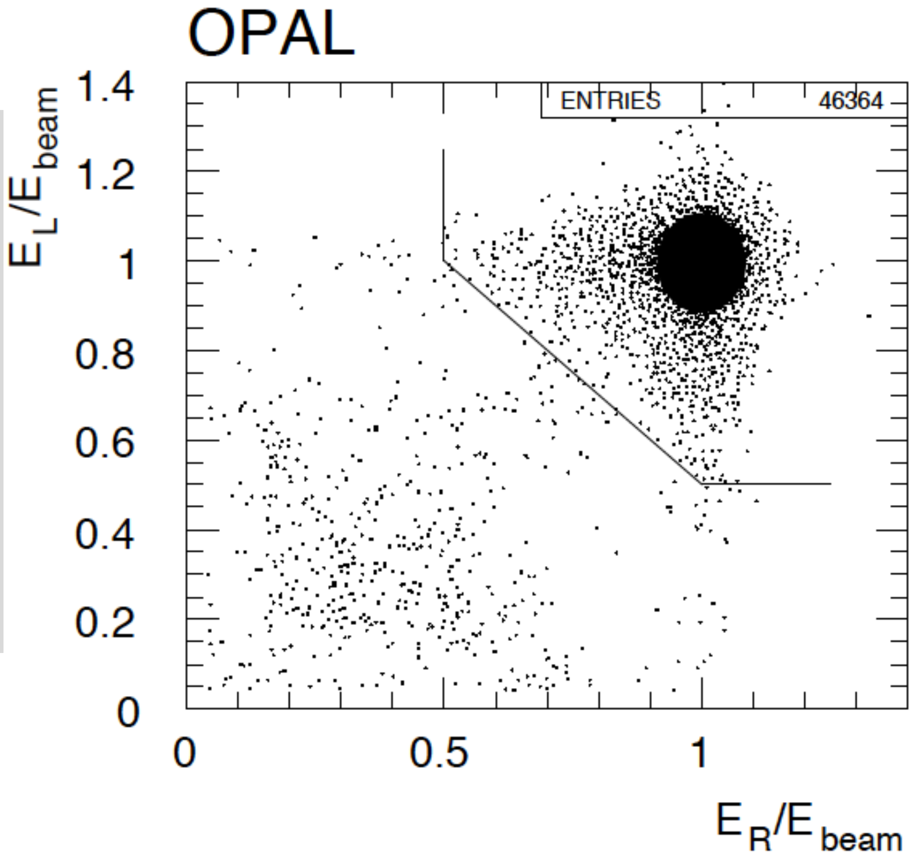

typical experimental signature of luminosity events

Problems of Luminosity Measurements at LEP

$$\sigma^{signal} = \frac{N^{signal}_{total}}{\mathcal{L}} = \frac{N_{selected} - N_{background}}{\mathcal{L} \cdot \varepsilon_{trigger} \cdot \varepsilon_{selection} \cdot Acceptance}$$

$$\mathcal{L} = \frac{N_{selected}}{\sigma^{signal} \cdot Acceptance}$$

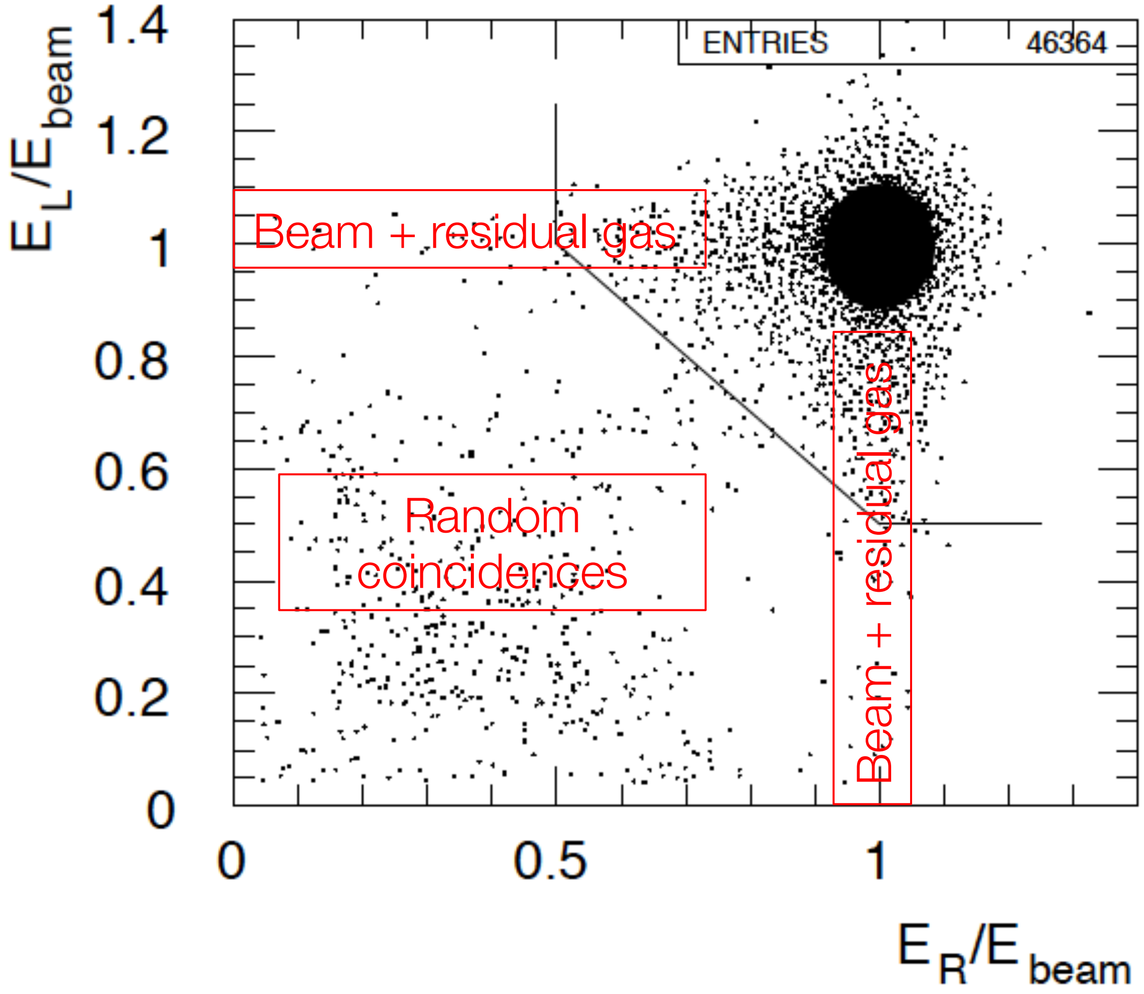

Very small background, very large sample of $N_{selected}$
BUT
the main systematic error from the definition of the geometrical acceptance for this process.

angular distribution falls like $1/\theta^4$
→ a precise knowledge of the inner radius of the calorimeter needed

The Bhabha cross-section at small scattering angles is dominated by the well-known QED t–channel scattering process known to ~ 0.05 %

LEP at High Energy: Phase-2

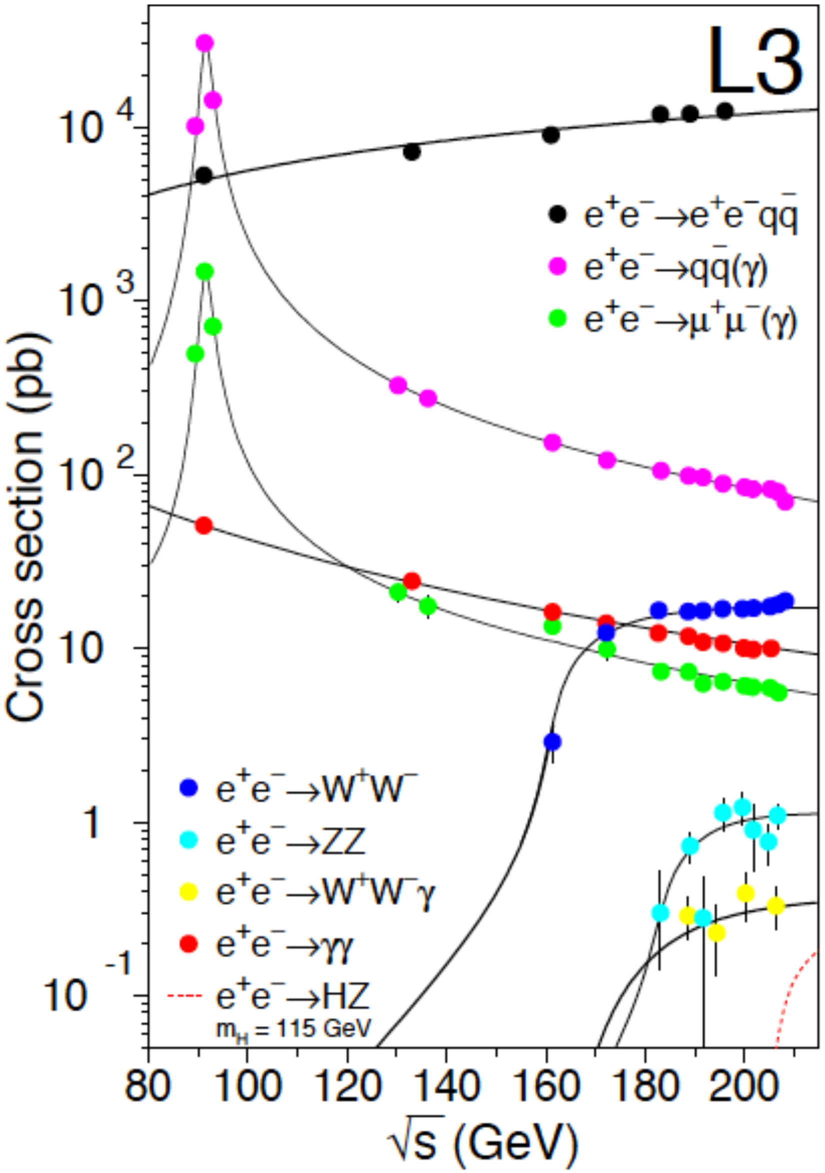

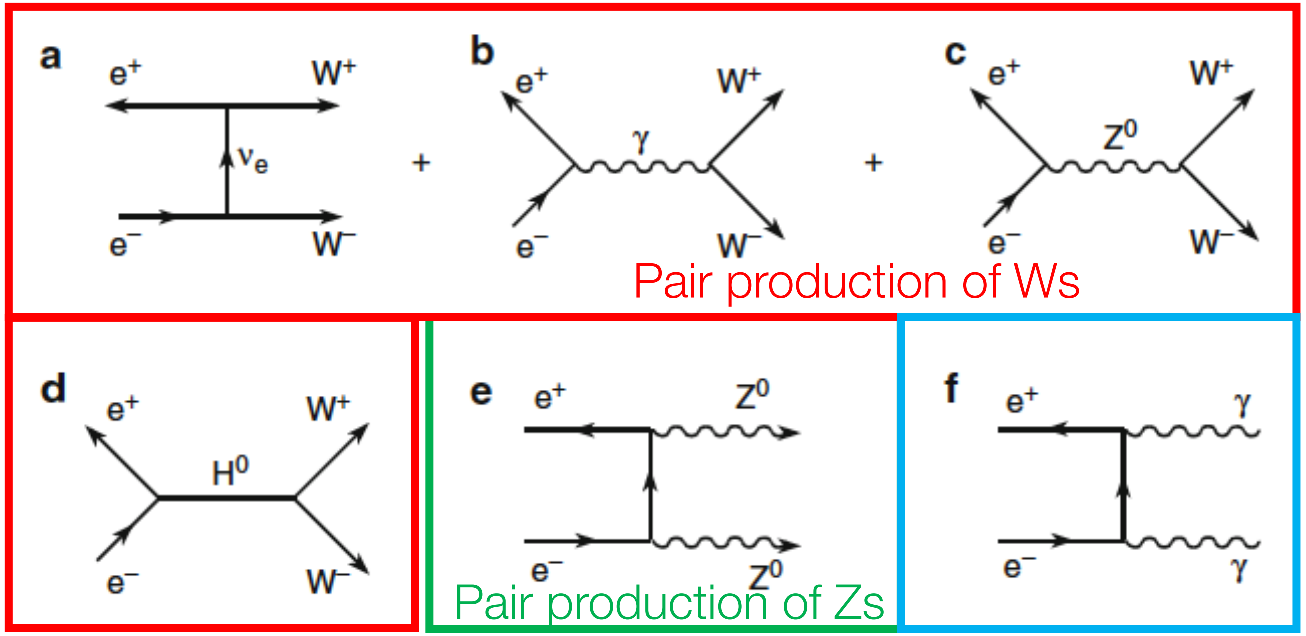

Pair production of Ws

Pair production of Zs

Pair production of γs

Lowest order Feynman diagrams (a), (b), (c), and (d) for the process $e^+e^- \to W^+W^-$, (e) the ZZ production and (f) the annihilation in two photons

W LEP Measurements & its Mass

$$e^+e^- \to W^+W^- \to q\overline{q}'q''\overline{q'''}$$

$$e^+e^- \to W^+W^- \to q\overline{q}'l\nu_l$$

W Mass at Colliders & Other Observables

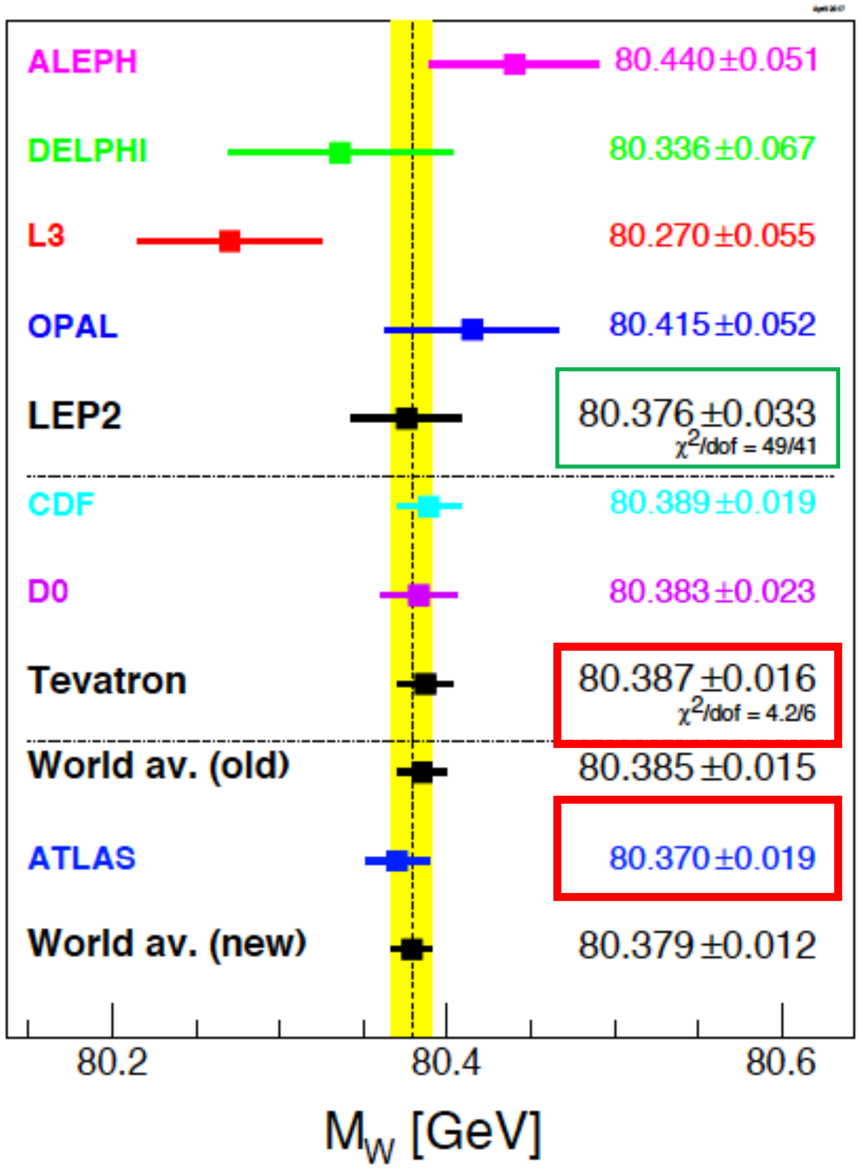

Standard Model: precise relations among many observables, → well defined ratios and/or relations.

- The mass of the W, of the Higgs, of the top quark are some of these observables.
- m_W is important because it is the best measured observable → check the consistency of the SM predictions with data.

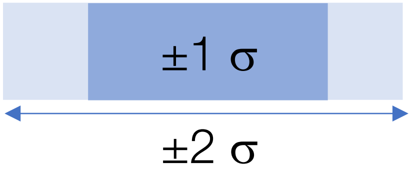

All these measurements must have an area of superposition

Inconsistencies could give possible indications of new physics

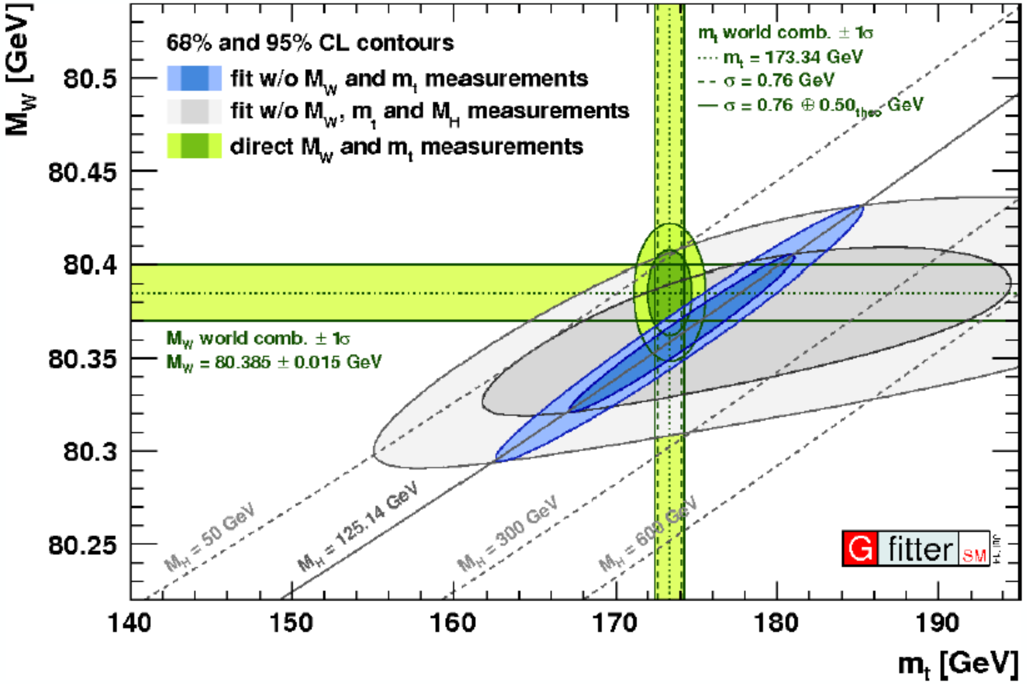

Methods to Measure the W Mass

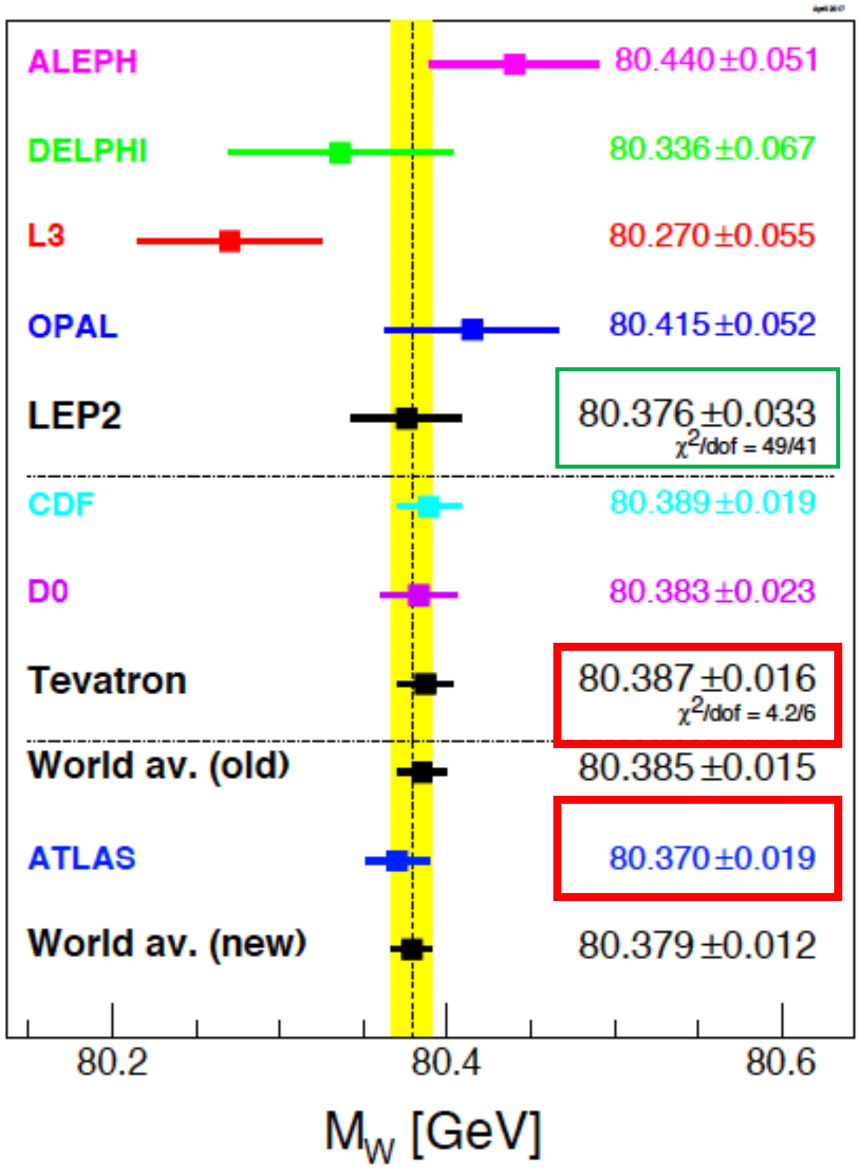

W mass and its width Γ_W is are the parameters that appear in a Breit-Wigner expression for the cross-section vs centre-of-mass-energy

Decay	$W^+W^- \to q\bar{q}'q''\overline{q'''}$	$W^+W^- \to q\bar{q}' l\nu_l$	$W^+W^- \to l\nu_l l\nu_l$
Fraction	46%	44%	10%
Topology	4 jets, no missing energy	2 jets + missing energy + lepton	No jet + missing energy

Machine	Method	Present precision
e^+e^-	1-cross-section at threshold, 2-direct reconstruction	±33 MeV
$p\bar{p}$	High p_T charged lepton from its decay. Due to the presence of νs the mass is determined by comparison of the transverse mass m_T with MC predictions	±16 MeV (CDF and D0) (±9 MeV?)
pp		±19 MeV (ATLAS only)

W mass measurement at Colliders

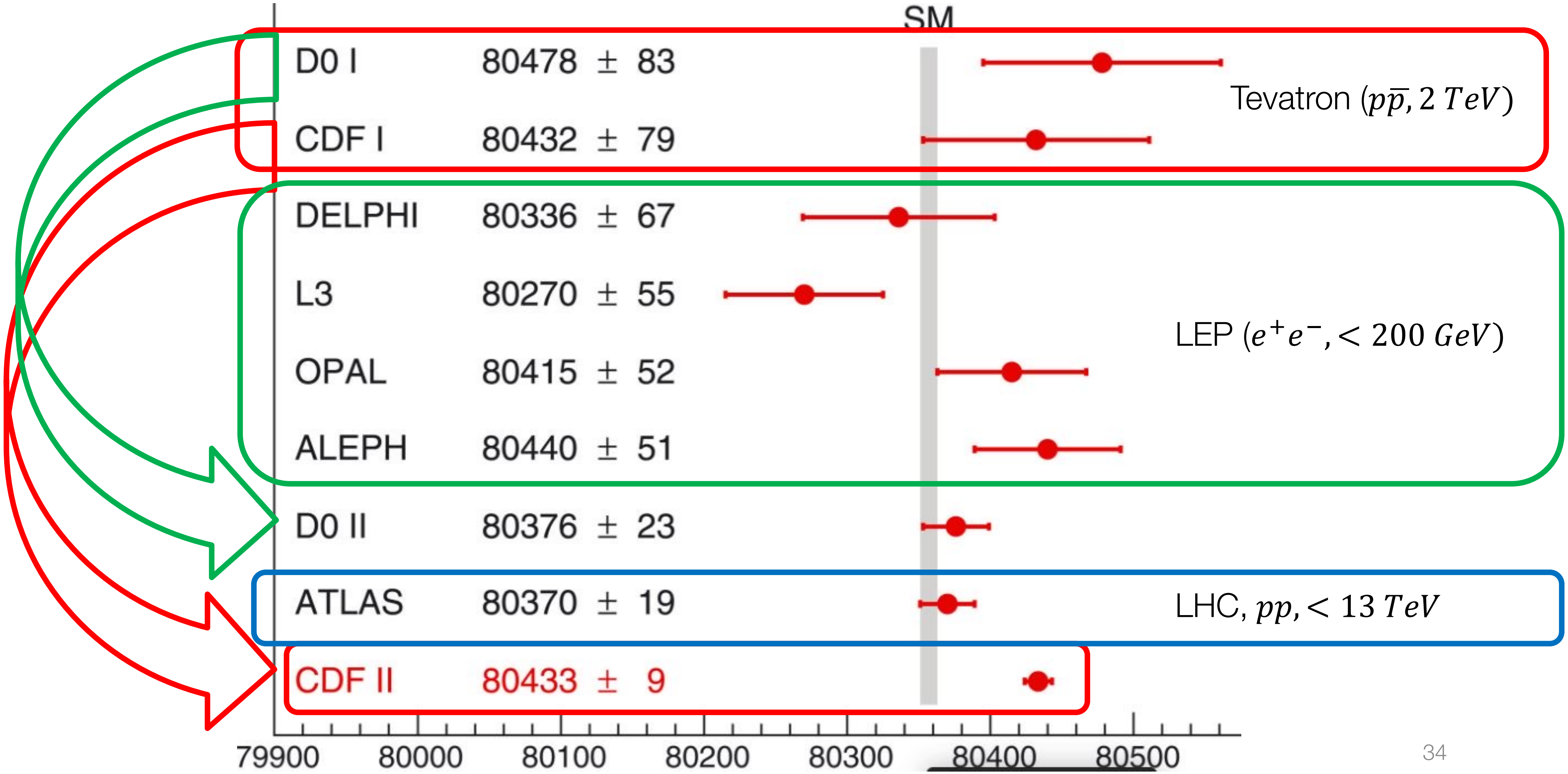

Tevatron ($p\bar{p}, 2\ TeV$)

LEP ($e^+e^-, < 200\ GeV$)

LHC, $pp, < 13\ TeV$

M_W at LEP

Toni Baroncelli: Precision Measurements

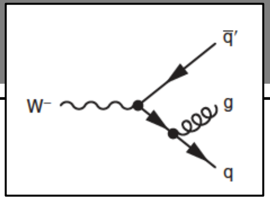

← gluon radiation, additional jet

Lowest order Feynman diagrams for the production of pairs of Ws and of Zs at LEP phase-2:

Centre-of-mass energy has to be larger than

$m_W\ (m_Z)\cdot 2$

- Fully hadronic: 44%, four jets whose energy sum is consistent with centre-of-mass-energy
- Semileptonic: ~46%
- Fully leptonic: 10%, **topology** two acoplanar energetic leptons with significant missing energy in detectors.

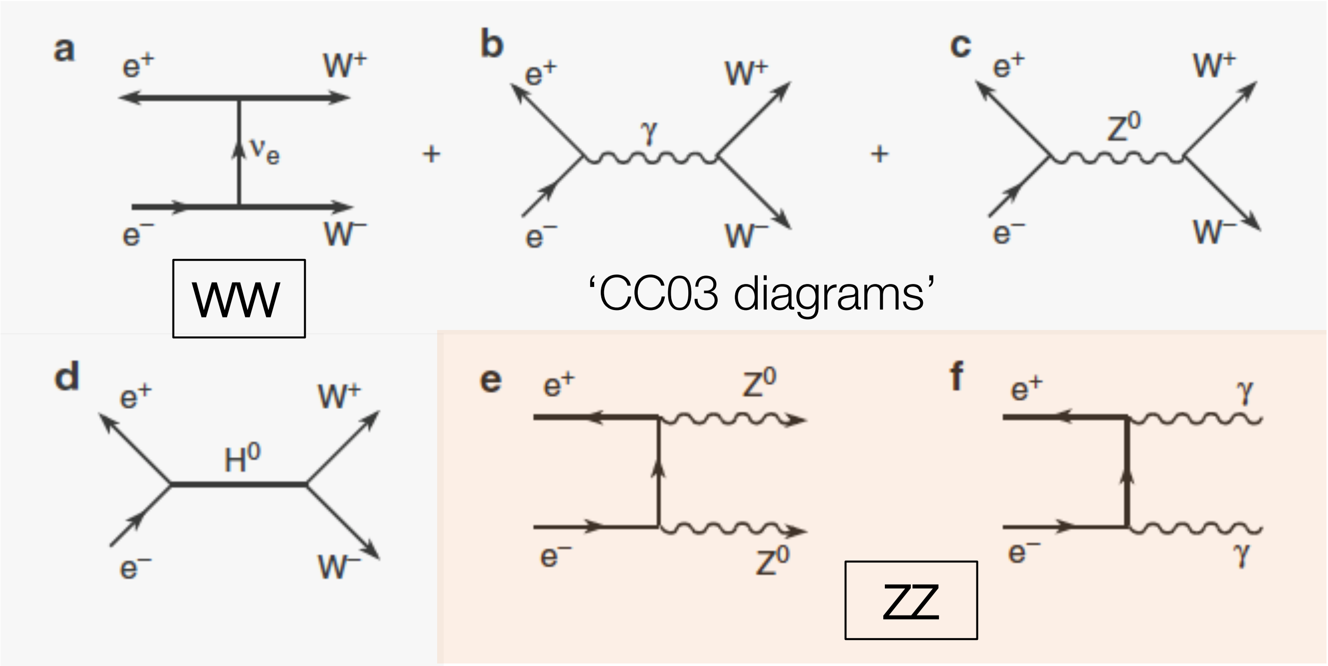

LEP Phase 2 → W properties (& quest for the Higgs)

Period	Energy (GeV)	Luminosity (pb^{-1})
1995	130/136	6.2
1996	161	12.1
1996	172	11.3
1997	183	63.8
1998	189	196.4
1999	192	30.

Typical situation at LEP for the WW selection (Aleph)

	Efficiency (%)	Purity (%)	Exp. N evts	Obs. N evts
$q\bar{q}q\bar{q}$	71.4	84.7	1173	1068
$q\bar{q}e\bar{\nu}_e$	81.3	92.7	371	358
$q\bar{q}\mu\bar{\nu}_\mu$	84.1	96.6	365	363
$q\bar{q}\tau\bar{\nu}_\tau$	41.5	95.4	176	159

W^+W^- Decay Topologies

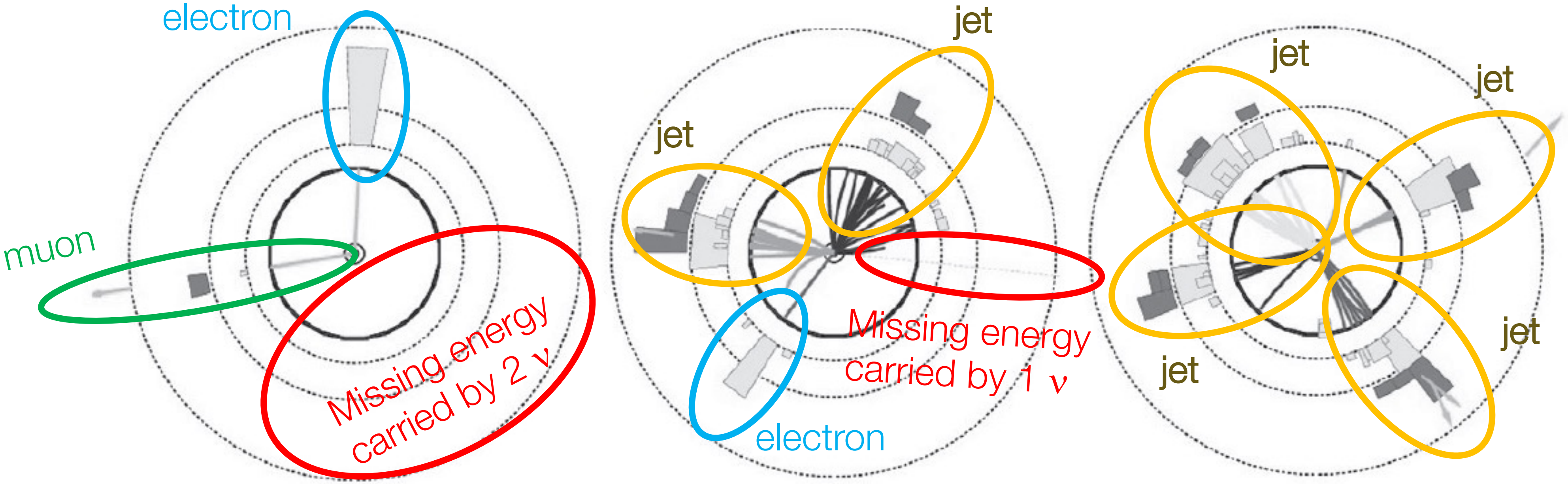

$W^+W^- \rightarrow e^-\bar{\nu}_e\mu^+\nu_\mu$

$W^+W^- \rightarrow e^-\bar{\nu}_e q_1\bar{q}_2$

$W^+W^- \rightarrow q_1\bar{q}_2q_3\bar{q}_4$

At LEP two point-like objects collide and this allowed the use of constraints:

- Total energy = $\sqrt{s}$ (= 2 x beam energy); → ν energy known
- Total momentum in 3 directions = 0;

At LEP rate is ~ low, events are clean, no pile-up!

→ adjust directions and p_T and E of objects to satisfy these constraints (fit) → improvement of m_W resolution

- If both Ws are reconstructed than also impose $m_W^1 = m_W^2$ (however in full hadronic topology 4 jets and 3 combinations; use pairing that gives best masses)

m_W Reconstruction at Threshold

Close to the W^+W^- threshold (161 GeV), the dependence of the W-pair production cross section rises as

$$\sigma_{WW} \propto \beta = \sqrt{1 - 4m_W^2/s}$$

→ The measurement of σ_{WW} at √s gives m_W (see plot on the right).
The most sensitive √s to m_W was determined to be √s = 161 GeV, but data at 172-183 GeV were also analysed to extract m_W.

The ***potential*** precision is similar to the direct reconstruction method, described below. However, LEP (mostly) operated at higher centre-of-mass energies (NP + precise EW) and only 3% of the full data set was taken at 161 GeV.

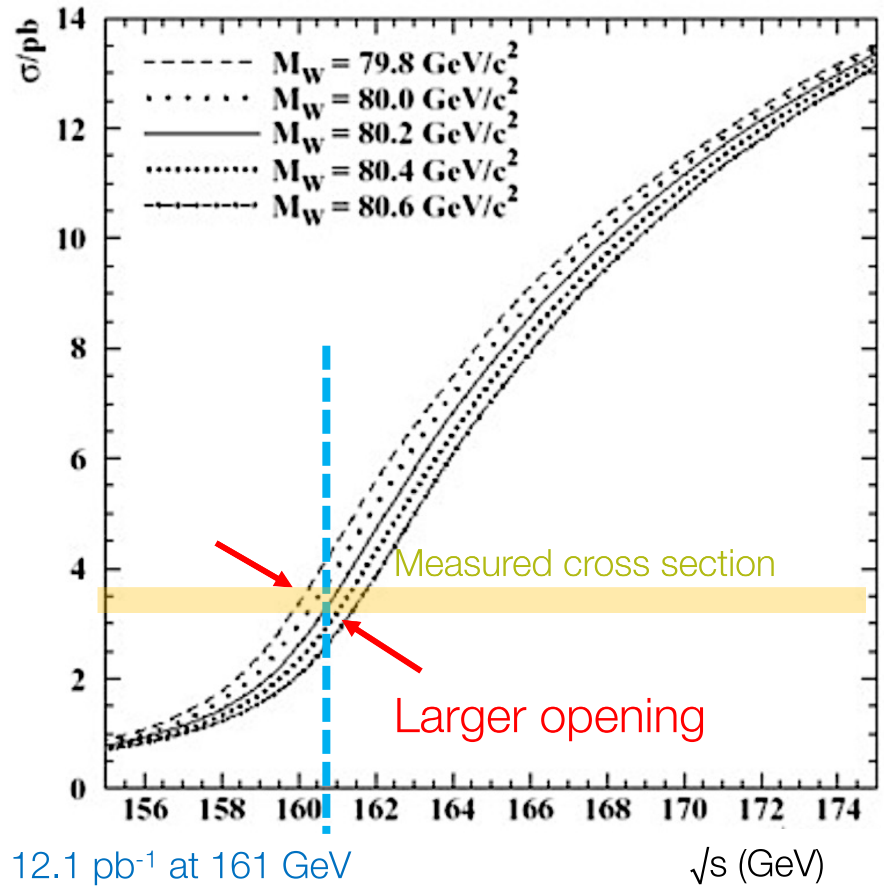

Measured cross section

Larger opening

12.1 pb^{-1} at 161 GeV

√s (GeV)

Threshold Analysis	
Experiment	m_W[GeV]
ALEPH	80.20 ± 0.34
DELPHI	$80.45^{+0.45}_{-0.41}$
L3	$80.78^{+0.48}_{-0.42}$
OPAL	$80.40^{+0.46}_{-0.43}$

The combination gives

$$m_W(\text{threshold}) = 80.42 \pm 0.20 \pm 0.03(E_{LEP})\ \text{GeV}$$

Δm_W~200 MeV, energy knowledge plays no role!

Direct Reconstruction of m_W

The direct mass reconstruction method was used at 172, 183 and 189 GeV centre-of-mass energies.

- W mass is reconstructed using the pairs of jets from each W decay.
- A constrained fit, mentioned before, is used
- fully hadronic and semileptonic channels are used
- In the fully hadronic channel ‘pairing problem’: (12+34, 13+24, 14+23) → combinatorial background.

Example: L3

qqeν: almost no background, no pairing problem

Full leptonic topology limited statistics (10% decays)

(a)

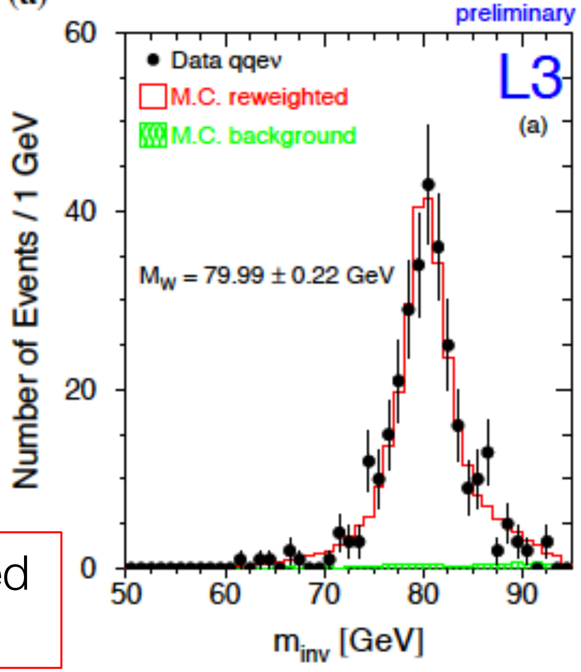

(b)

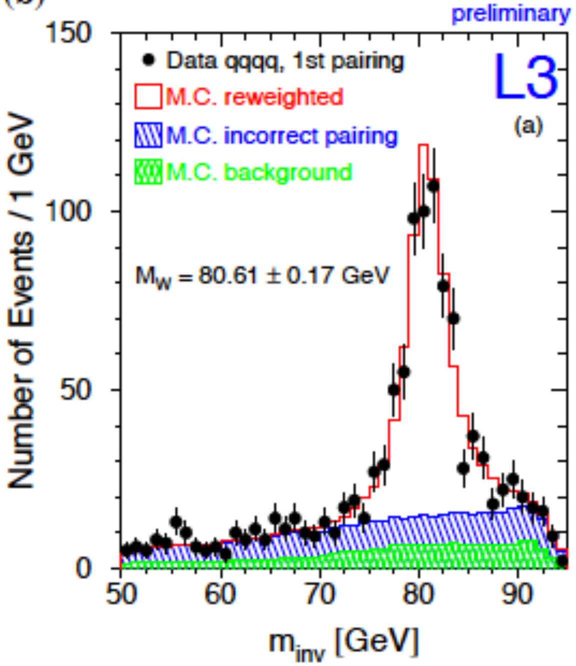

qqqq: some background, significant pairing contribution

→ similar precision to the semi-leptonic case even if statistics is larger

Toni Baroncelli: Precision Measurements

Getting the Mass and the Width

In the direct reconstruction method, the mass of the W boson is obtained by comparing data to simulated

$e^+e^- \to W^+W^-$

event samples generated with known values of m_W and Γ_W, in order to obtain those values which describe the data best.

These Monte-Carlo samples are of large statistics, typically 10^6 events. Since the generation of event samples for all possible parameter values is very computing time intensive, different methods are used to perform the m_W and Γ_W extraction in a more efficient, but still precise way (typically re-weight events).

The individual results of the four experiments are combined taking into account correlations

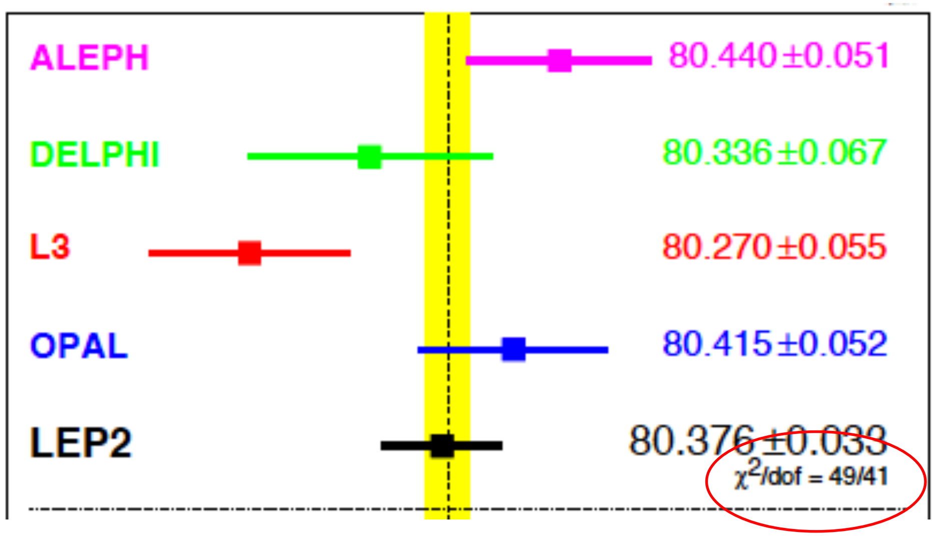

X^2/dof is ~good

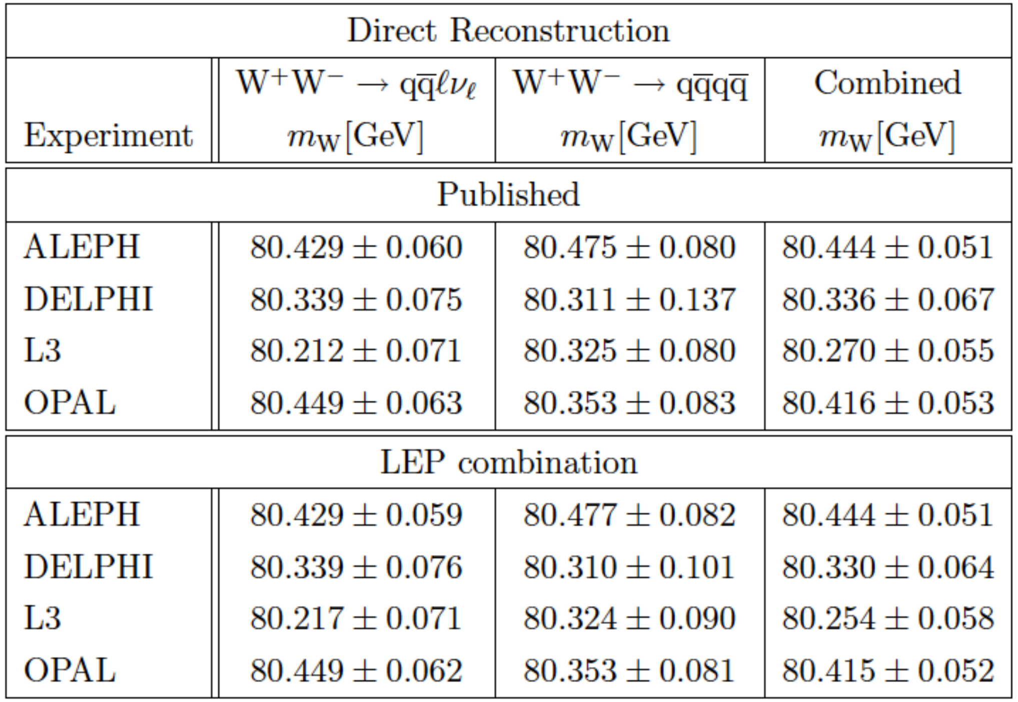

Direct Reconstruction			
Experiment	$W^+W^- \to q\bar{q}\ell\nu_\ell$ m_W[GeV]	$W^+W^- \to q\bar{q}q\bar{q}$ m_W[GeV]	Combined m_W[GeV]
Published			
ALEPH	80.429 ± 0.060	80.475 ± 0.080	80.444 ± 0.051
DELPHI	80.339 ± 0.075	80.311 ± 0.137	80.336 ± 0.067
L3	80.212 ± 0.071	80.325 ± 0.080	80.270 ± 0.055
OPAL	80.449 ± 0.063	80.353 ± 0.083	80.416 ± 0.053
LEP combination			
ALEPH	80.429 ± 0.059	80.477 ± 0.082	80.444 ± 0.051
DELPHI	80.339 ± 0.076	80.310 ± 0.101	80.330 ± 0.064
L3	80.217 ± 0.071	80.324 ± 0.090	80.254 ± 0.058
OPAL	80.449 ± 0.062	80.353 ± 0.081	80.415 ± 0.052

1

2

Higher Order Diagrams

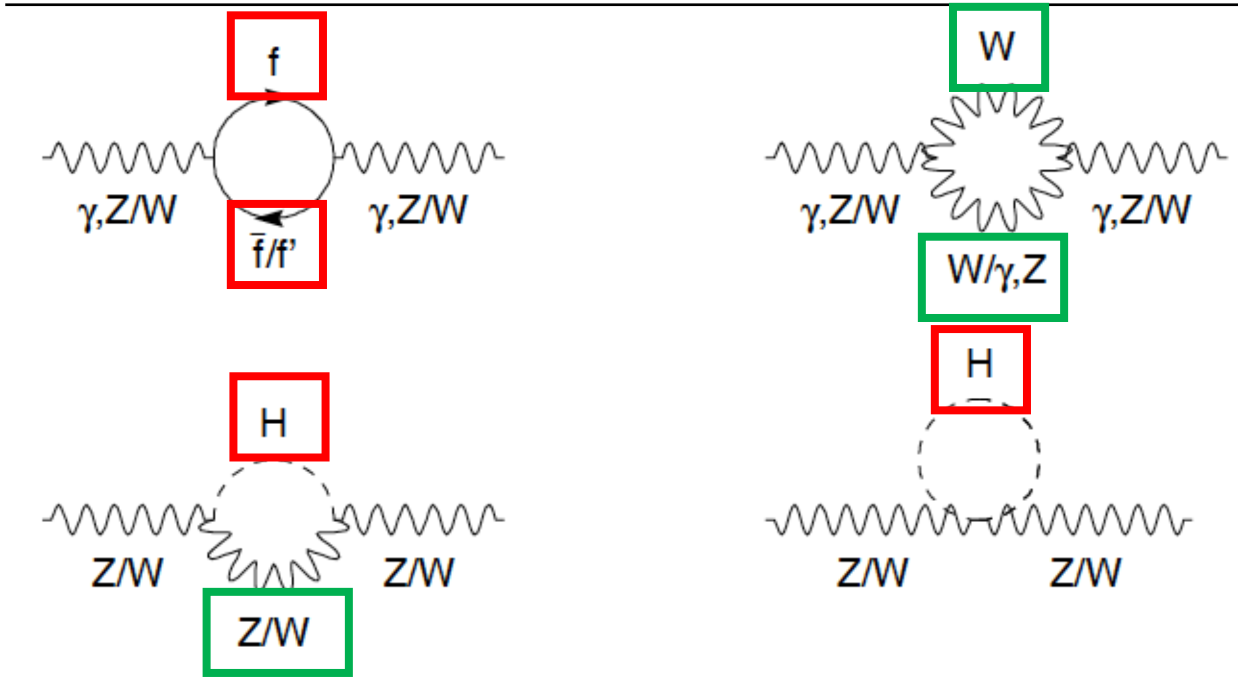

Higher order diagrams include loops with known and (at the time of LEP) yet unknown particles: the top quark and the Higgs boson.

The effect of these higher order diagrams is to modify slightly axial and vector couplings g_{Vf}, g_{Af}

$$\begin{aligned} \sin^2\theta^{f}_{eff} &\equiv \boxed{\kappa_f} \sin^2\theta_W \\ g_{Vf} &\equiv \boxed{\sqrt{\rho_f}}\,(T^{f}_{3} - 2Q_f \sin^2\theta^{f}_{eff}) \\ g_{Af} &\equiv \boxed{\sqrt{\rho_f}}\,T^{f}_{3}\,, \end{aligned}$$

$$\begin{aligned} \boxed{\rho_f} &\equiv \Re(\mathcal{R}_f) = 1 + \Delta\rho_{se} \\ \boxed{\kappa_f} &\equiv \Re(\mathcal{K}_f) = 1 + \Delta\kappa_{se} \end{aligned}$$

+ smaller terms

$$\begin{aligned} \boxed{\Delta\rho_{se}} &= \frac{3G_F m^2_W}{8\sqrt{2}\pi^2}\left[\frac{m^2_t}{m^2_W} - \frac{\sin^2\theta_W}{\cos^2\theta_W}\left(\ln\frac{m^2_H}{m^2_W} - \frac{5}{6}\right) + \cdots\right] \\ \boxed{\Delta\kappa_{se}} &= \frac{3G_F m^2_W}{8\sqrt{2}\pi^2}\left[\frac{m^2_t}{m^2_W}\frac{\cos^2\theta_W}{\sin^2\theta_W} - \frac{10}{9}\left(\ln\frac{m^2_H}{m^2_W} - \frac{5}{6}\right) + \cdots\right] \end{aligned}$$

→ one has some sensitivity on m_t and m_H:

- Dependence is quadratic on m_t → more visible
- Logarithmic on m_H → weak

At ~ low energy you open a small window on kinematically inaccessible regions

Global fits of all observables give some indication on m_t and m_H even before their direct discovery and measurement

m_t and m_H

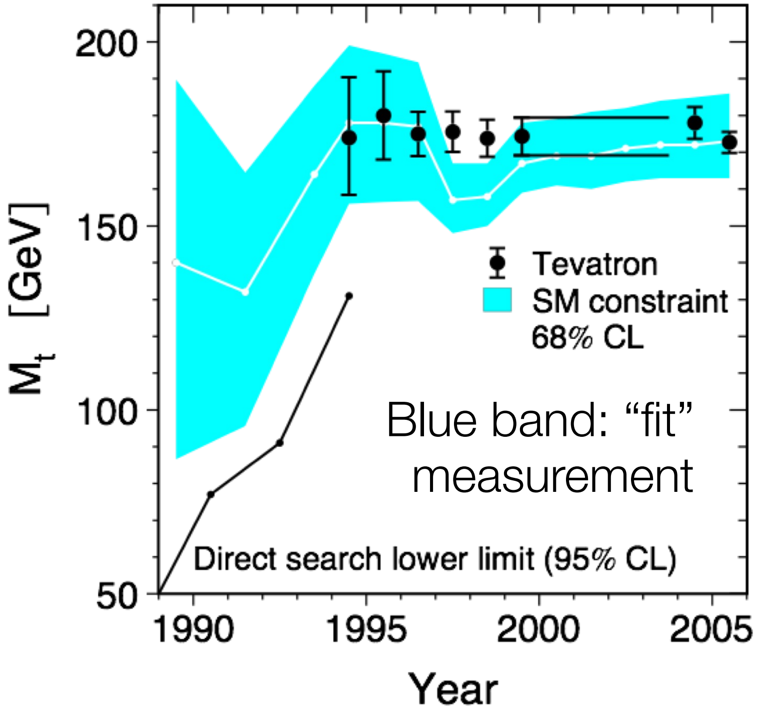

Blue band: “fit” measurement

Points: direct measurement

Parameter	Value	Correlations				
		$\Delta\alpha_{\mathrm{had}}^{(5)}(m_Z^2)$	$\alpha_S(m_Z^2)$	m_Z	m_t	$\log_{10}(m_H/\mathrm{GeV})$
$\Delta\alpha_{\mathrm{had}}^{(5)}(m_Z^2)$	0.02767 ± 0.00034	1.00				
$\alpha_S(m_Z^2)$	0.1188 ± 0.0027	−0.02	1.00			
m_Z [GeV]	91.1874 ± 0.0021	−0.01	−0.02	1.00		
m_t [GeV]	178.5 ± 3.9	−0.05	0.11	−0.03	1.00	
$\log_{10}(m_H/\mathrm{GeV})$	2.11 ± 0.20	−0.46	0.18	0.06	0.67	1.00
m_H [GeV]	129^{+74}_{-49}	−0.46	0.18	0.06	0.67	1.00

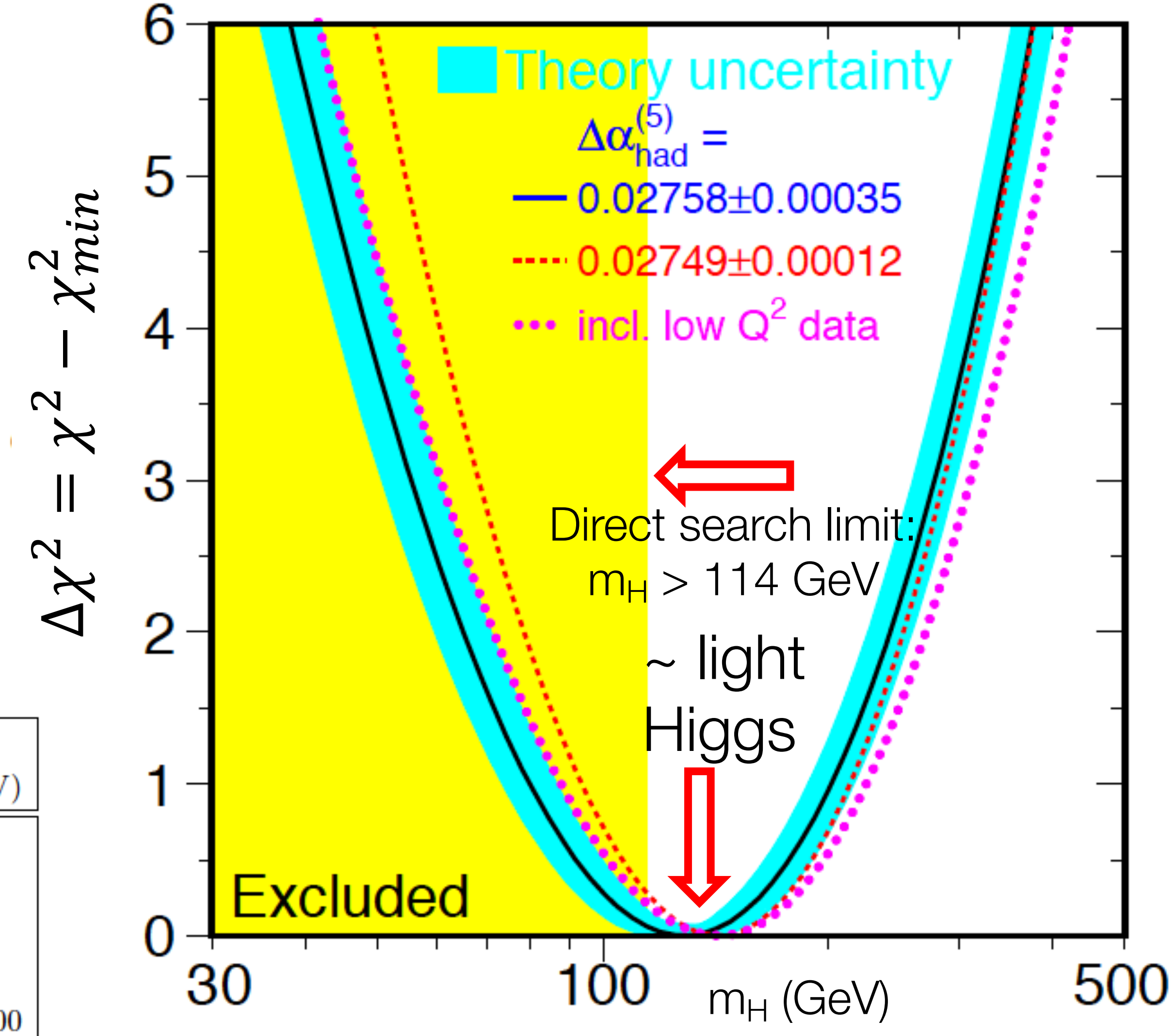

Direct search limit: m_H > 114 GeV

~ light Higgs

How Precisely one has to Measure m_W?

One could ask: down to which level do we need to know m_W?

the effect of higher order diagrams:

$$m_W^2\left(1-\frac{m_W^2}{m_Z^2}\right)=\frac{\pi\alpha}{\sqrt{2}G_F}(1+\Delta r)$$

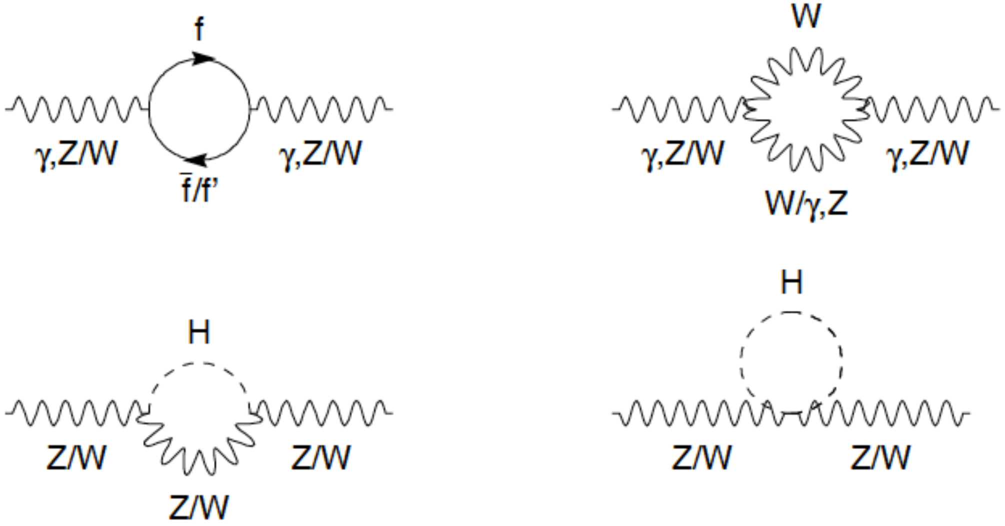

Δr:

- Dependence is quadratic on m_t → more visible
- Logarithmic on m_H → weak

In extended theories, Δr receives contributions from physics beyond the SM.

The current Particle Data Group gives the world average of m_W (dominated by the CDF and D0 measurements):

world average of $m_W = 80385 \pm 15$ MeV

Given the precisely measured values of , G_F and m_Z , and using m_t and m_H we can use the above relation to derive

SM prediction of $m_W = 80358 \pm 8$ MeV and $m_W = 80362 \pm 8$ MeV (different calculations).

The SM prediction uncertainty of 8 MeV represents therefore a target for the precision of future measurements of m_W.

W Mass Reconstruction at Colliders

We have seen that at LEP m_W could be reconstructed using ALL decays of the W. This is possible because

- Electrons and positrons are point-like objects
- The centre-of-mass energy is defined
- The background: both hadronic and leptonic decays
- Conservation of energy and momentum allows to calculate the momentum and direction of one undetected particle (like neutrinos in the decay $W \rightarrow \nu l$)

At hadronic collider machines there are difficulties in the use of hadronic decays:

- the QCD background is >>>>>>> the EW production of W's
- High energy W → the two jets $W \rightarrow qq'$ are ~merged. Sophisticated techniques look for internal structures in 'fat jets'.

In practice all m_W measurements at hadron colliders are based on the study of W's leptonic decays

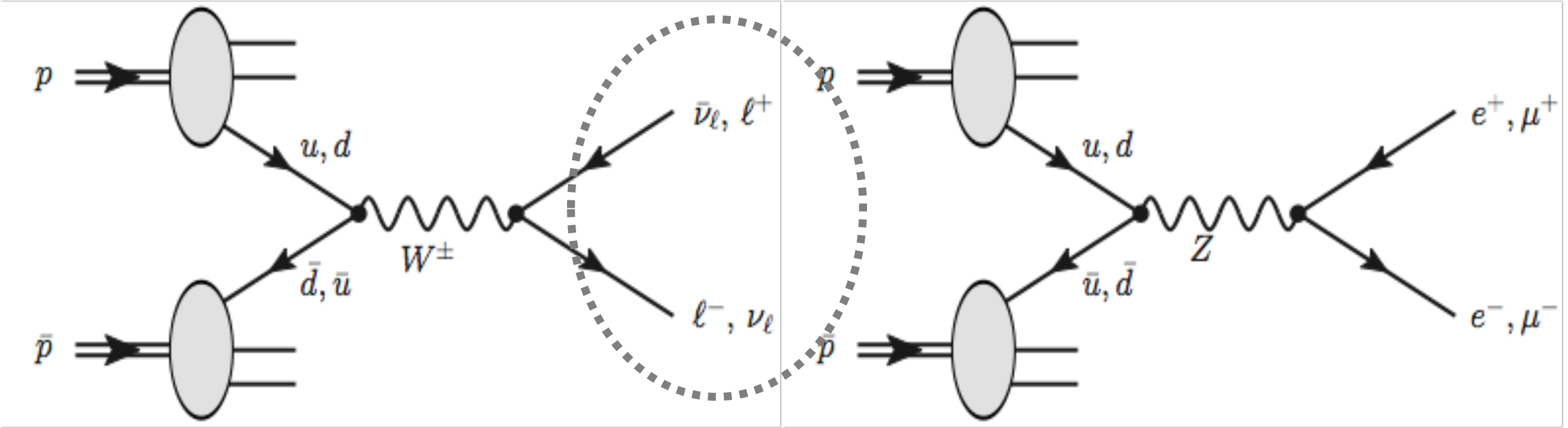

The Event Structure in W (and Z) Leptonic Decays

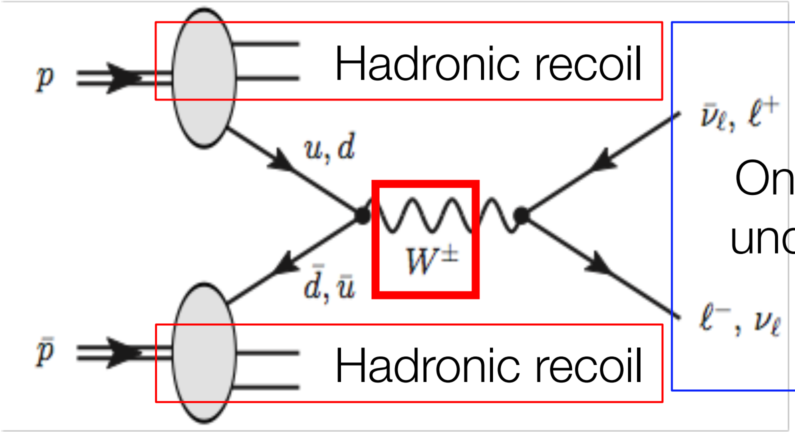

One lepton and one undetected neutrino

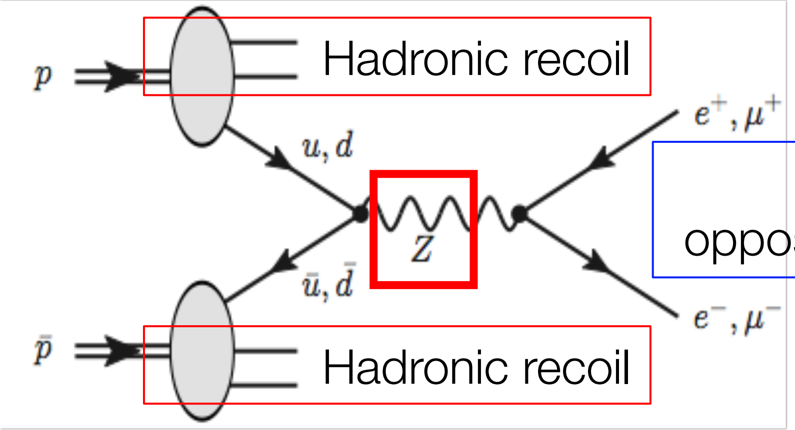

Two same flavour opposite charge leptons

Neutrino is not measured

$$\overrightarrow{p_T^{miss}} = -(\overrightarrow{p_T^l} + \overrightarrow{u_T})$$

Difficulty: p_T of the neutrino can be calculated only in the x-y plane.

→ how to compute the mass of the W using measurements in the transverse plane? → m_T

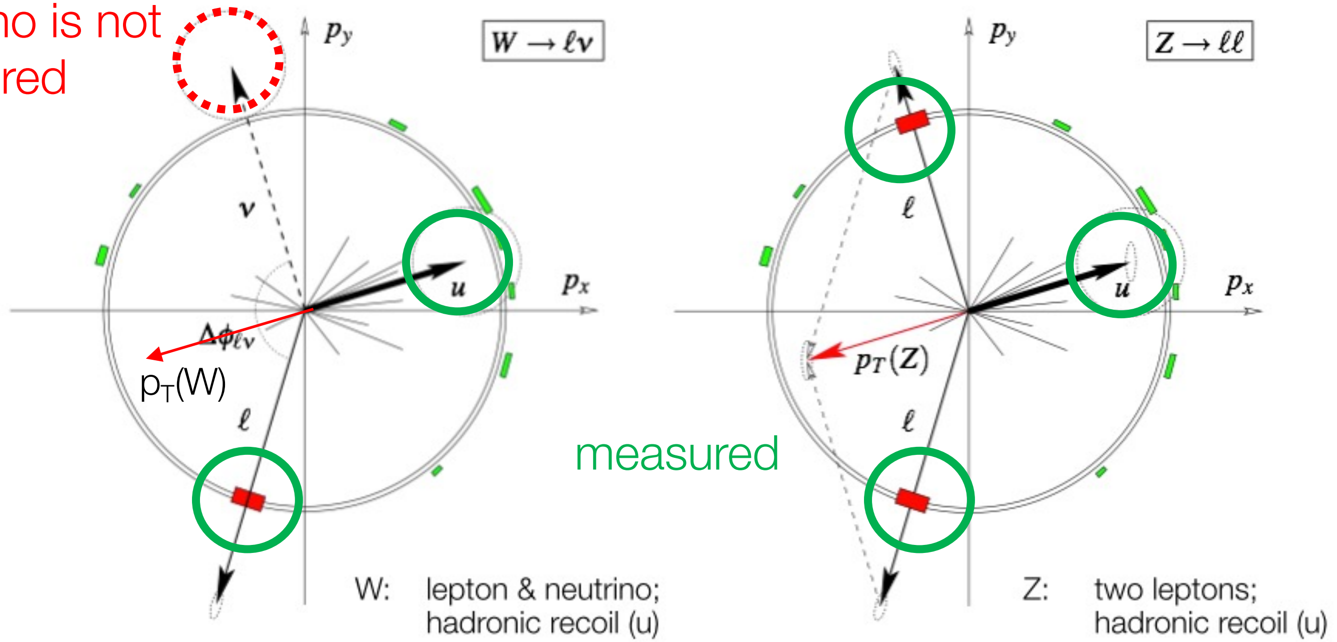

W: lepton & neutrino; hadronic recoil (u)

Z: two leptons; hadronic recoil (u)

W Mass Measurements at Hadron Colliders

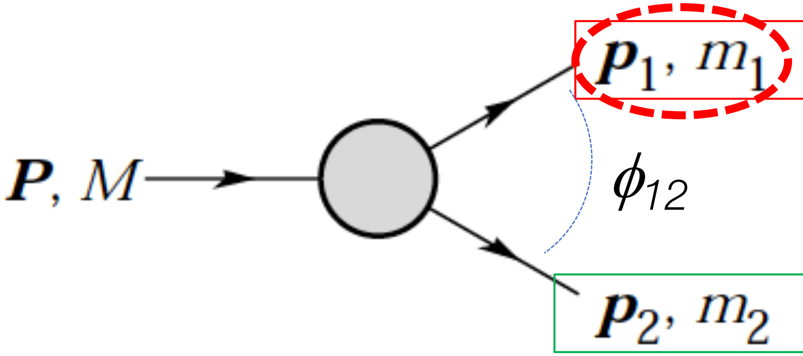

$\boldsymbol{p}_1, m_1$ Invisible particle (like νs in W decays)

$\boldsymbol{p}_2, m_2$ Visible particle (like leptons in W decays)

The mass of the parent particle can be constrained with the observable MT defined by

$$M_T^2 \equiv [E_T(1)+E_T(2)]^2 - [\boldsymbol{p}_T(1)+\boldsymbol{p}_T(2)]^2$$
$$= m_1^2+m_2^2+2[E_T(1)E_T(2)-\boldsymbol{p}_T(1)\cdot\boldsymbol{p}_T(2)]$$

where

$$p_T(1) = E_T^{miss}$$

For m1~m2~0→ $M_T^2 = 2|\boldsymbol{p}_T(1)||\boldsymbol{p}_T(2)|(1-\cos\phi_{12})$

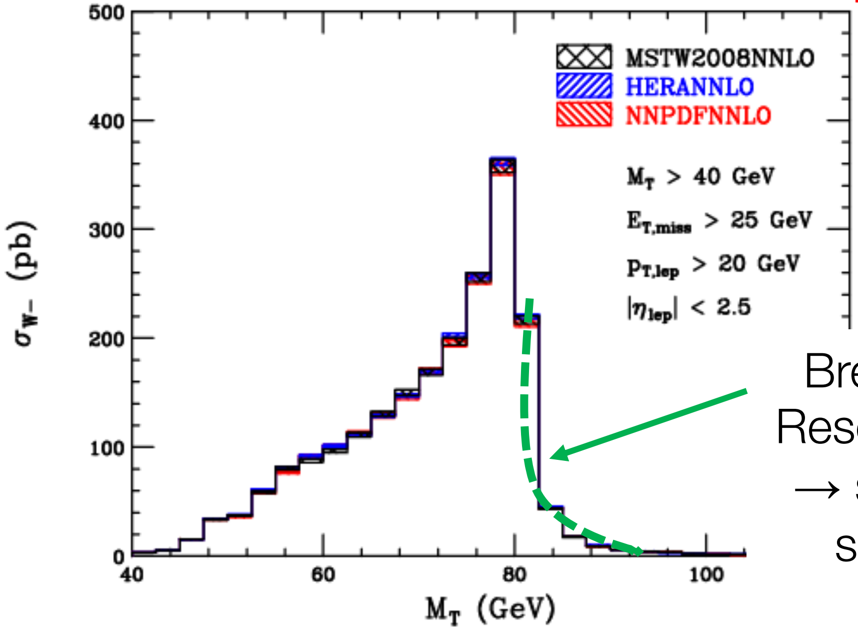

Breit-Wigner+
Resolution effect
→ sharp fall →
smooth fall

Important characteristic: the end point of this distribution is $M_T^{max} = M$

Also the distribution of the p$_T$ of the lepton has memory of m$_W$: the end-point is m$_W$/2

Effect on M_T of Resolution & Breit-Wigner Shape

Also the distribution of the p_T of the lepton has memory of m_W: the end-point is $m_W/2$

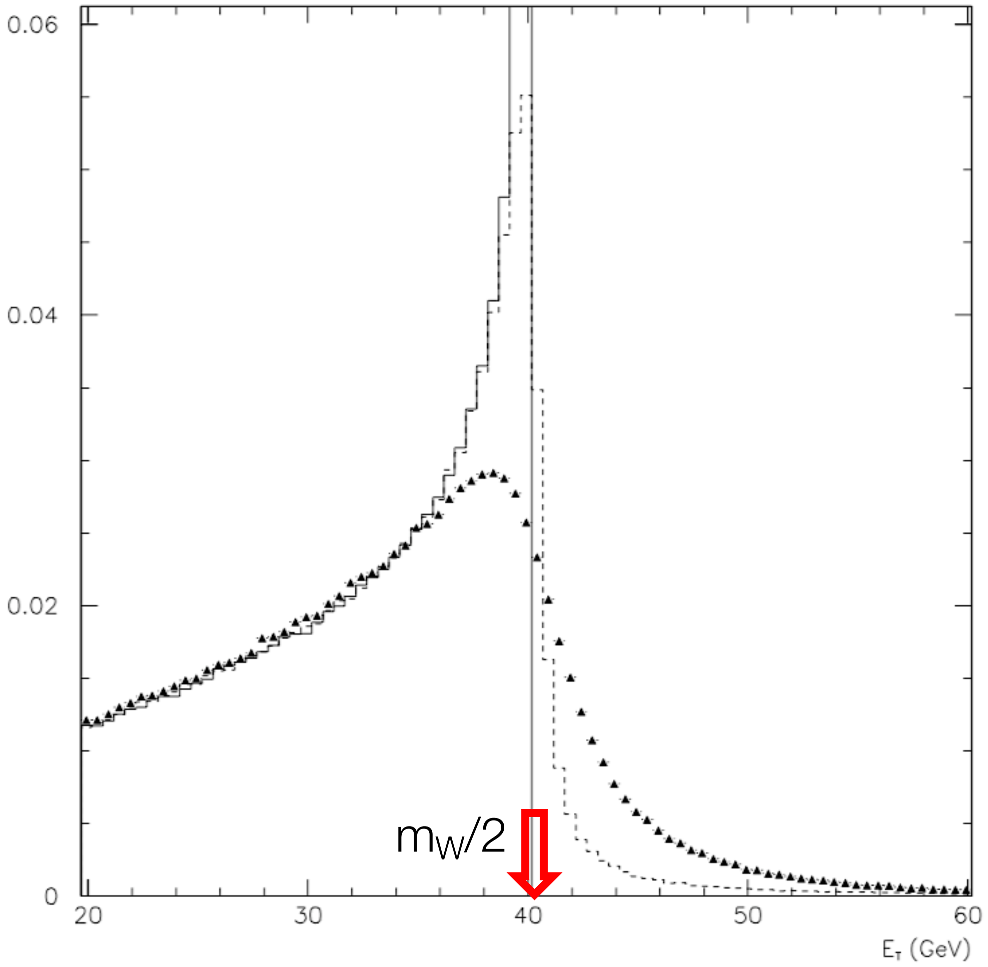

The figure ← shows the Jacobian peak of the p_T distribution when

- no Breit-Wigner distribution, ideal detector with perfect acceptance and resolution ———
- the W is produced according to a Breit-Wigner distribution, ideal detector with perfect acceptance and resolution ………
- Breit-Wigner distribution, detector with realistic acceptance and resolution ▲▲▲▲▲▲▲▲▲▲▲▲

→ the distribution becomes broader and broader

m_W and M_T (and p_T^l)

Strategy:

→ Generate MANY samples of simulated events including physics and detector effects with slightly different values of m_W and Γ_W and **find which one fits best the experimental M_T distribution.**

One needs to have excellent control of

- Physics effects (d(x), u(x) + QCD…)
- Detector effects

→ find ways to verify the quality of your simulation

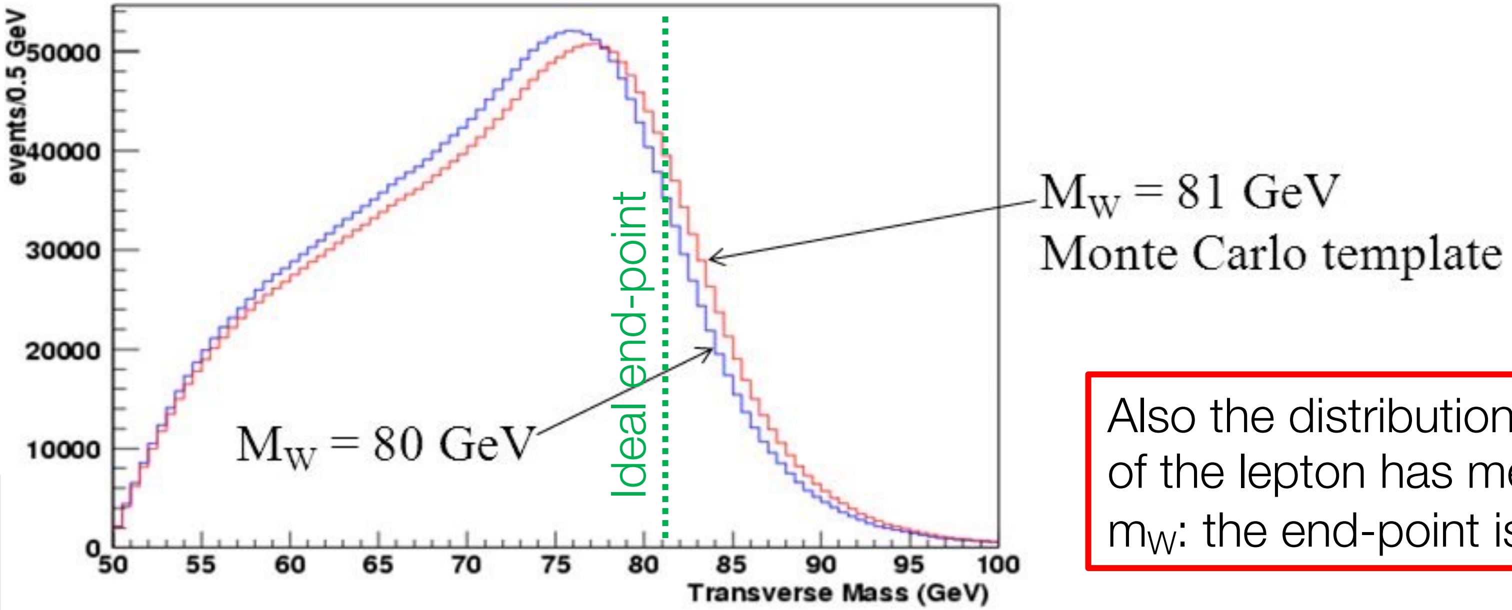

Also the distribution of the p_T of the lepton has memory of m_W: the end-point is $m_W/2$

m_W Measurement Strategy

The templates are compared to the observed distribution by means of a X^2 compatibility test.

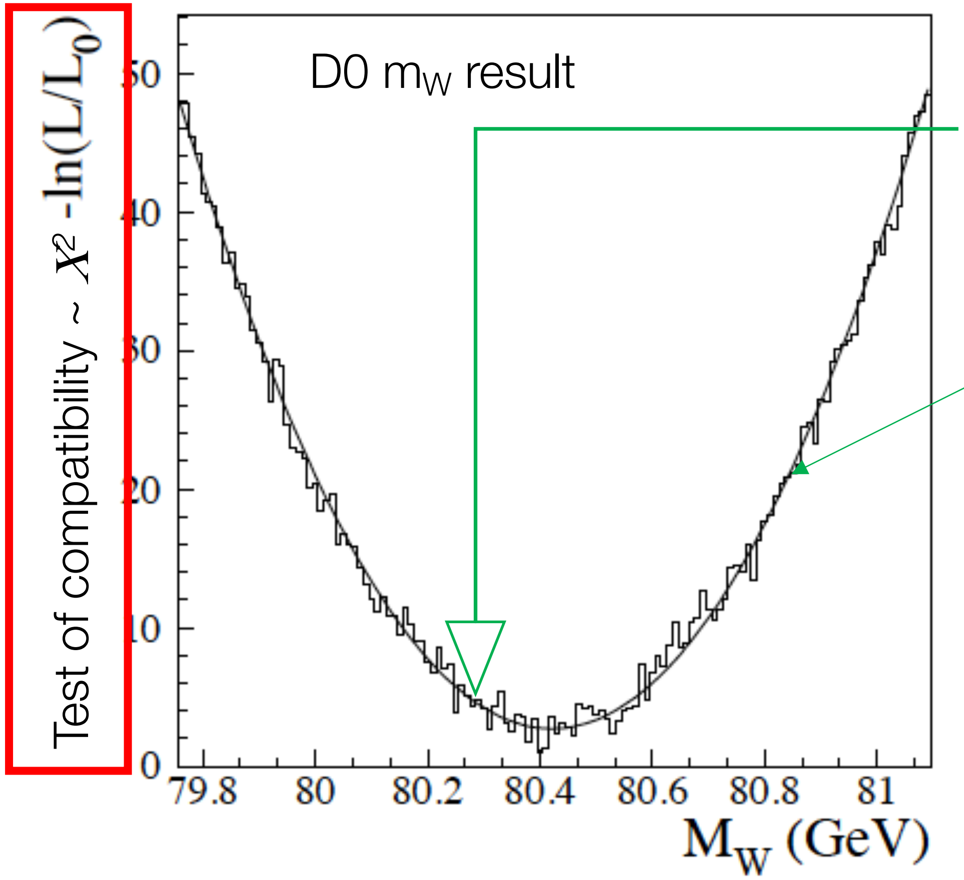

Each point of this ~parabola is the result of a comparison between data and simulated templates

The X^2 as a function of m_W is interpolated (solid line)

Problem: very many large (*) simulated samples with different values of m_W and Γ_W are needed.
Computer resources needed → affordable?
No!

The minimum of this curve gives the most probable value of m_W

(*) you want your simulated sample to be much larger than your data sample not to have a statistical error due to limited number of MC events!

$$N\ events\ \rightarrow \sigma_{stat} = \frac{1}{\sqrt{N}}$$

$$N_{simulated} \gg N_{data}$$

m_W Measurement Strategy: Simulation

- Predictions for different values of m_W from a single (.. a few) MC sample(s), by reweighting the W-boson Breit-Wigner distribution.
- In practice this is more complex but you manage to have many simulated samples starting from a few ones

Simulated samples are called “templates”

If you weight down $E<E_R$ and weight up $E>E_R$ you move to the right the peak of the Breit-Wigner

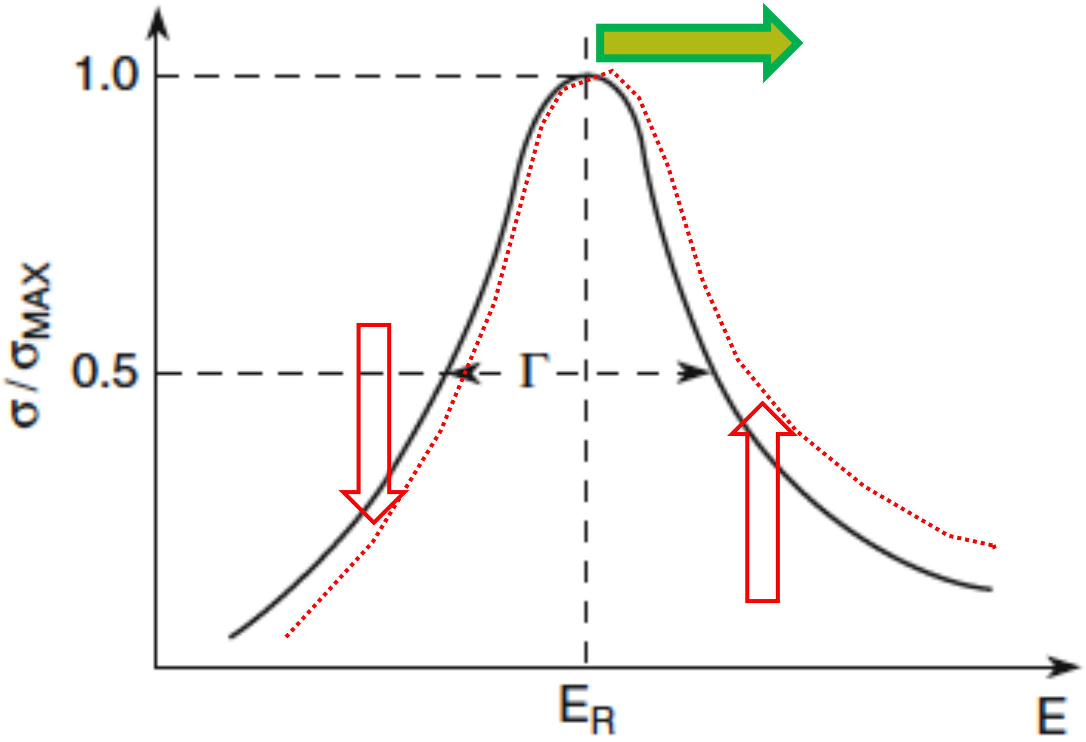

- The templates in small steps of of m_W:1 to 10 MeV around the reference value
- Systematic uncertainties due to physics-modelling corrections, detector-calibration corrections, and background subtraction, are studied.

m_W Measurement Strategy: Use Z Boson

- ~10^7 (10^6) W± to lν (Z to ll) → The sizes of these samples give a statistical error on m_W smaller than 10 MeV
- m_W is sensitive to the strange-quark and charm-quark distribution functions of the proton used in the of templates (less well known than u(x) and d(x)!)
- Use Z → *ll* events to calibrate the detector response: treat one of the reconstructed decay leptons as a neutrino.

The accuracy of this validation procedure is limited by Z-boson sample, ~ 10x smaller than the W sample.

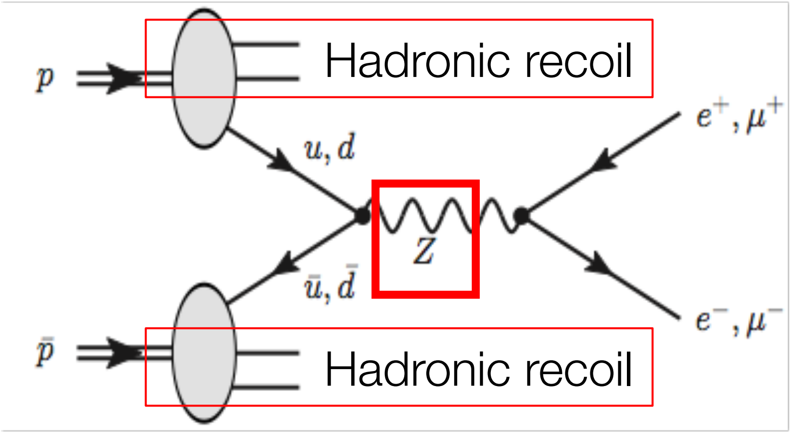

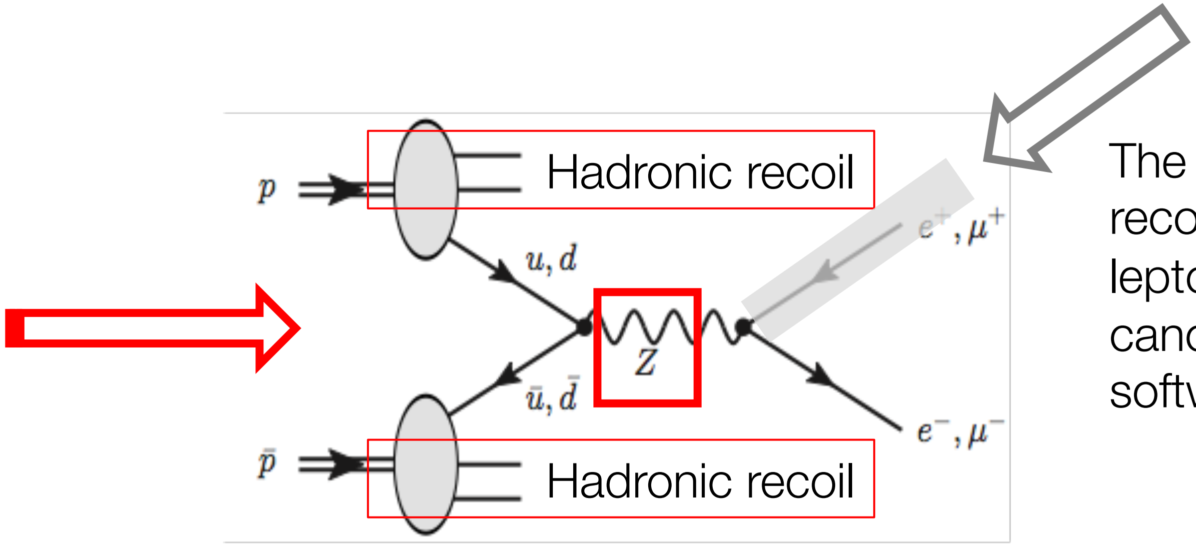

The reconstructed lepton is cancelled via software

CDF & D0

CDF

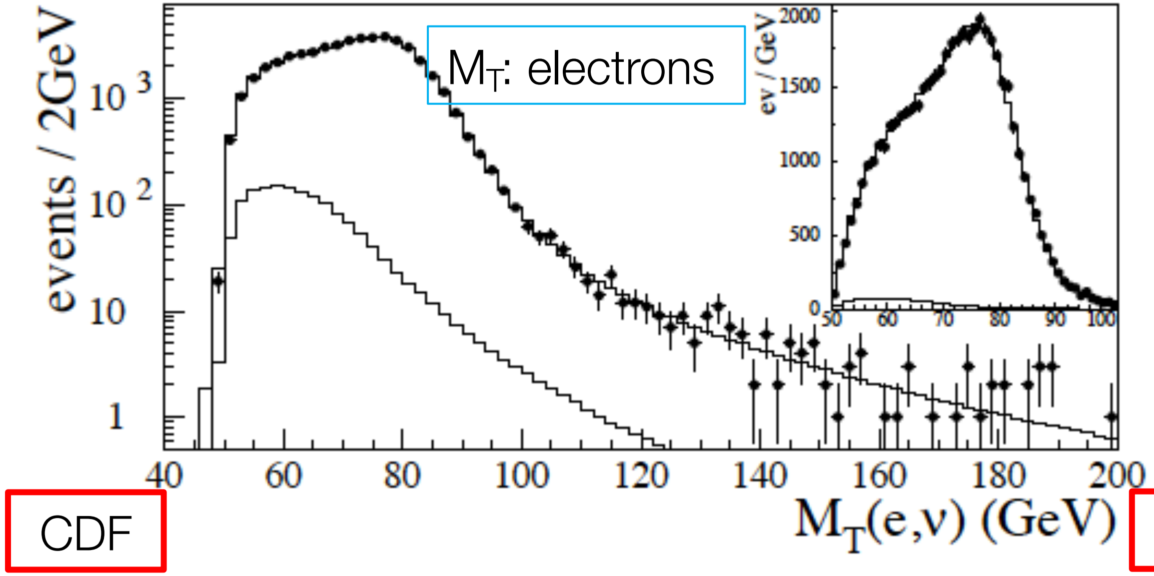
M_T: electrons

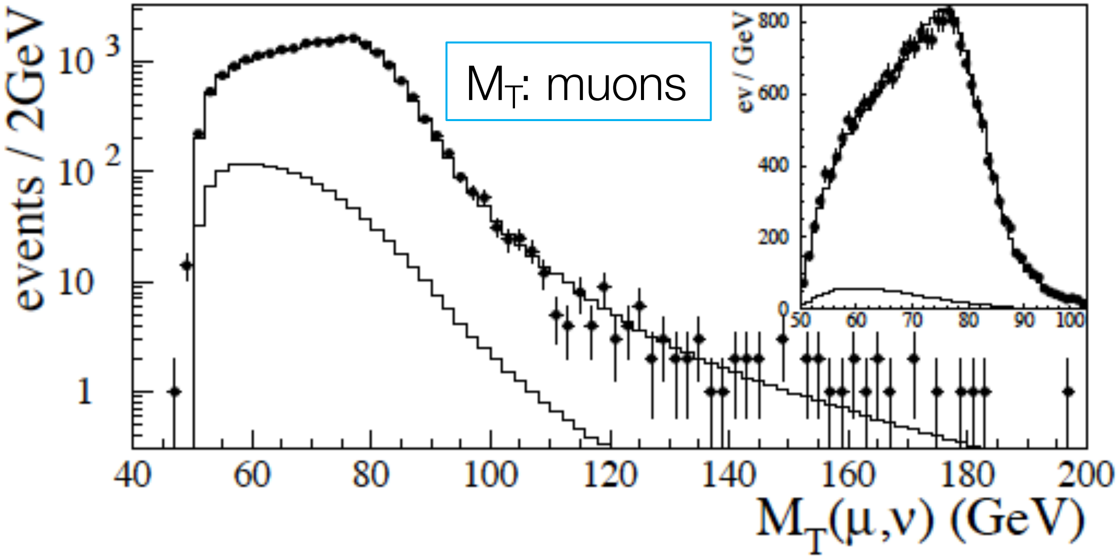
M_T: muons

D0

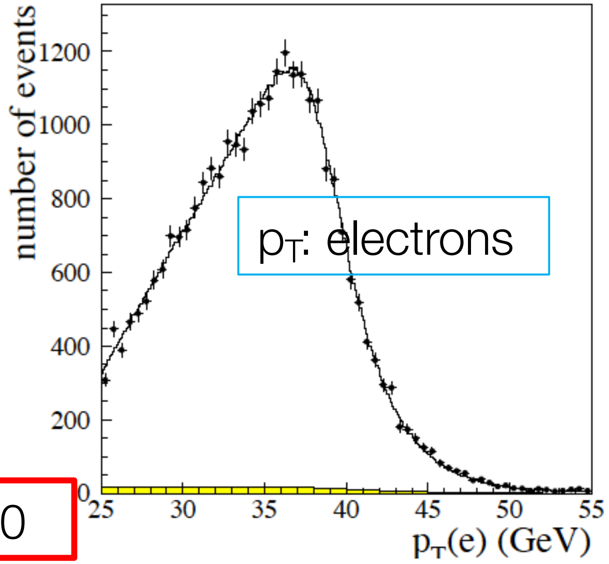
p_T: electrons

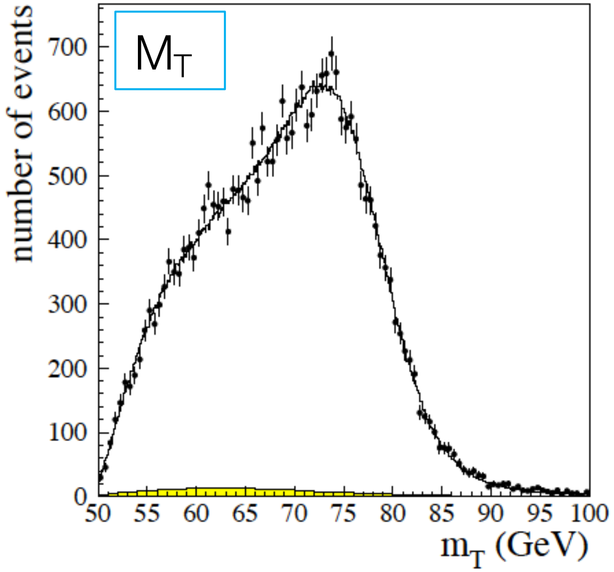
M_T

ATLAS: Uncertainty (Statistical and Systematic)

Result

Stat.Unc.

Systematic Unc.

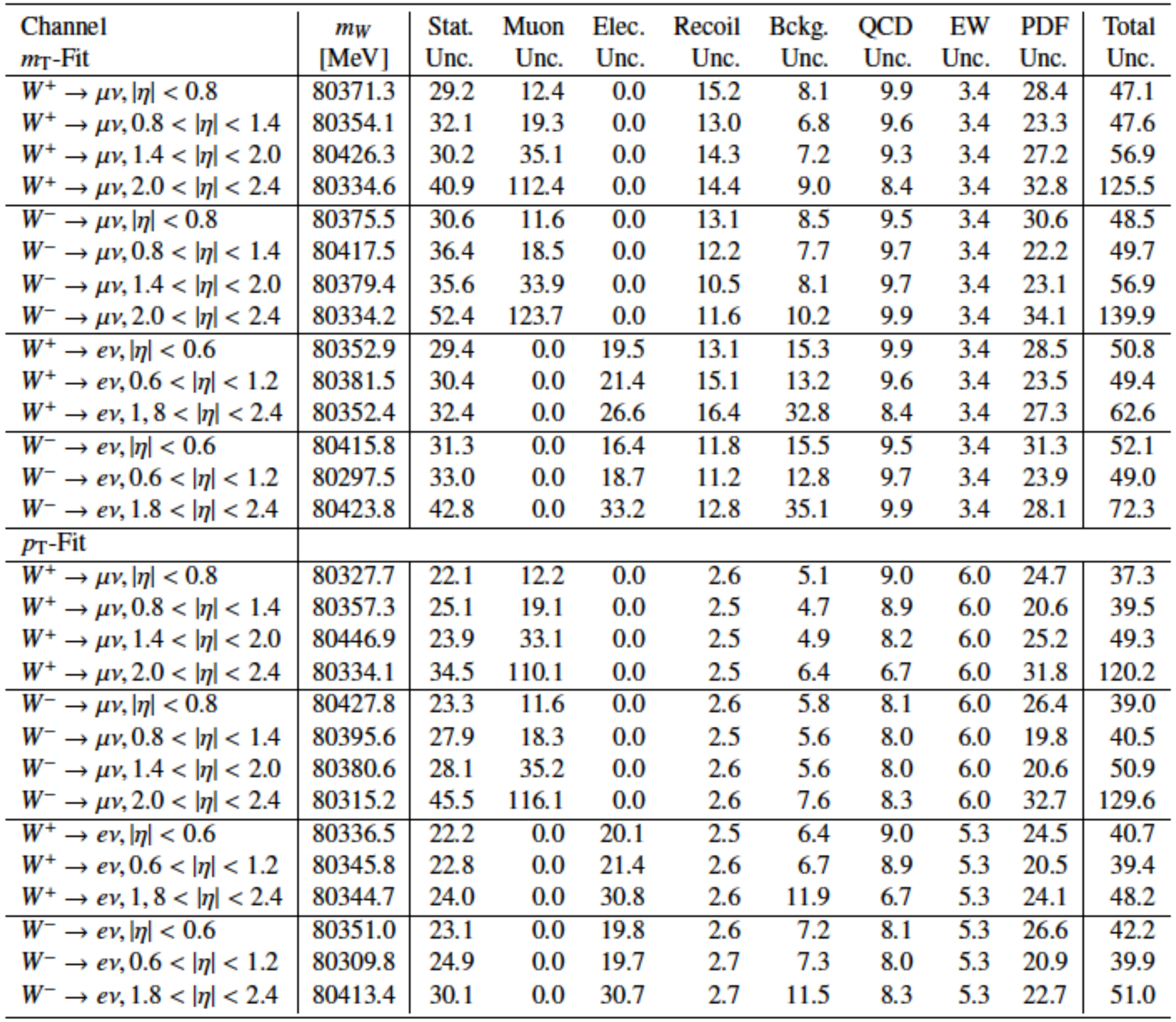

Channel m_T-Fit	m_W [MeV]	Stat. Unc.	Muon Unc.	Elec. Unc.	Recoil Unc.	Bckg. Unc.	QCD Unc.	EW Unc.	PDF Unc.	Total Unc.
$W^+ \to \mu\nu, \|\eta\| < 0.8$	80371.3	29.2	12.4	0.0	15.2	8.1	9.9	3.4	28.4	47.1
$W^+ \to \mu\nu, 0.8 < \|\eta\| < 1.4$	80354.1	32.1	19.3	0.0	13.0	6.8	9.6	3.4	23.3	47.6
$W^+ \to \mu\nu, 1.4 < \|\eta\| < 2.0$	80426.3	30.2	35.1	0.0	14.3	7.2	9.3	3.4	27.2	56.9
$W^+ \to \mu\nu, 2.0 < \|\eta\| < 2.4$	80334.6	40.9	112.4	0.0	14.4	9.0	8.4	3.4	32.8	125.5
$W^- \to \mu\nu, \|\eta\| < 0.8$	80375.5	30.6	11.6	0.0	13.1	8.5	9.5	3.4	30.6	48.5
$W^- \to \mu\nu, 0.8 < \|\eta\| < 1.4$	80417.5	36.4	18.5	0.0	12.2	7.7	9.7	3.4	22.2	49.7
$W^- \to \mu\nu, 1.4 < \|\eta\| < 2.0$	80379.4	35.6	33.9	0.0	10.5	8.1	9.7	3.4	23.1	56.9
$W^- \to \mu\nu, 2.0 < \|\eta\| < 2.4$	80334.2	52.4	123.7	0.0	11.6	10.2	9.9	3.4	34.1	139.9
$W^+ \to e\nu, \|\eta\| < 0.6$	80352.9	29.4	0.0	19.5	13.1	15.3	9.9	3.4	28.5	50.8
$W^+ \to e\nu, 0.6 < \|\eta\| < 1.2$	80381.5	30.4	0.0	21.4	15.1	13.2	9.6	3.4	23.5	49.4
$W^+ \to e\nu, 1, 8 < \|\eta\| < 2.4$	80352.4	32.4	0.0	26.6	16.4	32.8	8.4	3.4	27.3	62.6
$W^- \to e\nu, \|\eta\| < 0.6$	80415.8	31.3	0.0	16.4	11.8	15.5	9.5	3.4	31.3	52.1
$W^- \to e\nu, 0.6 < \|\eta\| < 1.2$	80297.5	33.0	0.0	18.7	11.2	12.8	9.7	3.4	23.9	49.0
$W^- \to e\nu, 1.8 < \|\eta\| < 2.4$	80423.8	42.8	0.0	33.2	12.8	35.1	9.9	3.4	28.1	72.3
p_T-Fit										
$W^+ \to \mu\nu, \|\eta\| < 0.8$	80327.7	22.1	12.2	0.0	2.6	5.1	9.0	6.0	24.7	37.3
$W^+ \to \mu\nu, 0.8 < \|\eta\| < 1.4$	80357.3	25.1	19.1	0.0	2.5	4.7	8.9	6.0	20.6	39.5
$W^+ \to \mu\nu, 1.4 < \|\eta\| < 2.0$	80446.9	23.9	33.1	0.0	2.5	4.9	8.2	6.0	25.2	49.3
$W^+ \to \mu\nu, 2.0 < \|\eta\| < 2.4$	80334.1	34.5	110.1	0.0	2.5	6.4	6.7	6.0	31.8	120.2
$W^- \to \mu\nu, \|\eta\| < 0.8$	80427.8	23.3	11.6	0.0	2.6	5.8	8.1	6.0	26.4	39.0
$W^- \to \mu\nu, 0.8 < \|\eta\| < 1.4$	80395.6	27.9	18.3	0.0	2.5	5.6	8.0	6.0	19.8	40.5
$W^- \to \mu\nu, 1.4 < \|\eta\| < 2.0$	80380.6	28.1	35.2	0.0	2.6	5.6	8.0	6.0	20.6	50.9
$W^- \to \mu\nu, 2.0 < \|\eta\| < 2.4$	80315.2	45.5	116.1	0.0	2.6	7.6	8.3	6.0	32.7	129.6
$W^+ \to e\nu, \|\eta\| < 0.6$	80336.5	22.2	0.0	20.1	2.5	6.4	9.0	5.3	24.5	40.7
$W^+ \to e\nu, 0.6 < \|\eta\| < 1.2$	80345.8	22.8	0.0	21.4	2.6	6.7	8.9	5.3	20.5	39.4
$W^+ \to e\nu, 1, 8 < \|\eta\| < 2.4$	80344.7	24.0	0.0	30.8	2.6	11.9	6.7	5.3	24.1	48.2
$W^- \to e\nu, \|\eta\| < 0.6$	80351.0	23.1	0.0	19.8	2.6	7.2	8.1	5.3	26.6	42.2
$W^- \to e\nu, 0.6 < \|\eta\| < 1.2$	80309.8	24.9	0.0	19.7	2.7	7.3	8.0	5.3	20.9	39.9
$W^- \to e\nu, 1.8 < \|\eta\| < 2.4$	80413.4	30.1	0.0	30.7	2.7	11.5	8.3	5.3	22.7	51.0

Error → Uncertainty, more correct

Systematic effects include knowledge of

- background,
- trigger efficiency,
- energy resolution,
- detector efficiency
- …

systematic error.

Strategy for handling systematic errors:

- All parameters of your analysis are known with some precision:
- You do your analysis with best values of your parameters;
- you repeat it with one ‘detector’ or ‘theory’ parameter changed by your uncertainty
  → the variation on your result is a systematic uncertainty

ATLAS Results

$W^+ \to e\nu$ $W^- \to e\nu$

p_T^l

M_T

p_T^{miss}

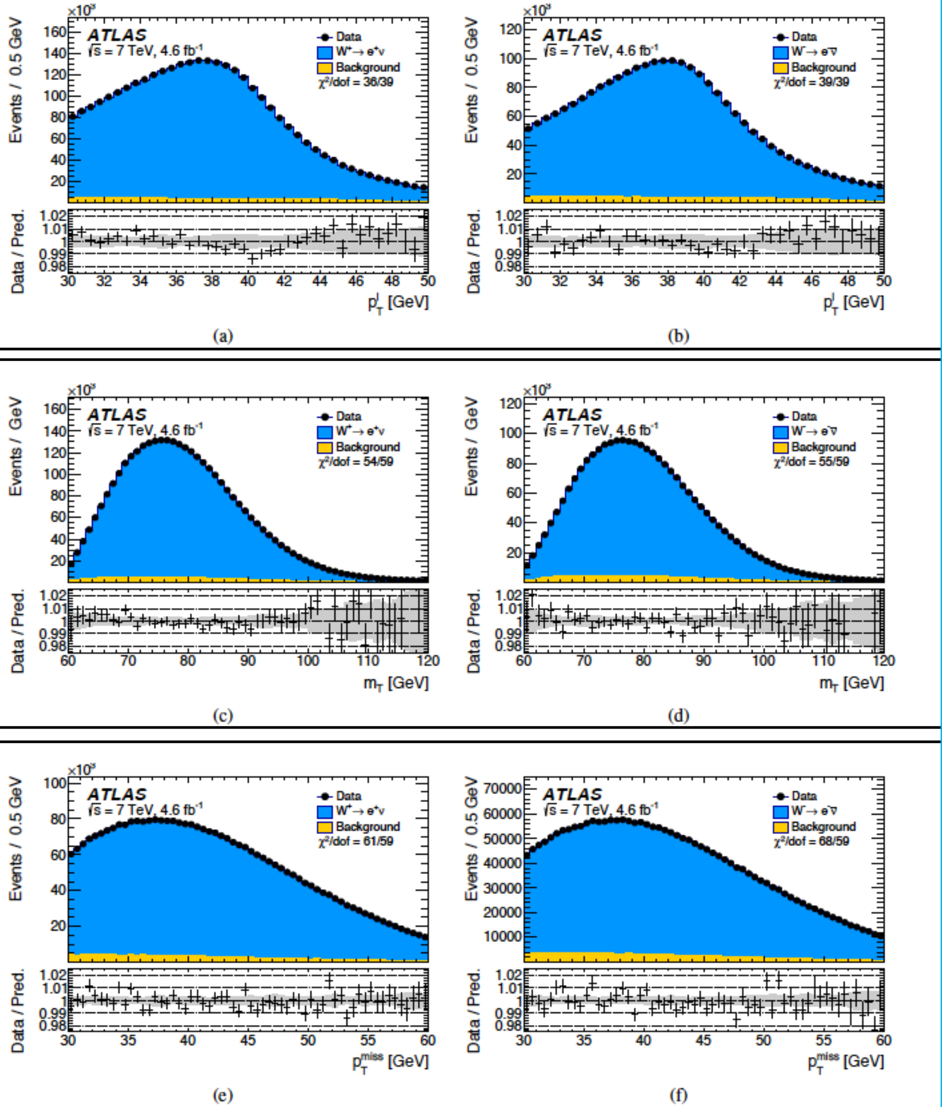

(a) (b) (c) (d) (e) (f)

$W^+ \to \mu\nu$ $W^- \to \mu\nu$

p_T^l

M_T

p_T^{miss}

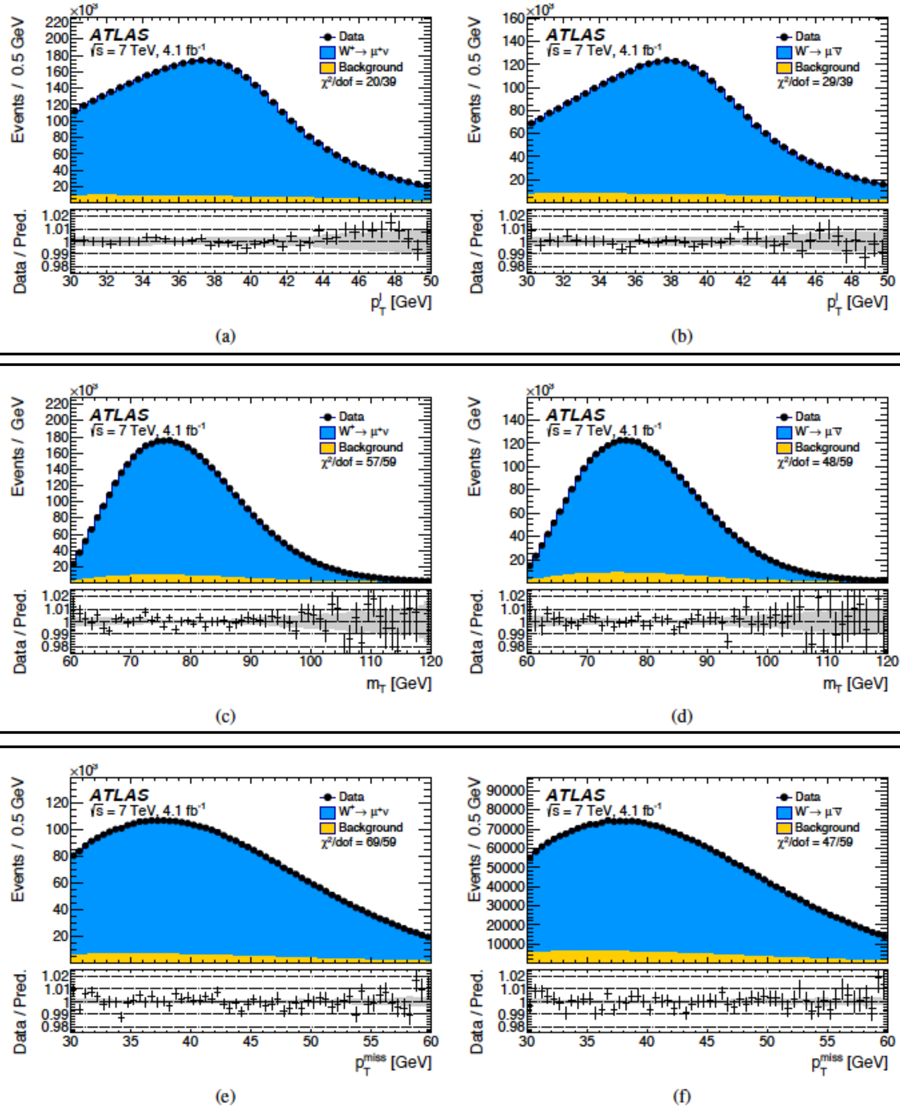

(a) (b) (c) (d) (e) (f)

$\frac{d\sigma}{d|\eta_l|}$ for W+ and W-

W+ cross section is larger and flatter than the corresponding W- cross section. Why?

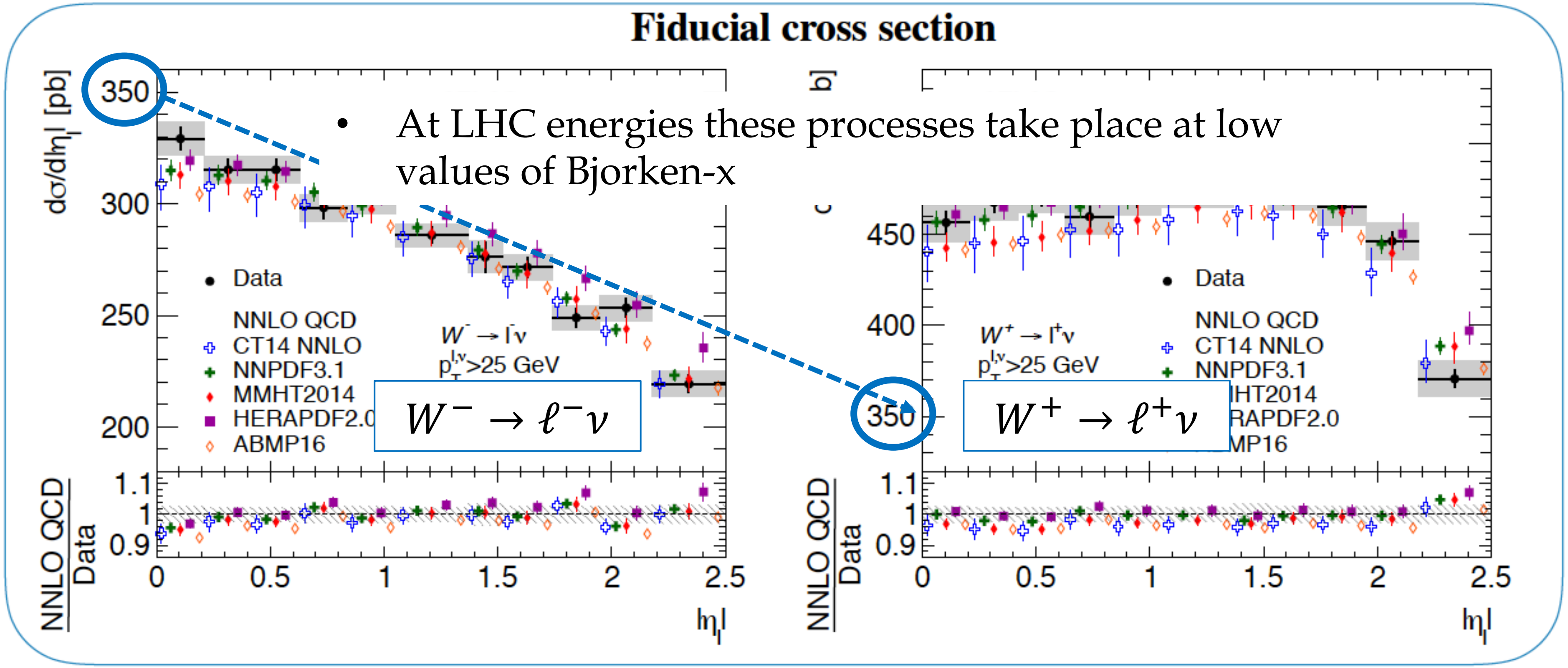

- At LHC energies these processes take place at low values of Bjorken-x

$W^- \rightarrow \ell^- \nu$

$W^+ \rightarrow \ell^+ \nu$

$$y = \frac{1}{2}\left(\frac{E+p_z}{E-p_z}\right)$$
$$\sim \eta \; for \; p \gg m$$

Z production main contributions:

$d\bar{d} \rightarrow Z$

$u\bar{u} \rightarrow Z$

W production main contributions:

$u\bar{d} \rightarrow W^+$

$d\bar{u} \rightarrow W^-$

These processes need both quarks and anti-quarks

$$proton = uud, \overline{proton} = \bar{u}\bar{u}\bar{d}$$

→ Tevatron ($p\bar{p}$ collider) has both quarks and valence anti-quarks → ~high values of Bjorken x

→ LHC (pp collider) has quarks and sea anti-quarks → low values of Bjorken x

$\frac{d\sigma}{d|\eta_l|}$ for W+ and W-

W production main contributions: $u\bar{d} \rightarrow W^+$; $d\bar{u} \rightarrow W^-$ $(proton = uud \rightarrow 1d + 2u)$

Assuming $\bar{d} \approx \bar{u} \rightarrow {}^{\sigma_{W+}}/_{\sigma_{W-}} \approx \frac{u\bar{d}}{d\bar{u}} \approx \frac{u}{d} \rightarrow \frac{{}^{d\sigma}/_{d\eta}(W^-)}{{}^{d\sigma}/_{d\eta}(W^+)} \approx \frac{d(x)\bar{u}(x)}{u(x)\bar{d}(x)} \approx \frac{d(x)}{u(x)}$

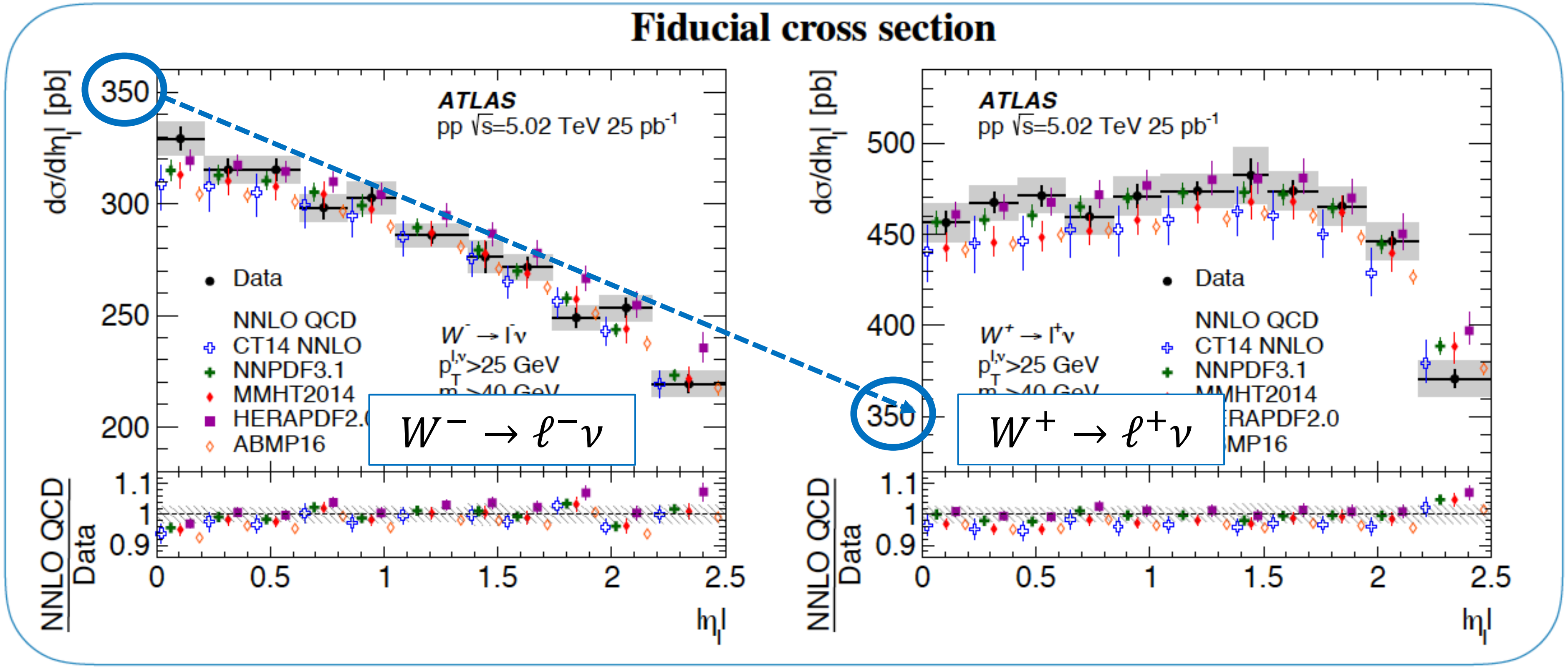

→ at LHC

$\sigma(W^-) \approx \frac{1}{2}\sigma(W^+)$

W Physics at LHC

$$\text{Assuming } \bar{d} \approx \bar{u} \rightarrow {}^{\sigma_{W^+}}/_{\sigma_{W_-}} \approx \frac{u\bar{d}}{d\bar{u}} \approx \frac{u}{d} \rightarrow \frac{{}^{d\sigma}/_{d\eta}(W^-)}{{}^{d\sigma}/_{d\eta}(W^+)} \approx \frac{d(x)\bar{u}(x)}{u(x)\bar{d}(x)} \approx \frac{d(x)}{u(x)}$$

$(proton = uud \rightarrow 1d + 2u)$

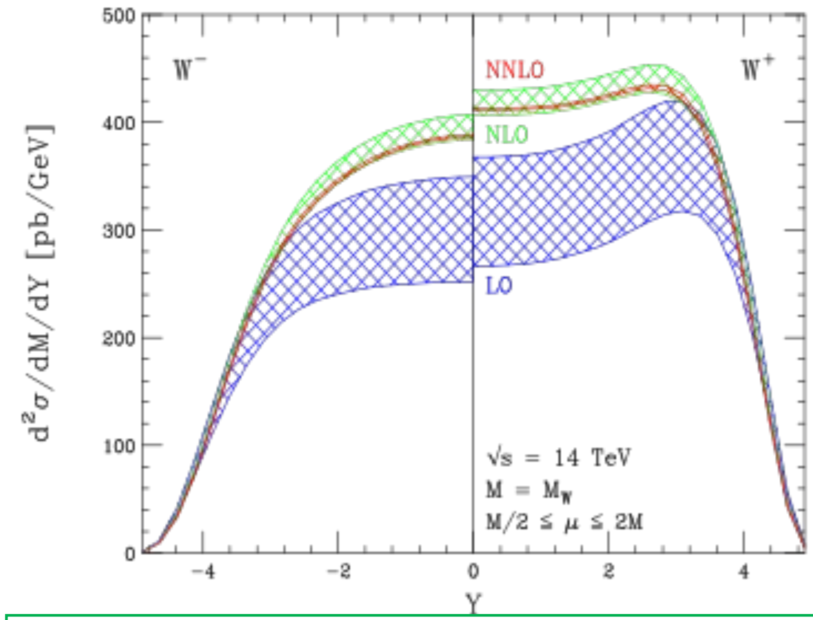

$$y = \frac{1}{2}\ln\left(\frac{E+p_z}{E-p_z}\right) \qquad y = \frac{1}{2}\ln\frac{\cos^2(\theta/2)+m^2/4p^2+\ldots}{\sin^2(\theta/2)+m^2/4p^2+\ldots}$$

$$\approx -\ln\tan(\theta/2) \equiv \eta$$

Proton-Proton Collider:

→ u(x) > d(x) for large x (valence quarks) → more W⁺ at positive rapidity

always more W⁺ than W⁻

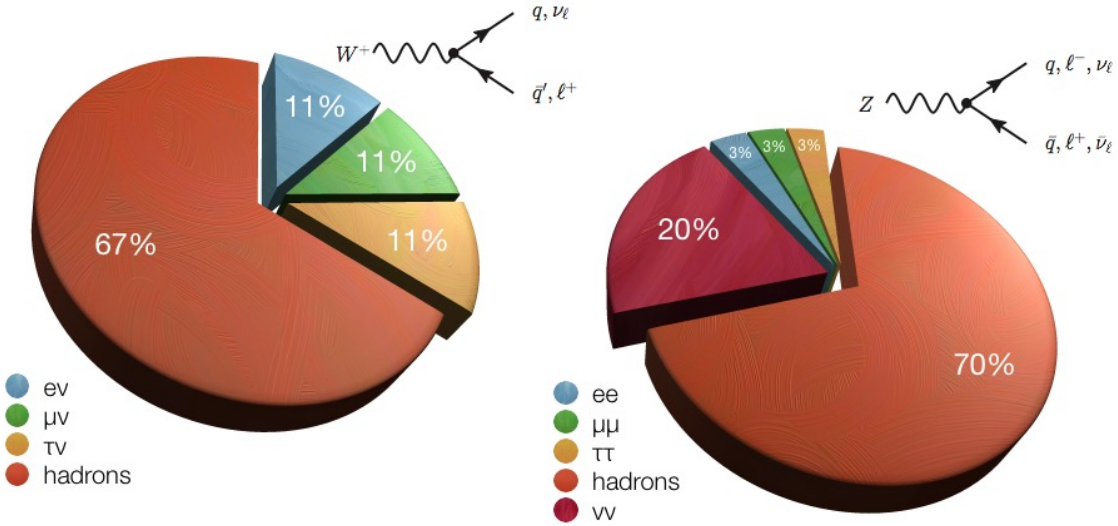

Global EW fits – Input Parameters

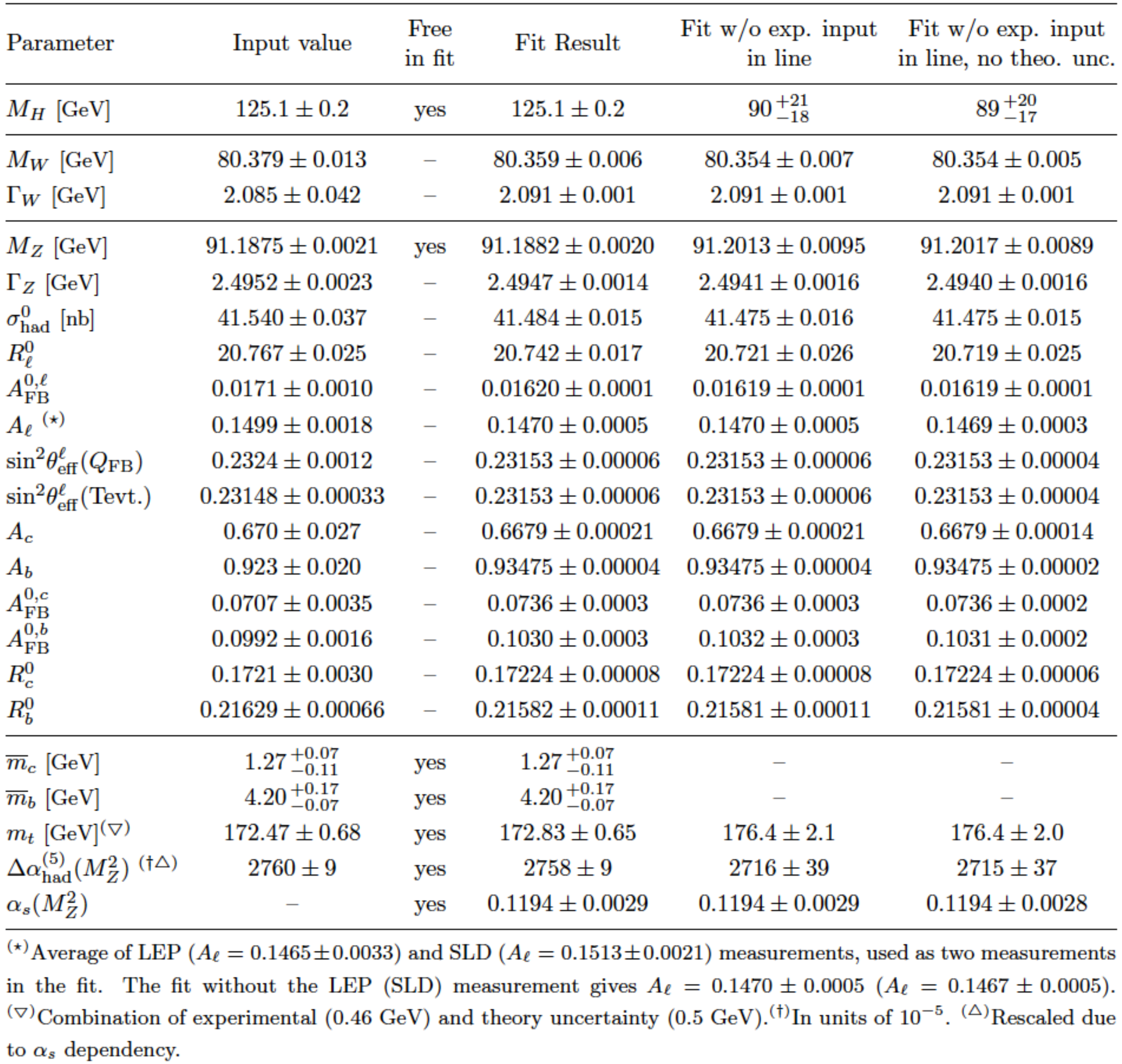

Parameter	Input value	Free in fit	Fit Result	Fit w/o exp. input in line	Fit w/o exp. input in line, no theo. unc.
M_H [GeV]	125.1 ± 0.2	yes	125.1 ± 0.2	90^{+21}_{-18}	89^{+20}_{-17}
M_W [GeV]	80.379 ± 0.013	–	80.359 ± 0.006	80.354 ± 0.007	80.354 ± 0.005
Γ_W [GeV]	2.085 ± 0.042	–	2.091 ± 0.001	2.091 ± 0.001	2.091 ± 0.001
M_Z [GeV]	91.1875 ± 0.0021	yes	91.1882 ± 0.0020	91.2013 ± 0.0095	91.2017 ± 0.0089
Γ_Z [GeV]	2.4952 ± 0.0023	–	2.4947 ± 0.0014	2.4941 ± 0.0016	2.4940 ± 0.0016
$\sigma^0_{\rm had}$ [nb]	41.540 ± 0.037	–	41.484 ± 0.015	41.475 ± 0.016	41.475 ± 0.015
R^0_ℓ	20.767 ± 0.025	–	20.742 ± 0.017	20.721 ± 0.026	20.719 ± 0.025
$A^{0,\ell}_{\rm FB}$	0.0171 ± 0.0010	–	0.01620 ± 0.0001	0.01619 ± 0.0001	0.01619 ± 0.0001
A_ℓ $^{(\star)}$	0.1499 ± 0.0018	–	0.1470 ± 0.0005	0.1470 ± 0.0005	0.1469 ± 0.0003
$\sin^2\theta^\ell_{\rm eff}(Q_{\rm FB})$	0.2324 ± 0.0012	–	0.23153 ± 0.00006	0.23153 ± 0.00006	0.23153 ± 0.00004
$\sin^2\theta^\ell_{\rm eff}$(Tevt.)	0.23148 ± 0.00033	–	0.23153 ± 0.00006	0.23153 ± 0.00006	0.23153 ± 0.00004
A_c	0.670 ± 0.027	–	0.6679 ± 0.00021	0.6679 ± 0.00021	0.6679 ± 0.00014
A_b	0.923 ± 0.020	–	0.93475 ± 0.00004	0.93475 ± 0.00004	0.93475 ± 0.00002
$A^{0,c}_{\rm FB}$	0.0707 ± 0.0035	–	0.0736 ± 0.0003	0.0736 ± 0.0003	0.0736 ± 0.0002
$A^{0,b}_{\rm FB}$	0.0992 ± 0.0016	–	0.1030 ± 0.0003	0.1032 ± 0.0003	0.1031 ± 0.0002
R^0_c	0.1721 ± 0.0030	–	0.17224 ± 0.00008	0.17224 ± 0.00008	0.17224 ± 0.00006
R^0_b	0.21629 ± 0.00066	–	0.21582 ± 0.00011	0.21581 ± 0.00011	0.21581 ± 0.00004
$\overline{m}_c$ [GeV]	$1.27^{+0.07}_{-0.11}$	yes	$1.27^{+0.07}_{-0.11}$	–	–
$\overline{m}_b$ [GeV]	$4.20^{+0.17}_{-0.07}$	yes	$4.20^{+0.17}_{-0.07}$	–	–
m_t [GeV]$^{(\triangledown)}$	172.47 ± 0.68	yes	172.83 ± 0.65	176.4 ± 2.1	176.4 ± 2.0
$\Delta\alpha^{(5)}_{\rm had}(M_Z^2)$ $^{(\dagger\triangle)}$	2760 ± 9	yes	2758 ± 9	2716 ± 39	2715 ± 37
$\alpha_s(M_Z^2)$	–	yes	0.1194 ± 0.0029	0.1194 ± 0.0029	0.1194 ± 0.0028

$^{(\star)}$Average of LEP ($A_\ell = 0.1465 \pm 0.0033$) and SLD ($A_\ell = 0.1513 \pm 0.0021$) measurements, used as two measurements in the fit. The fit without the LEP (SLD) measurement gives $A_\ell = 0.1470 \pm 0.0005$ ($A_\ell = 0.1467 \pm 0.0005$). $^{(\triangledown)}$Combination of experimental (0.46 GeV) and theory uncertainty (0.5 GeV).$^{(\dagger)}$In units of 10^{-5}. $^{(\triangle)}$Rescaled due to α_s dependency.

Input values and fit results for the observables used in the global electroweak fit.

1. the observables/parameters used in the fit
2. their experimental values or estimates
3. indicates whether a parameter is floating in the fit.
4. the results of the fit including all experimental data.
5. fit results are given without using the corresponding experimental or phenomenological estimate in the given row (indirect determination).
6. result using the same setup as in the fifth column, but ignoring all theoretical uncertainties.

Toni Baroncelli: Precision Measurements

Global EW fits - 1

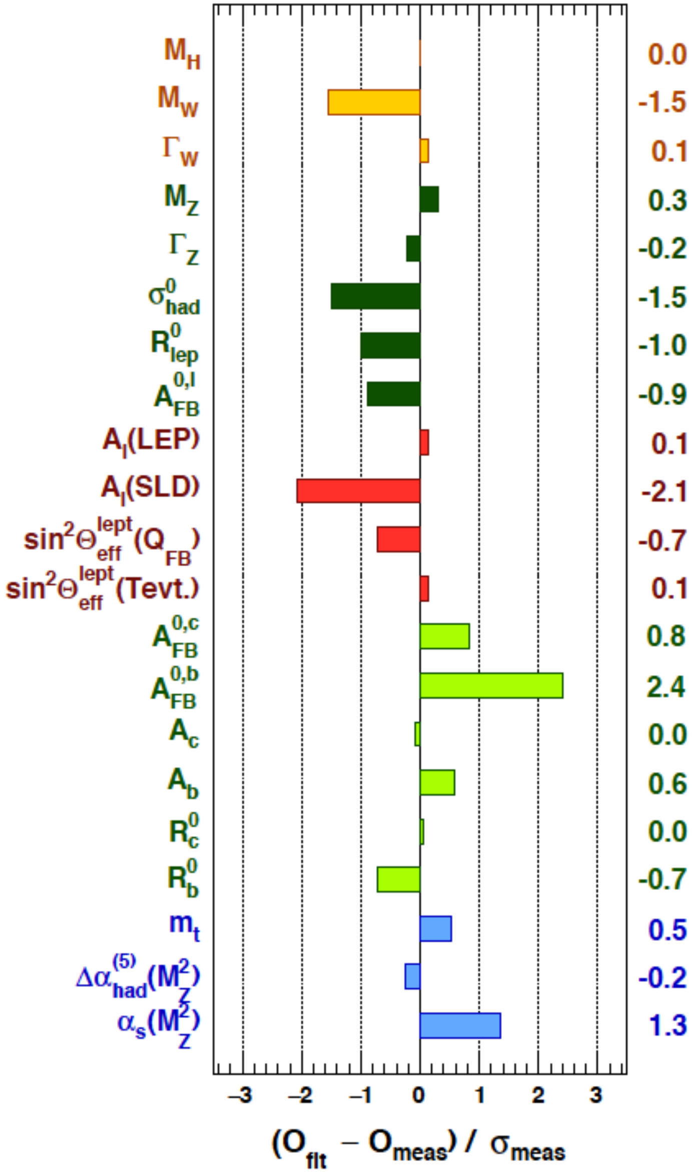

Comparison of the results with the indirect determination in units of the total uncertainty, defined as the uncertainty of the direct measurement and that of the indirect determination added in quadrature.

The indirect determination of an observable corresponds to a fit without using the corresponding direct constraint from the measurement.

$$\boxed{\frac{Result - Indirect\ Determination}{\sqrt{\sigma^2_{Result} + \sigma^2_{Ind.Det.}}}}$$

In the context of global fits to the SM parameters, constraints on physics beyond the SM are currently limited by the measurement of the W-boson mass. Therefore improving the precision of the measurements of m_W is of high importance for testing the overall consistency of the SM.

ATLAS paper

Toni Baroncelli: Precision Measurements

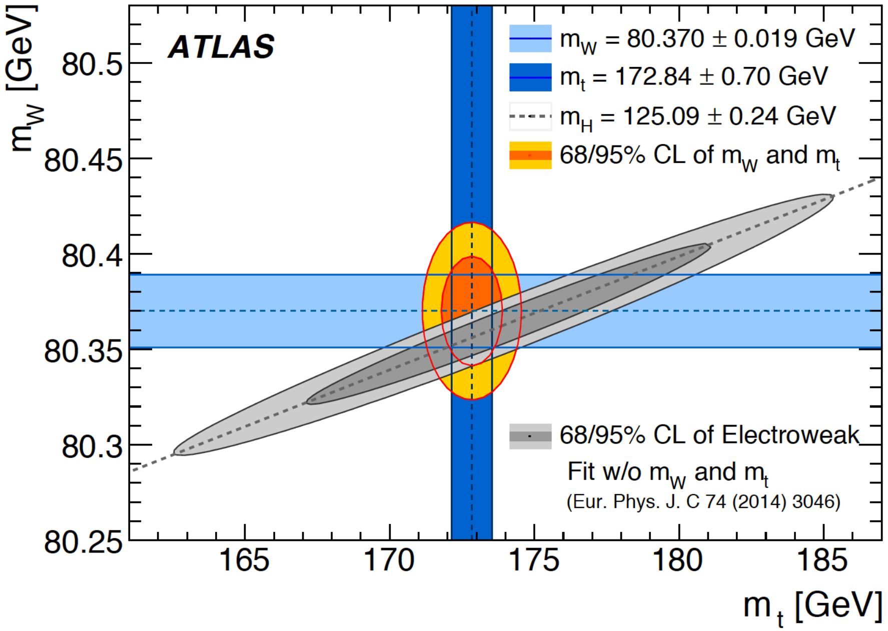

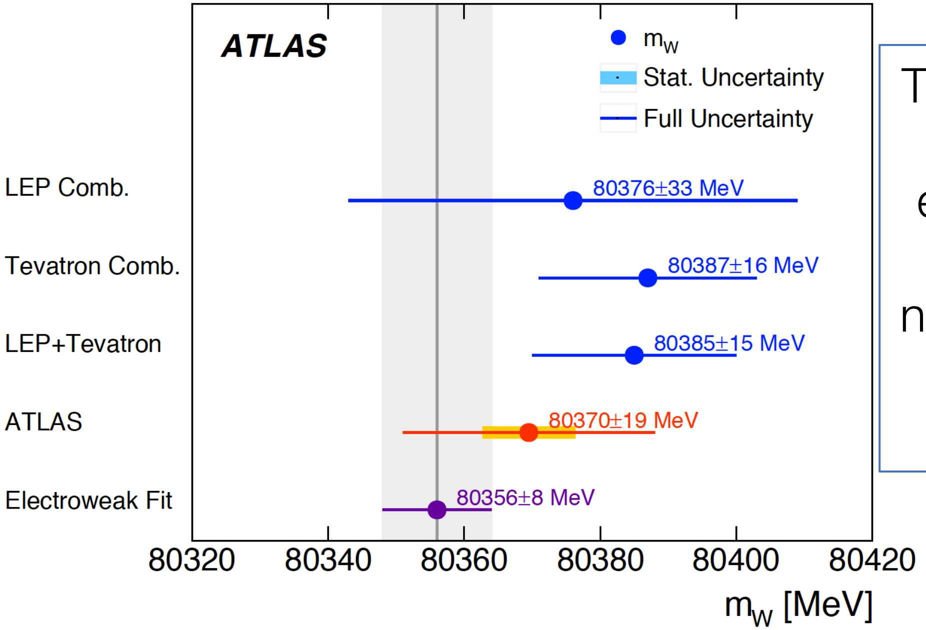

The determination of m_W from the global fit of the electroweak parameters has an uncertainty of 8 MeV → natural target for the precision of the experimental measurement of m_W.

Need to improve:

- The modelling uncertainties, which currently dominate the overall uncertainty of the m_W
- Better knowledge of the PDFs, as achievable with the inclusion in PDF fits of recent precise measurements of W- and Z-boson rapidity cross sections
- Improved QCD and electroweak predictions for Drell–Yan production

All these uncertainties are crucial for future measurements of the W-boson mass at the LHC.

Not only m_W: EW Measurements at LHC: CMS

Measurements of many different EW processes have been performed:

Many different cross sections have been measured at different centre-of-mass energies, spanning over ~9 orders of magnitude.

The comparison with SM predictions is also shown.

Agreement is generally good.

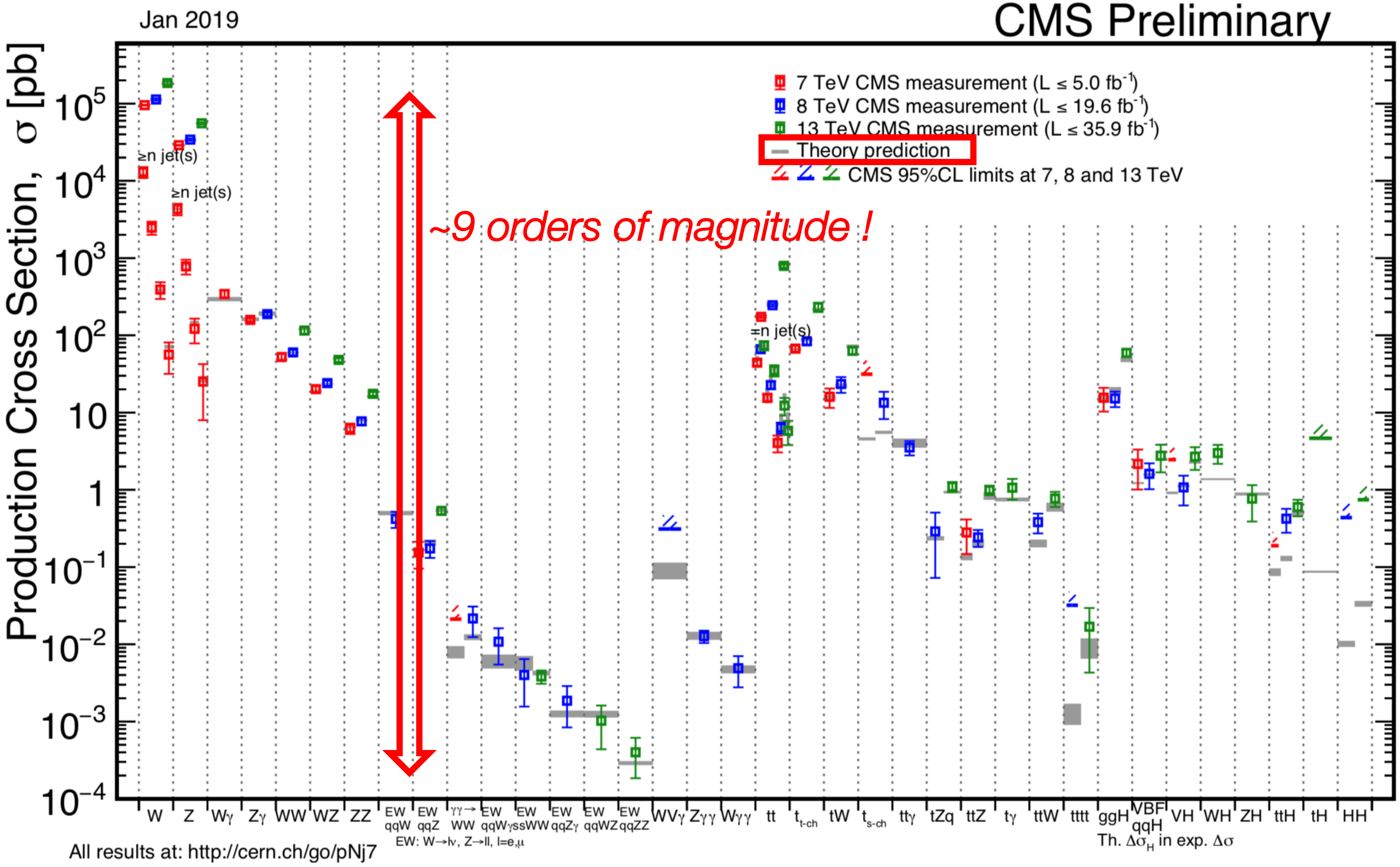

~9 orders of magnitude !

Not only m_W: EW Measurements at LHC: ATLAS

Very similar situation in ATLAS →

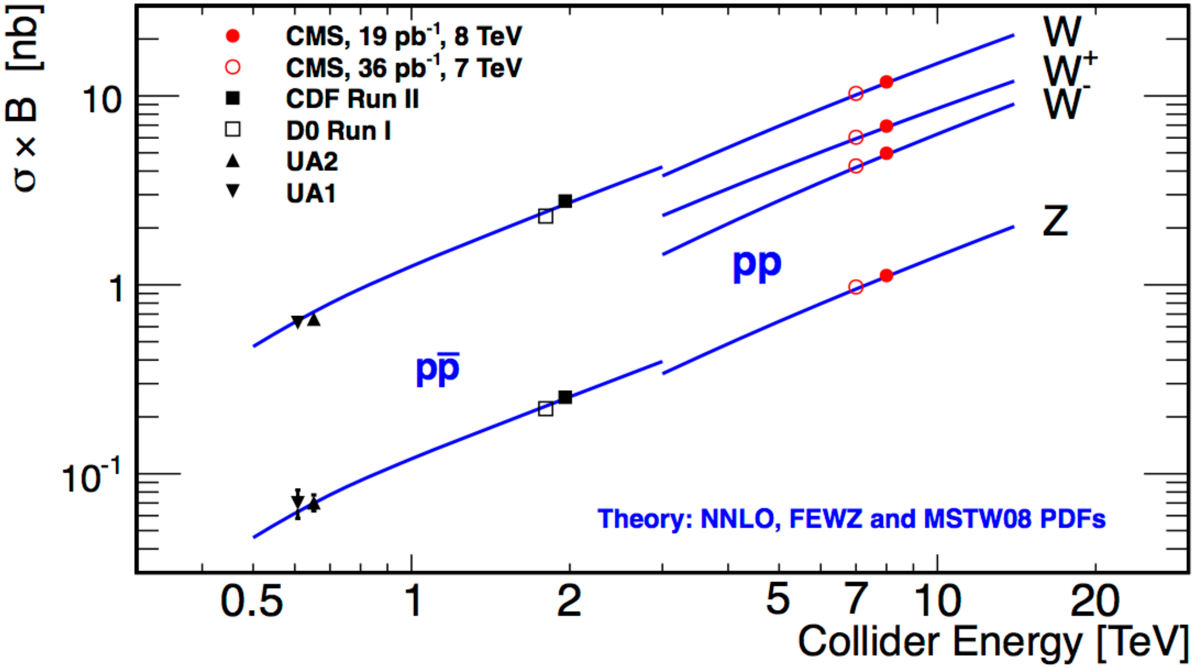

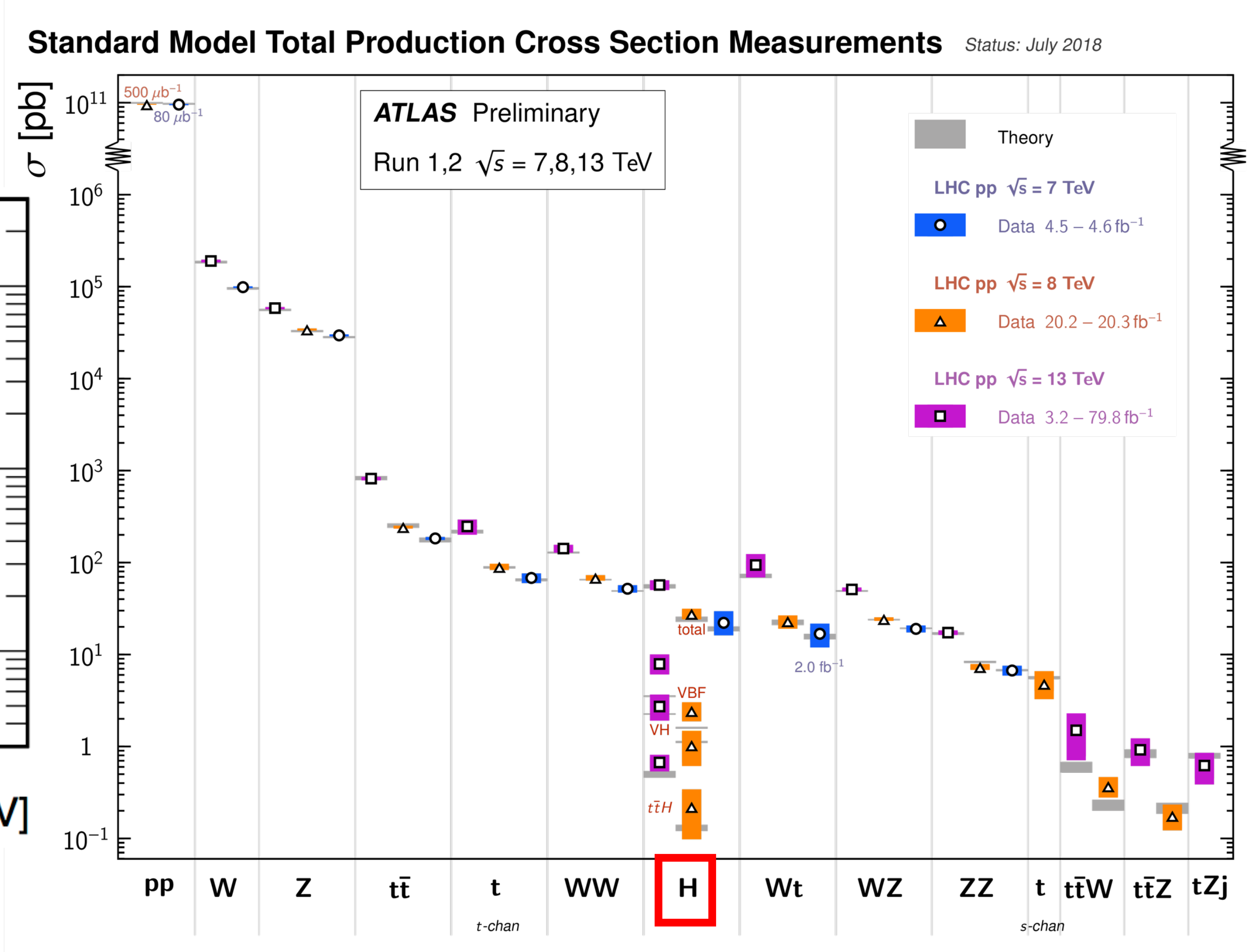

As an example the inclusive cross-section for the production of Ws and Zs is also shown compared to theory.

This is the end of the SM? Do we need to measure some observable to a better precision?

EW cross-sections as Measured by ATLAS

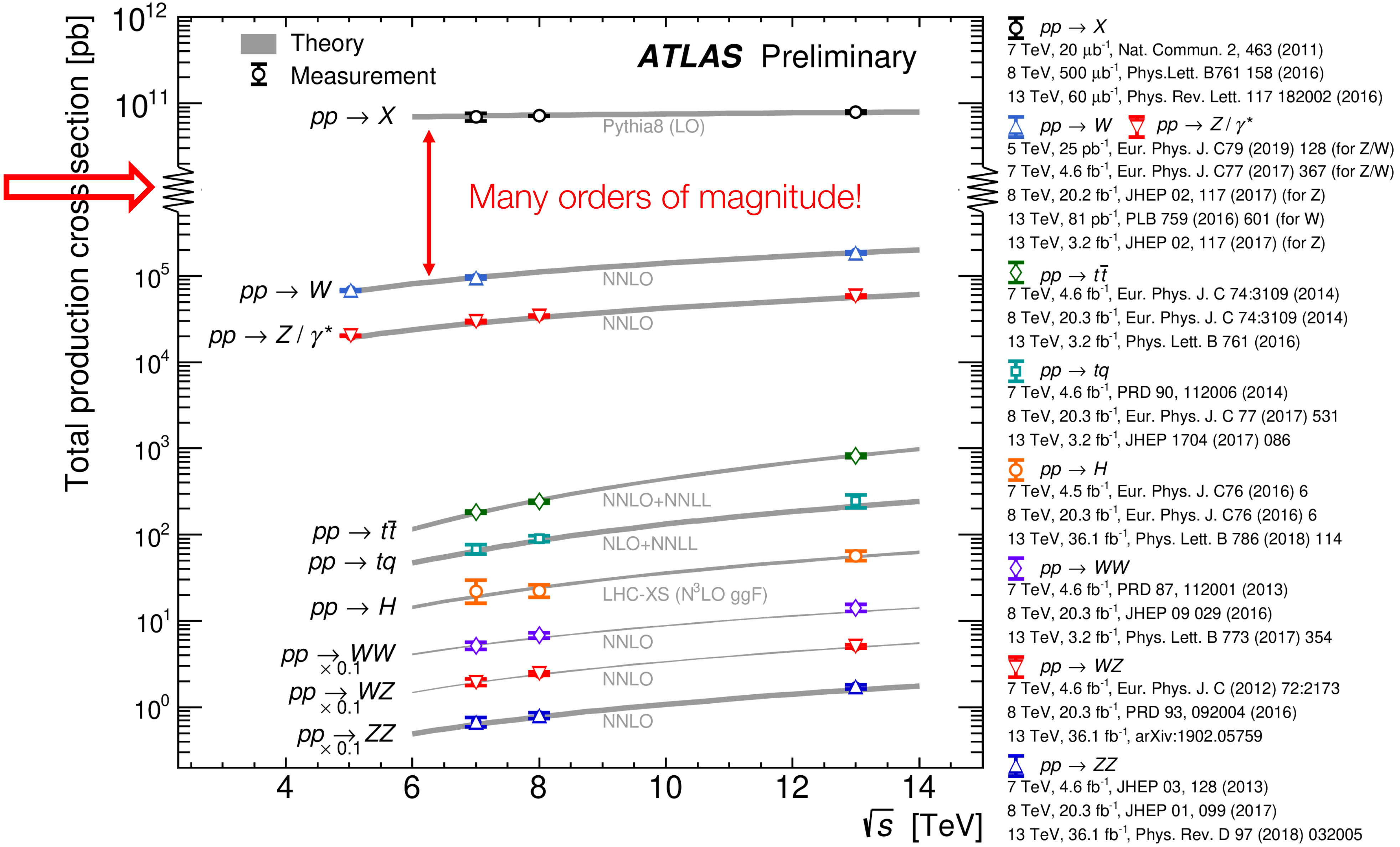

Many orders of magnitude!

References

1) J. J. Aubert et al. , “Experimental Observation of a Heavy Particle J.” Phys. Rev. Lett. , 33 , 1404 (1974).
2) J.-E. Augustin et al. , “Discovery of a Narrow Resonance in e+e– Annihilation.” Phys. Rev. Lett. , 33 , 1406 (1974).
3) C. Bacci et al. , “Preliminary Result of Frascati (ADONE) on the Nature of a New 3.1 GeV Particle Produced in e^+e^- Annihilation.” Phys. Rev. Lett. , 33 , 1408 (1974).
4) LEP and SLD Collaborations. 2006. Phys. Rept., 427, 257–454
5) W-PAIR PRODUCTION AT LEP P.AZZURRI European Organization for Nuclear Research CERN, EP Division, CH-1211 Geneve 23, Switzerland
6) Electroweak Measurements in Electron-Positron Collisions at W-Boson-Pair Energies at LEP The ALEPH, DELPHI, L3, OPAL Collaborations, the LEP Electroweak Working Group
7) Sylvie Braibant, Giorgio Giacomelli, Maurizio Spurio, Particles and Fundamental Interactions; An Introducton to Particle Physics. Springer

Precision Measurements

Particle Physics
Toni Baroncelli
Haiping Peng
USTC

End of Precision Measurements

Let’s consider the case of a W produced at rest. The cross section can be expressed as

$$\frac{d\sigma}{d(\cos\hat{\theta})} = \sigma_0(\hat{s})(1+\cos^2\hat{\theta})$$

where s is the center of mass energy of the colliding quarks and where θ is the polar angle of the electron with respect to the proton beamline. The function $\theta_0(\widehat{s})$ is proportional to a Breit-Wigner distribution.

We define the quantity $\mathrm{E} = \sqrt{\hat{\mathrm{s}}}$ and $\mathrm{E_T} = \sqrt{\hat{\mathrm{s}}} * \sin(\theta)$

This quantity is useful because it is invariant under longitudinal boosts. In the W rest frame we can write the differential cross section in E_T as

$$\begin{aligned}\frac{d\sigma}{dE_T} &= \frac{2}{\sqrt{\hat{s}}}\frac{d\sigma}{d(\sin\hat{\theta})} \\ &= \frac{2}{\sqrt{\hat{s}}}\frac{d\sigma}{d(\cos\hat{\theta})}\left|\frac{d(\cos\hat{\theta})}{d(\sin\hat{\theta})}\right| \\ &= \frac{2}{\sqrt{\hat{s}}}\sigma_0(\hat{s})(1+\cos^2\hat{\theta})|\tan\hat{\theta}| \\ &= \sigma_0(\hat{s})\frac{4E_T}{\hat{s}}(2-4E_T^2/\hat{s})\frac{1}{\sqrt{1-4E_T^2/\hat{s}}}\end{aligned}$$

$$
\begin{aligned}
\frac{d\sigma}{dE_T} &= \frac{2}{\sqrt{\hat{s}}}\frac{d\sigma}{d(\sin\hat{\theta})} \\
&= \frac{2}{\sqrt{\hat{s}}}\frac{d\sigma}{d(\cos\hat{\theta})}\left|\frac{d(\cos\hat{\theta})}{d(\sin\hat{\theta})}\right| \\
&= \frac{2}{\sqrt{\hat{s}}}\sigma_0(\hat{s})(1+\cos^2\hat{\theta})|\tan\hat{\theta}| \\
&= \sigma_0(\hat{s})\frac{4E_T}{\hat{s}}(2-4E_T^2/\hat{s})\frac{1}{\sqrt{1-4E_T^2/\hat{s}}}
\end{aligned}
$$

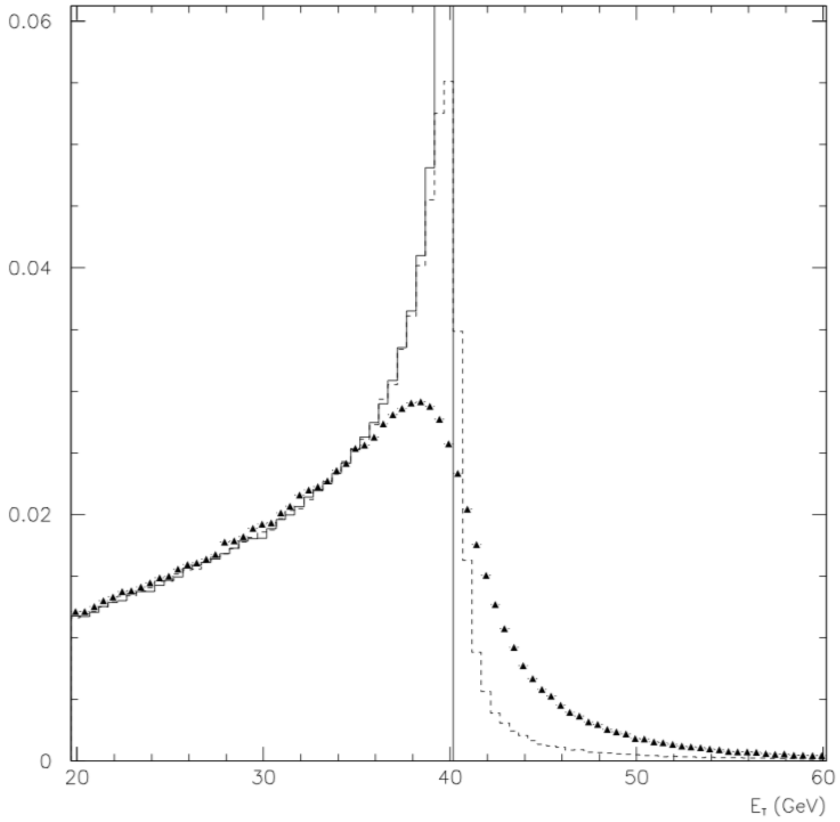

For $E_T = \sqrt{\hat{s}}/2$ we have a singularity! However σ_0 has the shape of a Breit-Wigner thus all these values are smeared and the discontinuity is recovered

The Properties of the W-Boson

Toni Baroncelli: Precision Measurements

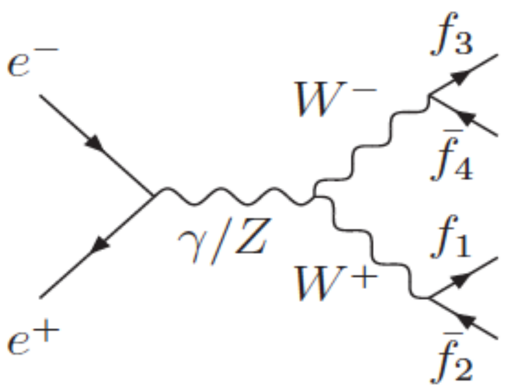

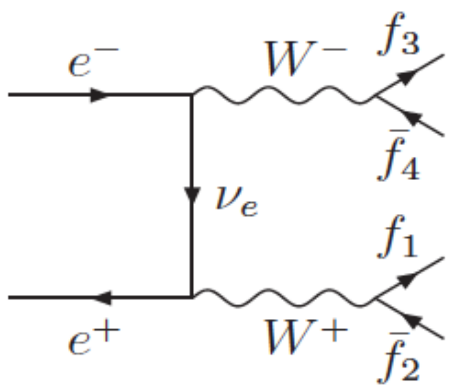

W Leptonic Branching Ratios

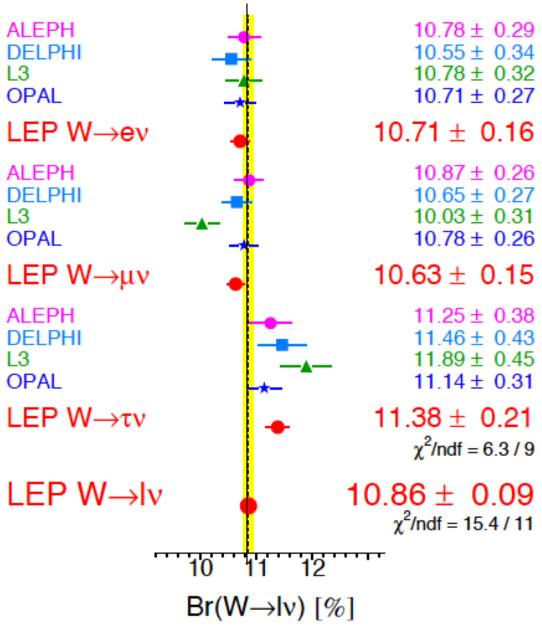

W Hadronic Branching Ratio